# Performance Evaluation of Precast Reinforced Concrete after Early-Age Carbonation Curing

# **Duo Zhang**

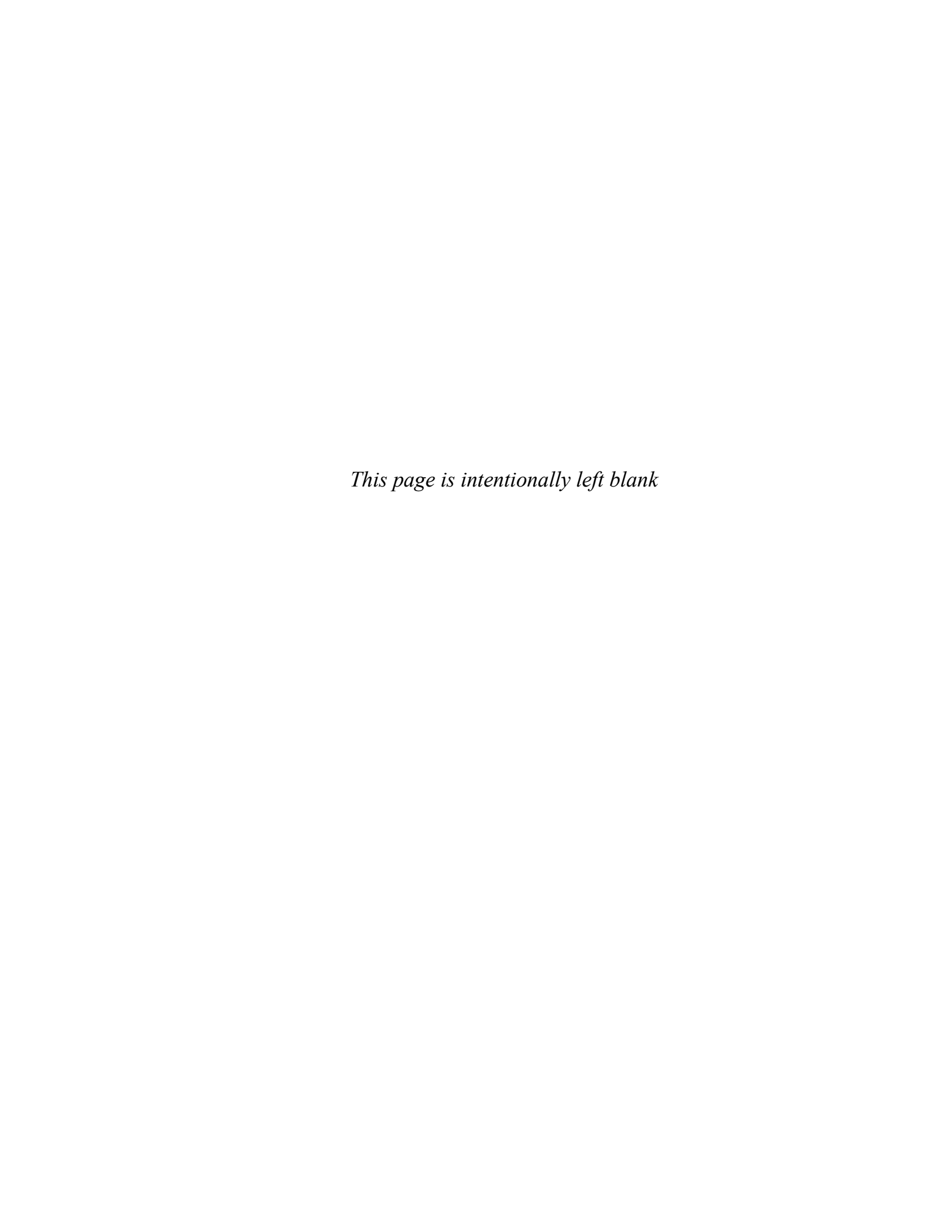
Department of Civil Engineering and Applied Mechanics McGill University, Montreal

July 2016



A thesis submitted to McGill University in partial fulfillment of the requirements of the degree of Doctor of Philosophy in Engineering

© Duo Zhang, 2016 All Rights Reserved



#### **ABSTRACT**

Early carbonation curing of precast concrete accelerates early strength and promotes carbon dioxide utilization. Reinforced concrete represents the majority of precast concrete products and thus the application of early-age carbonation technology in reinforced concrete curing is able to enhance the carbon dioxide utilization potential by concrete products for emission reduction and performance improvement. This thesis aims to develop a special carbonation process suitable to high slump precast concrete. The performance of both ordinary Portland cement (OPC) concrete and fly ash-OPC concretes were evaluated. Early carbonation behavior was assessed by carbon uptakes, pH values, compressive strength and process shrinkage. The effect of early carbonation curing on cement reaction, pozzolanic reaction and pore structure was also examined to interpret the mechanisms of durability performance including freeze-thaw resistance, chloride penetration and weathering carbonation. It was found that carbonation curing had reduced both pore volume and pore size. Gel pores became dominant which were responsible for the improved resistance to permeation and freeze-thaw damage. Chemically cement reaction was accelerated in the early age by carbonation curing and concrete pH values could be compensated by subsequent re-hydration. It was concluded that the carbonation curing was suited to the precast reinforced concrete with or without fly ash incorporation in order to gain improved early strength, enhanced durability and permanent carbon dioxide sequestration as an added-value for environmental benefit.

#### RÉSUMÉ

La cure précoce de la carbonatation des produits préfabriqués en béton accélère la résistance initiale et permet de promouvoir l'utilisation du dioxide de carbone. Le béton armé représante la majorité des produits de béton préfabriqués, ainsi, l'application de la technologie de de la carbonatation précoce sur la cure du béton armé est capable d'améliorer le potential d'utlisation du dioxyde de carbone par les produits fabriqués en béton pour la réduction des émissions et l'amélioration de la péreformance. Cette thèse vise a développer un processus spécial de cabonatation adapté à l'affaissement du béton préfabriqué. Le fonctionnement du béton composé de ciment ordinaire de Portland (OPC) ainsi que celui du béton avec cendres volantes a été évaluée. Le fonctionnement de la carbonatation précoce a été évalué par l'absorption du carbone, les valeurs de pH, la résistance à la compression, ainsi que par le processus de retrait. L'effet de la cure précoce de la carbonatation sur la réaction du ciment, réaction pouzzolanique et la structure des pores, a également été examinée afin d'interpréter les mécanismes de durabilité des performances, comprenant la résistance au gel-dégel, la pénétration des chlorures et la carbonatation intempérie. Il a été déduit que la cure de la carbonatation a réduit le volume ainsi que la taille des pores. Les pores du gel sont devenus dominants, ceux-ci étant responsables de l'amélioration de la résistance à la perméation et des dégâts dûs au gel-degél. Chimiquement, la réaction du ciment a été accélérée par la cure de la carbonatation et les valeurs pH du béton pourraient être compensées par la réhydratation ultérieure. Il a était conclu que la cure de la carbonatation serait adapté au béton préfabriqué, avec ou sans l'incorporation de cendres volantes afin d'obtenir l'amélioration

de la résistance initiale, une durabilité accrue, et la séquestration du dioxyde de carbone permanent comme une valeur ajoutée environmental supplémentaire.

#### **ACKNOWLEDGEMENTS**

I am grateful to my supervisor, Prof. Yixin Shao, for the inspiration, patience and guidance throughout the past three years. I sincerely appreciate his exclusive contribution of time and ideas which lead me into research.

I would like to express my special thanks to Prof. Xinhua Cai at Wuhan University for assistance and discussion. Chemistry experiments were carried out with technical assistance of Ms. Monique Riendeau and Mr. Robert Paquette at Department of mining and material engineering, McGill University. I am also grateful for the long time aid from Mr. Zhuoran Wang specifically in microscopic analysis. Many thanks to Mr. Jie Zhou for portion of microstructure experiment conducted at University of Alberta.

Technical support from John Bartczak, Bill Cook and Damon Kiperchuk are greatly appreciated. In the meanwhile I would like to thank all my colleagues in the research group for the wonderful time working together.

I would like to express my most sincere gratitude to my parents who are accompanying, understanding and motivating me all the time. Thank you for sharing all my happiness and frustration in these years. And thank you for granting me the happiest family ever. I am also grateful to my supervisor of master degree, Prof. Shunquan Qin, for his mentorship of my life which is always driving me to pursue excellence.

Lastly I would like to thank Mr. Robert Rizk, for translating the abstract to French.

#### STATEMENT OF ORIGINALITY

- A unique process including in-mold curing, de-mold conditioning, carbonation curing and subsequent rehydration was developed for precast reinforced concrete with high workability.
- The relationship between pozzolanic reaction and carbonation reaction was systematically studied.
- The pore structure of carbonation cured concrete was characterized and the mechanism of durability improvement by early carbonation was elucidated.
- The effect of carbonation curing on chloride penetration and weathering carbonation was investigated.

#### *Publications:*

Duo Zhang, Yixin Shao. (2016), Early age carbonation curing for precast reinforced concrete, Construction and Building Materials, 113, 134-143.

This paper is published based on Chapter 3.

Duo Zhang, Xinhua Cai, Yixin Shao. (2016), *Carbonation curing of precast fly ash concrete*, <u>Journal of Materials in Civil Engineering</u>, <u>ASCE</u>, 04016127

This paper is published based on Chapter 4.

Duo Zhang, Yixin Shao. *Pore structure of cementitious pastes subject to carbonation curing and its effect on concrete performance*, submitted to <u>Cement and Concrete Composites</u>.

This paper is published based on Chapter 5.

Duo Zhang, Yixin Shao. Effect of early carbonation curing on chloride penetration and weathering carbonation in concrete, Construction and Building Materials, accepted, in press

This paper is published based on Chapter 6.

#### **CONTRIBUTIONS OF AUTHORS**

The manuscripts included in this thesis (Chapters 3 to 6) have been submitted for publication in scientific journals. The author was responsible for conducting the research, analyzing the data, and preparing the manuscripts. The author's supervisor, Dr. Yixin Shao, provided general guidance and editorial revisions throughout the entire thesis. Also, Dr. Xinhua Cai of Wuhan University assisted in performing the selective acid dissolution tests in Chapter 4.

# TABLE OF CONTENTS

CHAPTER 1 - INTRODUCTION	1 -
1.1. OVERVIEW	1-
1.1.1. CURING OF CONCRETE PRODUCTS	2 -
1.1.2. CARBONATION CURING TECHNOLOGY	3 -
1.1.3. CARBON DIOXIDE EMISSION AND SEQUESTRATION	4-
1.2. RESEARCH OBJECTS	5 -
1.3. THESIS STRUCTURE	6-
REFERENCES	8-
CHAPTER 2 - LITERATURE REVIEW	9 -
2.1. CARBONATION	9 -
2.1.1. WEATHERING CARBONATION	9 -
2.1.2. EARLY AGE CARBONATION	11 -
2.1.3. QUANTIFICATION OF CARBON DIOXIDE CONTENT	12 -
2.1.4. CARBONATION PRODUCTS	13 -
2.2. SUPPLEMENTARY CEMENTITIOUS MATERIALS	14 -
2.3. PORE STRUCTURE	16 -
2.3.1. GEL PORES	17 -
2.3.2. CAPILLARY PORES	18 -
2.3.3. Entrained voids	18 -
2.3.4. Pore structure evolution	19 -
2.3.5. MERCURY INTRUSION POROSIMETRY (MIP)	20 -
2.3.6. GAS ADSORPTION	23 -
2.3.7. COMPARISON OF VARIOUS CHARACTERIZATION METHODS	25 -
2.4. CORROSION	26 -
2.4.1. CHI ODIDE INDUCED CODDOCION	27

2.4.2. CARBONATION-INDUCED CORROSION	28 -
3.5. SUMMARY	28 -
REFERENCES	30 -
CHAPTER 3 - EARLY AGE CARBONATION CURING FOR PREC	CAST
REINFORCED CONCRETES	42 -
Preface	42 -
3.1. Introduction	43 -
3.2. EXPERIMENTAL PROGRAM	45 -
3.2.1. MATERIALS AND MIXTURE PROPORTIONS	45 -
3.2.2. CARBONATION CURING PROCEDURE.	47 -
3.2.3. CO <sub>2</sub> uptake estimation	49 -
3.2.4. Performance evaluation	50 -
3.2.5. ACCELERATED WEATHERING CARBONATION TEST	52 -
3.2.6. Preconditioning shrinkage of reinforced concrete beam	53 -
3.3. RESULTS AND DISCUSSIONS	54 -
3.3.1. CARBONATION CURING OF WET-MIX CONCRETE	54 -
3.3.2. EFFECT OF CARBONATION CURING ON PH OF CONCRETE	63 -
3.3.3. Effect of Early Carbonation on Weathering Carbonation	64 -
3.3.4. Preconditioning shrinkage of reinforced concrete beams	66 -
3.3.5. UTILIZATION CAPACITY OF CARBON DIOXIDE AND COST ANALYSIS	70 -
3.4. CONCLUSIONS	71 -
ACKNOWLEDGEMENT	73 -
REFERENCES	74 -
CHAPTER 4 - CARBONATION CURING OF PRECAST FLY ASH CONCRETE	- 76 -
Preface	
4.1. Introduction	
4.2. EXPERIMENTAL PROGRAM	

4.2.1. MATERIALS AND MIX PROPORTION	80 -
4.2.2. Samples preparation	80 -
4.2.3. MEASUREMENT OF CARBONATION DEGREE	84 -
4.2.4. Compression test	85 -
4.2.5. DETERMINATION OF FLY ASH REACTION DEGREE	86 -
4.2.6. DETERMINATION OF CEMENT REACTION DEGREE	88 -
4.2.7. Concrete test	89 -
4.3. RESULTS AND DISCUSSIONS	91 -
4.3.1. Degree of Carbonation reaction	91 -
4.3.2. Compressive strength of fly ash-OPC pastes	92 -
4.3.3. REACTION DEGREE OF FLY ASH	96 -
4.3.4. REACTION DEGREE OF CEMENT	97 -
4.3.5. Properties of Carbonated fly ash concrete	102 -
	105 -
4.4. CONCLUSIONS	
	107 -
ACKNOWLEDGEMENT	
ACKNOWLEDGEMENT	108 - STES ON
ACKNOWLEDGEMENT  REFERENCES  CHAPTER 5 - PORE STRUCTURE OF CEMENTITIOUS PASUBJECT TO CARBONATION CURING AND ITS EFFECT CONCRETE PERFORMANCE	108 - STES ON 110 -
ACKNOWLEDGEMENT  REFERENCES  CHAPTER 5 - PORE STRUCTURE OF CEMENTITIOUS PASUBJECT TO CARBONATION CURING AND ITS EFFECT CONCRETE PERFORMANCE  PREFACE	STES ON 110 -
ACKNOWLEDGEMENT  REFERENCES  CHAPTER 5 - PORE STRUCTURE OF CEMENTITIOUS PASUBJECT TO CARBONATION CURING AND ITS EFFECT CONCRETE PERFORMANCE  PREFACE  5.1. INTRODUCTION	STES ON 110 - 110 - 112 -
ACKNOWLEDGEMENT  REFERENCES  CHAPTER 5 - PORE STRUCTURE OF CEMENTITIOUS PASUBJECT TO CARBONATION CURING AND ITS EFFECT CONCRETE PERFORMANCE  PREFACE  5.1. INTRODUCTION  5.2. EXPERIMENTAL PROGRAM	STES ON 
ACKNOWLEDGEMENT  REFERENCES  CHAPTER 5 - PORE STRUCTURE OF CEMENTITIOUS PASUBJECT TO CARBONATION CURING AND ITS EFFECT CONCRETE PERFORMANCE  PREFACE  5.1. INTRODUCTION  5.2. EXPERIMENTAL PROGRAM  5.2.1. MATERIALS AND MIX PROPORTION	STES ON
ACKNOWLEDGEMENT  REFERENCES	STES ON
ACKNOWLEDGEMENT	STES ON
ACKNOWLEDGEMENT  REFERENCES	STES ON
ACKNOWLEDGEMENT	STES ON - 110 110 112 114 114 117 120 121 -
ACKNOWLEDGEMENT REFERENCES	STES ON - 110 110 112 114 114 117 120 CONCRETE - 121 -

5.3.4. COMPARISON OF MIP AND NAD ON INK-BOTTLE PORES	133 -
5.3.5. EFFECT OF PORE STRUCTURE CHANGE ON CONCRETE PERFORMANCE	135 -
5.4. CONCLUSIONS	140 -
ACKNOWLEDGEMENT	142 -
REFERENCES	143 -
	<b>™</b> T
CHAPTER 6 - EFFECT OF EARLY CARBONATION CURING OF CHLORIDE PENETRATION AND WEATHERING CARBONATION	
CONCRETE	146 -
PREFACE	146 -
6.1. Introduction	148 -
6.2. EXPERIMENTAL PROGRAM	150 -
6.2.1. MATERIALS AND MIX PROPORTION	150 -
6.2.2. Sample preparation and carbonation curing process	150 -
6.2.3. ABSORPTION AND SURFACE ELECTRICAL RESISTIVITY	154 -
6.2.4. CHLORIDE PENETRATION AND WEATHERING CARBONATION TESTS	155 -
6.2.5. DETERMINATION OF CHLORIDE AND WEATHERING CARBONATION EXT	ent 156 -
6.3. RESULTS AND DISCUSSIONS	157 -
6.3.1. EARLY CARBONATION BEHAVIOR OF CONCRETE	157 -
6.3.2. Effect of weathering carbonation on chloride penetration .	161 -
6.3.3. EFFECT OF EARLY CARBONATION CURING ON CHLORIDE PENETRATION	(AIR
DRYING)	163 -
6.3.4. Effect of early carbonation curing on chloride penetration	AT THE
PRESENCE OF WEATHERING CARBONATION	166 -
6.3.5. Effect of Early Carbonation curing on Weathering Carbona	γιον - 167 -
6.3.6. CHLORIDE PROFILE EVOLUTION	169 -
6.3.7. EFFECT OF EARLY CARBONATION CURING ON FREE CHLORIDE PROFILE	170 -
6.4. SUMMARY AND CONCLUSIONS	173 -
ACKNOWLEDGEMENT	175 -
Defendances	176

CHAPTER 7 - CONCLUSIONS AND FUTURE WORK	179
7.1. CONCLUSIONS	- 179
7.2. SUGGESTIONS FOR FUTURE WORK	- 182

# LIST OF TABLES

Table 2.1. pH threshold of carbonation corrosion	28 -
Table 3.1. Mixture proportions of concrete	47 -
Table 3.2. CO <sub>2</sub> uptake of concrete (12 hours carbonation)	56 -
Table 3.3. pH and carbon content distribution in concrete by 12 hours carbonation .	63 -
Table 3.4. Effect of early carbonation on weathering carbonation (mix A)	64 -
Table 3.5. Early carbonation of reinforced concrete beam	68 -
Table 4.1. Chemical composition of as-received materials (%)	81 -
Table 4.2. Mixture proportions (kg/m <sup>3</sup> )	83 -
Table 4.3. Calcium hydroxide content in hydrated and carbonated cement pastes	- 101 -
Table 4.4. Carbonation profile and pH distribution in concrete	- 103 -
Table 4.5. Surface resistivity of concrete.	- 104 -
Table 5.1. Chemical compositions of cement and fly ash (%)	- 114 -
Table 5.2. Mixture proportions of pastes and concretes	- 115 -
Table 5.3. Carbonation and hydration performance of pastes and concretes	- 122 -
Table 5.4. Total pore volume and porosity by MIP	- 124 -
Table 5.5. Critical and threshold diameter of pastes measured by MIP	- 128 -
Table 5.6. Pore volume by NAD	- 129 -
Table 5.7. Permeable porosity of concrete	- 134 -
Table 6.1. Chemical compositions of cement and fly ash (%)	- 151 -
Table 6.2. Mixture proportion of concrete	- 151 -
Table 6.3. Results of carbonation curing	- 157 -
Table 6.4. Surface electrical resistivity ( $k\Omega$ .cm)	- 159 -
Table 6.5. Weathering carbonation depth (mm)	- 167 -
Table 6.6. The bound chloride to total chloride ratio (%)	- 172 -

# LIST OF FIGURES

Fig. 3.1. Sieve analysis of aggregate	46 -
Fig. 3.2. Carbonation curing procedure for wet-mix concrete	48 -
Fig. 3.3. Schematic of carbonation curing setup.	49 -
Fig. 3.4. Schematic of reinforced concrete beam	54 -
Fig. 3.5. Effect of water removal on CO <sub>2</sub> uptake	55 -
Fig. 3.6. Effect of carbonation time on CO <sub>2</sub> uptake.	56 -
Fig. 3.7. Effect of gas pressure on CO <sub>2</sub> uptake	57 -
Fig. 3.8. Compressive strength of concrete.	58 -
Fig. 3.9. Electrical resistivity in wet cast concrete after carbonation curing	59 -
Fig. 3.10. SEM micrograph and EDS spectrum.	61 -
Fig. 3.11. Carbonation depth after early age carbonation curing	62 -
Fig. 3.12. Carbonation depth in weathering carbonation	65 -
Fig. 3.13. Shrinkage of reinforced concrete beam due to fan drying conditioning	67 -
Fig. 3.14. Carbonation depth in reinforced concrete beam due to carbonation curing	68 -
Fig. 4.1. Procedure of carbonation curing.	82 -
Fig. 4.2. CO <sub>2</sub> uptake mass curves of paste and concrete samples	90 -
Fig. 4.3. Compressive strength of hydrated OPC and fly ash-OPC pastes	92 -
Fig. 4.4. Compressive strength of carbonated OPC pastes	93 -
Fig. 4.5. Compressive strength of carbonated OPC pastes	94 -
Fig. 4.6. Fly ash reaction degree of 20% fly ash-OPC pastes	95 -
Fig. 4.7. Fly ash reaction degree of 50% fly ash-OPC pastes	96 -
Fig. 4.8. Typical TG/DTG curve of fly ash-OPC pastes at 360 days	98 -
Fig. 4.9. Cement reaction degree in OPC paste	99 -
Fig. 4.10. Cement reaction degree in 20% fly ash-OPC paste	100 -
Fig. 4.11. Cement reaction degree in 50% fly ash-OPC paste	101 -
Fig. 4.12. Compressive strength of hydrated and carbonated concrete	102 -
Fig. 5.1. Carbonation curing apparatus	116 -
Fig. 5.2. Pore size distribution of OPC pastes by MIP	125 -
Fig. 5.3. Pore size distribution of fly ash-OPC pastes by MIP	126 -

Fig. 5.4. Relation between pore volume and pore size by MIP 12	27 -
Fig. 5.5. Pore size distribution of OPC pastes by NAD 13	31 -
Fig. 5.6. Pore size distribution of fly ash-OPC pastes by NAD 13	32 -
Fig. 5.7. Specific surface area calculated by BET 13	33 -
Fig. 5.8. Comparison of MIP with NAD for OPC pastes 13	35 -
Fig. 5.9. Comparison of MIP with NAD for fly ash-OPC pastes 13	36 -
Fig. 5.10. Concrete surface resistivity13	37 -
Fig. 5.11. Concrete mass loss due to freeze-thaw cycles 13	37 -
Fig. 5.12. Concrete scaling damage after 150 freeze-thaw cycles 13	38 -
Fig. 6.1. Experimental flow chart	53 -
Fig. 6.2. Setup of early carbonation apparatus 1:	54 -
Fig. 6.3. CO <sub>2</sub> content along the thickness 1:	58 -
Fig. 6.4. Distribution of pH values along the thickness 10	60 -
Fig. 6.5. Permeable porosity of hydrated and carbonated concrete 10	61 -
Fig. 6.6. Total chloride content in hydrated OPC concrete 10	62 -
Fig. 6.7. Total chloride content in hydrated fly ash-OPC concrete 10	62 -
Fig. 6.8. Effect of early carbonation curing on chloride penetration in OPC concrete	
exposed to chloride immersion and air drying cycles 10	63 -
Fig. 6.9. Effect of early carbonation curing on chloride penetration in fly ash-OPC	
concrete exposed to chloride immersion and air drying cycles 10	65 -
Fig. 6.10. Total chloride content in OPC concrete exposed to chloride immersion and	
accelerated weathering carbonation cycles 10	65 -
Fig. 6.11. Total chloride content in fly ash-OPC concrete exposed to chloride immersion	on
and accelerated weathering carbonation cycles 10	66 -
Fig. 6.12. Evolution of total chloride content in OPC concrete 10	68 -
Fig. 6.13. Evolution of total chloride content in fly ash-OPC concrete 10	68 -
Fig. 6.14. Free chloride content in OPC concrete after 50 <sup>th</sup> cycle 1	70 -
Fig. 6.15. Free chloride content in fly ash-OPC concrete after 50 <sup>th</sup> cycle17	70 -

## **CHAPTER 1**

\_

## **INTRODUCTION**

#### 1.1. OVERVIEW

Weathering carbonation of concrete occurred between hydration products and atmospheric carbon dioxide. It was progressive and took into effect after over 10 to 20 years' exposure. Weathering carbonation was usually considered detrimental to reinforced concrete. It decomposed calcium hydroxide (CH) and calcium silicate hydrates (C-S-H) into silica gel (SiO<sub>2</sub>) and calcium carbonate (CaCO<sub>3</sub>), leading to pH reduction in concrete pore solution and increasing corrosion risk of reinforcing steel. However, if implemented at the early age through curing process carbonation could be beneficial. The major reactions happened between carbon dioxide and anhydrous phase in cement to form C-S-H. Early carbonation was successfully applied to masonry block production (El-Hassan et al., 2013a). High early strength was generated and concrete durability was improved (Rostami et al., 2011b). Early carbonation was also an uptake process of carbon dioxide. Precast concrete products were able to be utilized for emission reduction. To increase the capacity of carbon dioxide uptake, more concrete products should be

considered. Since the process was carried out in an enclosure currently early carbonation curing was suited only to precast products.

Precast concrete products were generally categorized to two types including drymix and wet-mix. The dry-mix concrete was typically designed with zero slump and low cement content. Consequently the fresh mixture was usually consolidated by vibration compaction and able to be demolded immediately after casting. The typical products included masonry blocks, paving stones, concrete pipes and hollow core slabs. In contrast, wet-cast concretes with high slump constituted the majority of precast products. Superplasticizer was normally added to adjust sufficient workability. Higher content of cement and water prohibited the immediate demolding. Durability of precast concrete relied on several factors including mixture design, materials and early age curing approach. While carbonation curing of dry-mix concrete was successful in obtaining accelerated strength gain and improved durability, special process was needed to be developed on wet-mix concrete to implement the technique to general precast products for carbon utilization. It was also necessary to reveal the effect of early age carbonation on microstructure formation and long term durability performance of precast concrete products.

# 1.1.1. Curing of concrete products

It was generally considered that curing was of vital importance on both concrete strength and durability (Kosmatka and Wilson, 2011). Fresh concrete was kept in suitable temperature and moisture for early age cement hydration. Steam curing was frequently

applied as acceleration of hydration for precast products via exposure in controlled temperature and humidity. In reduction of turnaround time of framework during industrial manufacture, autoclaving was utilized in cases. The process was energy extensive though being proved with high early strength and thus faster fabrication (Meeks and Carino, 1999).

#### 1.1.2. Carbonation curing technology

Being firstly introduced in 1970s, chemical reactions of early age carbonation were systematically studied in theory (Goodbrake et al., 1979; Berger et al., 1972). Calcium silicates in cement reacted with carbon dioxide in considerably high rate and resulted in notable strength gain in few minutes to hours (Young et al., 1974). Intensive research of its application appeared after late 1990s. It was recognized that concrete cured through early age carbonation maintained not only enhanced early strength, but also observed economic benefits (El-Hassan et al., 2013a). Comparing to steam curing, energy consumption of early age carbonation was proved to be significantly lower even with consideration of energy cost during carbon dioxide gas purification and transport. In the long term, carbonation curing was reported to produce more durable concrete products in exposure to extreme conditions (Rostami et al., 2011b). Less permeability and higher resistance against frost damage were observed (Rostami et al., 2011a). This technology was becoming more attractive in the background of carbon dioxide sequestration and reutilization (Bertos et al., 2004).

# 1.1.3. Carbon dioxide emission and sequestration

Portland cement industry was energy intensive and accounted for more than 7% of global greenhouse gas emission. Besides optimization of its manufacture process, reduction of its usage was of primary concern in regard to the environmental effect. Partial replacement of cement by supplementary cementitious materials (SCMs) was among the primary solutions currently available. In practice SCMs, such as fly ash, slag and metakaolin, was commonly used in concrete as 15-20% by mass of the cementitious material (Scrivener and Kirkpatrick, 2008). High volume dosage of 50-60% was also reported in cases (Lothenbach et al., 2011).

Carbonation curing was a utilization process of carbon dioxide. Carbon dioxide reacted with calcium silicates in aqueous condition and was permanently converted into the form of calcium carbonate binding with hydration products (El-Hassan et al., 2013b). It was reported that concrete block unit with mass of 18 kg containing 10% cement by mass was able to uptake at least 0.18 kg of CO<sub>2</sub> gas (El-Hassan et al., 2013a). For precast products made of dry-mix concrete, the capacity of CO<sub>2</sub> uptake could reach up to 10% by mass of cement. Thus it was estimated that the annual capture amount of 2.5 million tons gaseous carbon dioxide was able to be reached by precast blocks or bricks alone. If the technique could be applied on wet-mix concrete this environmental effect is dramatically higher due to the widely usage.

#### 1.2. RESEARCH OBJECTS

This proposed research sought to develop the early age carbonation technology for wet-mix reinforced concrete products with high workability. Special manufacturing process was formulated and the long term performance including strength evolution, pH values, pore structure change and chloride penetration was evaluated. The carbonation cured structure was characterized by both physical and chemical methods and the effect of early carbonation on reinforced concrete corrosion was assessed.

Unlike the dry-mix concrete with compact casting, majority of precast reinforced concrete was generally cast from wet mixture. Mineral admixtures were widely used such as fly ash, silica fume or slag. Their addition might change the pattern of carbonation curing and consequently formed products and pore structure distinguished from plain Portland cement mixture. The effect was to be clearly understood before being implemented on reinforced concrete. The following tasks would be carried out in regard to the carbonation curing of precast reinforced concrete products:

- To develop a controlled carbonation curing process at early age to facilitate carbon dioxide utilization while avoiding carbonation-induced corrosion;
- To quantify the effect of early age carbonation on cement reaction degree in both short and long term;
- To investigate the relationship between early age carbonation reaction and pozzolanic reaction in fly ash / Portland cement system;

- To characterize the pore structure evolution (including pore volume, pore size distribution, specific surface area) due to carbonation curing in both early and late ages;
- To examine the freeze-thaw resistance and transport behavior of carbonation cured concrete due to the pore structure change;
- To assess the resistance to chloride penetration in concrete subject to carbonation curing;
- To evaluate corrosion potential of carbonation cured reinforced concrete subject to exposure of both chloride ambient and atmospheric weathering carbonation.

#### 1.3. THESIS STRUCTURE

This thesis followed manuscript-based structure. Chapter 1 introduced the background, significance and aim of the proposed research. Chapter 2 provided detailed literature review in which previous research was summarized in the domain of cement and concrete carbonation. Chapter 3, 4, 5 and 6 were focused on individual aspects on wet-mix concrete carbonation curing varying from chemical to physical and microscope to macro performance. Each chapter followed a preface which highlighted its objectives and connections to other chapters. Brief literature review of past research was given on each specific topic to highlight the contribution of each chapter. Chapter 3 developed the manufacture approach feasible on precast reinforced concrete based on extensive parameter studies. The basic process of initial curing – carbonation curing – subsequent hydration was determined and optimized. Chapter 4 and 5 studied the mechanism of

carbonation curing in scope of chemistry and physics, respectively. The addition of fly ash and its interaction with carbonation curing were highlighted. Low volume (20%) and high volume (50%) fly ash were treated with different carbonation degree and studied the short and long term performance including 1, 28, 90, 180 and 360 days. Chapter 4 focused on the chemical aspect of carbonation curing and traced the evolution of cement hydration and pozzolanic reaction with age up to 360 days. Various experimental approaches were introduced in order for the determination of reaction degree including thermal gravimetric analysis, selective acid dissolution, concrete pyrolysis, etc. The corresponding compressive strength, fly ash reaction degree, carbon content and durability performance were correlated. The physical evolution of pore structure was discussed in detail by Chapter 5. Mercury intrusion porosimetry and nitrogen gas adsorption / desorption were applied to present an overview on the porous media subjected to carbonation curing with pore diameter range from nanometers to hundreds of micrometers. Features of pore structure were discussed such as pore volume, pore size and pore shape etc. The effect on durability of concrete was further discussed with more deeply illustrations on the mechanism of "carbon densification". Transport behavior and freeze-thaw resistance were investigated and the mechanism was explained in aspect of pore structure. Chapter 6 emphasized on effect of carbonation curing on reinforcement corrosion potential in concrete exposed to both chloride and atmospheric carbon dioxide condition. Long term experimental studies were conducted referring to coastal structures, especially splash zone. The complexed effects from both chemistry and physics aspects were involved. Conclusions were summarized in Chapter 7 with suggestions of future work.

#### REFERENCES

- BERGER, R., YOUNG, J. & LEUNG, K. 1972. Acceleration of hydration of calcium silicates by carbon dioxide treatment. *Nature*, 240, 16-18.
- BERTOS, M. F., SIMONS, S., HILLS, C. & CAREY, P. 2004. A review of accelerated carbonation technology in the treatment of cement-based materials and sequestration of CO<sub>2</sub>. *Journal of hazardous materials*, 112, 193-205.
- EL-HASSAN, H., SHAO, Y. & GHOULEH, Z. 2013a. Effect of initial curing on carbonation of lightweight concrete masonry units. *ACI Materials Journal*, 110, 441-450.
- EL-HASSAN, H., SHAO, Y. & GHOULEH, Z. 2013b. Reaction Products in Carbonation-Cured Lightweight Concrete. *Journal of Materials in Civil Engineering*, 25, 799-809.
- GOODBRAKE, C. J., YOUNG, J. F. & BERGER, R. L. 1979. Reaction of Beta-Dicalcium Silicate and Tricalcium Silicate with Carbon Dioxide and Water Vapor. *Journal of the American Ceramic Society*, 62, 168-171.
- KOSMATKA, S. H. & WILSON, M. L. 2011. Design and Control of Concrete Mixtures: The guide to applications, methods, and materials, Portland Cement Association.
- LOTHENBACH, B., SCRIVENER, K. & HOOTON, R. 2011. Supplementary cementitious materials. *Cement and Concrete Research*, 41, 1244-1256.
- MEEKS, K. W. & CARINO, N. J. 1999. Curing of high-performance concrete: Report of the state-of-the-art, Citeseer.
- ROSTAMI, V., SHAO, Y. & BOYD, A. J. 2011a. Carbonation curing versus steam curing for precast concrete production. *Journal of Materials in Civil Engineering*, 24, 1221-1229.
- ROSTAMI, V., SHAO, Y. & BOYD, A. J. 2011b. Durability of concrete pipes subjected to combined steam and carbonation curing. *Construction and Building Materials*, 25, 3345-3355.
- SCRIVENER, K. L. & KIRKPATRICK, R. J. 2008. Innovation in use and research on cementitious material. *Cement and Concrete Research*, 38, 128-136.
- YOUNG, J., BERGER, R. & BREESE, J. 1974. Accelerated curing of compacted calcium silicate mortars on exposure to CO<sub>2</sub>. *Journal of the american ceramic society*, 57, 394-397.

# **CHAPTER 2**

\_

#### LITERATURE REVIEW

#### 2.1. CARBONATION

## 2.1.1. Weathering carbonation

Mature concrete was vulnerable to the reaction with carbon dioxide (CO<sub>2</sub>) in atmosphere. The reaction happened between cement hydration products and CO<sub>2</sub> at rather slow rate. It took years to show the effects on concrete. The main elements in hydrated cement included calcium hydroxide (CH) and calcium-silicate-hydrate (C-S-H), both of which were susceptible to the reaction with CO<sub>2</sub>. The reaction consumed calcium hydroxide first and resulted in lower pH in pore solution as shown in Eq. 2.1. The neutralization effect reduced pH to below 9 comparing to non-carbonated pH of 13 (Chang and Chen, 2006).

$$Ca(OH)_2 + CO_2 \rightarrow CaCO_3 + H_2O$$
 (2.1)

Carbonation of C-S-H gel were studied thoroughly. It was generally believed that portion of calcium in C-S-H gel was departed due to the reaction and formed calcium

carbonates as shown in Eq. 2.2. Calcium to silicate ratio (C/S) in C-S-H gel was reduced as a result of the decalcification-polymerization effect (Morandeau et al., 2014).

$$xCaO \cdot ySiO_2 \cdot zH_2O + xCO_2 \rightarrow xCaCO_3 + ySiO_2 \cdot tH_2O + (z-yt)H_2O$$
 (2.2)

Besides of calcium hydroxide and C-S-H gel (composing more than 85% of hydrated cement), aluminum phase in hydration products including ettringite and monosulphoaluminate were also susceptible to carbonation as reported in past studies (Nishikawa et al., 1992; Venhuis and Reardon, 2001).

$$6\text{CaO} \cdot \text{Al}_2\text{O}_3 \cdot 3\text{SO}_3 \cdot 32\text{H}_2\text{O} + 3\text{CO}_2 \rightarrow$$

$$3CaCO_3 + 3CaO \cdot SO_3 \cdot 2H_2O + Al_2O_3 \cdot xH_2O + (26-x)H_2O$$
 (2.3)

 $4\text{CaO} \cdot \text{Al}_2\text{O}_3 \cdot \text{SO}_3 \cdot 12\text{H}_2\text{O} + 3\text{CO}_2 \rightarrow$ 

$$3CaCO_3 + CaO \cdot SO_3 \cdot 2H_2O + Al_2O_3 \cdot 3H_2O + 7H_2O$$
 (2.4)

In most cases, weathering carbonation was considered as detrimental effect especially in reinforced concrete. The primary reason was the reduced pH in pore solution which increased possibility of steel rebar corrosion. It was reported that in natural atmospheric exposure, steel reinforcement could be affected in 10 to 50 years in regard to ambient environment (Kobayashi et al., 1994; Castro et al., 2000). It was an important parameter in life-cycle assessment of structure durability.

In spite of the risk to corrosion, higher compressive strength was observed owing to weathering carbonation. Explanation of this phenomenon laid on the densification effect of microstructure. Physically, less porous structure was formed as result of weathering carbonation (Arandigoyen et al., 2006; Lawrence et al., 2007). In the

meanwhile, it was also observed loss of bound water and shrinkage during weathering carbonation (Persson, 1998; Chen et al., 2006).

#### 2.1.2. Early age carbonation

Instead of reaction on mature cement or concrete, CO<sub>2</sub> was purposely reacted with fresh or partially hydrated cement during carbonation in the early age. Unlike weathering carbonation, this early reaction took place between CO<sub>2</sub> and anhydrous phase in cement (specifically calcium silicates) as shown in Eqs. 2.5 to 2.6.

$$3\text{CaO} \cdot \text{SiO}_2 + (3-x)\text{CO}_2 + y\text{H}_2\text{O} \rightarrow x\text{CaO} \cdot \text{SiO}_2 \cdot z\text{H}_2\text{O} + (3-x)\text{CaCO}_3$$
 (2.5)

$$2\text{CaO} \cdot \text{SiO}_2 + (2-x)\text{CO}_2 + y\text{H}_2\text{O} \rightarrow x\text{CaO} \cdot \text{SiO}_2 \cdot z\text{H}_2\text{O} + (2-x)\text{CaCO}_3$$
 (2.6)

Early age carbonation happened in rather fast rate and generated considerably high strength in a short period. It was recognized that compressive strength of cement paste after 81 min carbonation could reach over 67 MPa (Young et al., 1974). It was believed that late stage of hydration still maintained after the intensive reaction of the short period. Residual cement (mainly calcium silicates) was further reacted with water following the mechanism of conventional hydration.

Due to the effect of accelerated strength gain, early age carbonation was applied on concrete as curing method and named as carbonation curing (Monkman and Shao, 2009; Monkman and Shao, 2010). The approach was attempted on dry-mixed pure concrete blocks (El-Hassan et al., 2013). To gain desired CO<sub>2</sub> uptake fresh concrete underwent the process including casting, initial water loss and high pressure carbonation.

Compressive strength was reported highly improved with 10% CO<sub>2</sub> uptake based on cement mass. Controlled carbonation curing was proposed in consideration of pH and later stage hydration. It was reported that pH was able to be recovered to higher than 12.0 after 27 days subsequent hydration (Rostami et al., 2011a). Durability performance was compared among concrete cured by carbonation, natural hydration and high pressure steaming. Carbonation curing was found with better resistance to frost damage and sulphate attack (Rostami et al., 2011b).

#### 2.1.3. Quantification of carbon dioxide content

Carbonation degree of concrete, in consideration of both atmospheric and early age carbonation, was generally measured through spray of phenolphthalein on cross section. The depth of carbonation was used as indicator of reaction extent.

In early age carbonation, CO<sub>2</sub> uptake could also be measured through mass difference before and after the reaction. There were two methods built on this principle, mass gain method and mass curve method (El-Hassan et al., 2013). CO<sub>2</sub> uptake in mass gain method was measured by the sample mass change and water loss amount during carbonation as shown in Eq. 2.7. Unlike mass gain method, weight of the whole system (sample + chamber) was recorded and the weight increase was measured as CO<sub>2</sub> uptake.

Mass gain (%) = 
$$\frac{Final\ mass + Mass\ of\ water\ loss - Initial\ mass}{Mass\ of\ cement}$$
(2.7)

Other determination methods commonly used included acid titration, thermal pyrolysis, NMR, SEM/EDS, etc. Details could be found in past literatures (Anstice et al., 2005; Villain et al., 2007; Justnes et al., 1990).

#### 2.1.4. Carbonation products

It was widely accepted that the reaction between calcium silicates and carbon dioxide created calcium silicate hydrate (C-S-H) and calcium carbonate as illustrated in Eqs. 2.5 to 2.6. It was suggested that the two compounds intermixed each other making it difficult to distinguish the morphology of each product (Berger et al., 1972). Nevertheless, most studies believed that C-S-H generated from early carbonation appeared gel-like and amorphous structure (Young et al., 1974). Besides being intermingled with calcium carbonate, C-S-H gel formed during early carbonation was proved quite different from normal hydration products. Reduced calcium to silicate ratio was observed in carbonation formed C-S-H (Groves et al., 1991). Scanning electron microscopy (SEM) suggested that the C-S-H gel was silica-rich and might be surrounded by SiO<sub>2</sub> and calcium carbonate. The method to determine Ca to Si ratio in C-S-H gel was through SEM/EDS in spite that presence of calcium carbonate in C-S-H might affect the accuracy.

Another product during early carbonation was calcium carbonate, of which research remained major controversial, specifically on its morphology. Since mixed with C-S-H gel, calcium carbonate was usually difficult to be distinguished in SEM image. Thus experimental research in this area was commonly conducted on pure tricalcium

silicate ( $C_3S$ ),  $\beta$ -dicalcium silicate ( $\beta$ - $C_2S$ ) and calcium hydroxide (CH), respectively (Goodbrake et al., 1979; Moorehead, 1986). The morphology was mostly considered as calcite crystallites smaller than 1  $\mu$ m in most cases (Young et al., 1974; Cizer et al., 2008). However, aragonite was observed to be formed in prolonged carbonation of  $C_3S$  and  $\beta$ - $C_2S$  in vapor condition or dried out sample with presence of liquid water (Goodbrake et al., 1979). Some studies believed that calcium carbonate was chemically bonded with C-S-H gel to form the amorphous calcium silicate hydrocarbonate. As crystalline polymorph, calcite was formed from carbonation of  $C_3S$ ,  $\gamma$ - $C_2S$  while aragonite was intensively observed in carbonation product of  $\beta$ - $C_2S$  (Goto et al., 1995). It was noted that aragonite and vaterite were metastable polymorph and may recrystallize in some circumstances to form calcite which was the stable polymorph of calcium carbonate (Morse et al., 2007). The formation of basic calcium carbonates (BCC) and amorphous basic calcium carbonates (ABCC) was also mentioned (Goto et al., 1995).

## 2.2. SUPPLEMENTARY CEMENTITIOUS MATERIALS

Supplementary cementitious materials (SCMs) were extensively used in concrete either as blended cement or separated addition in concrete mix. Most commonly used SCMs included silica fume, fly ash and slag etc.

Silica fume was firstly introduced in concrete during 1970s. The bulk density ranged from 200 to 300 kg/m<sup>3</sup> and specific gravity was around 2.20 (<u>Toutanji et al.</u>, <u>2004</u>). Due to the fine grain, the addition of silica fume improved compressive strength in the early age while the late strength remained comparable to OPC concrete (<u>Mazloom et</u>

<u>al., 2004</u>). It was recognized that the small particle size of silica fume filled spaces in cement paste (micro filler effect) and thus improved packing effect and reduced permeability (<u>Duval and Kadri, 1998</u>). The resistance to corrosion was also improved with addition of silica fume (<u>Dotto et al., 2004</u>). However, concrete with silica fume was reported less resistant against frost damage (<u>Sabir, 1997</u>).

Unlike silica fume, fly ash concrete gained strength at much lower rate. The reaction of fly ash, also referred to as pozzolanic reaction, took place between fly ash and calcium hydroxide (CH) and generated C-S-H gel. The reaction was slow in normal temperature. Thus some specifications permitted only 20-40% usage of fly ash in consideration of early strength (Mehta and Gjørv, 1982). It was also found that reaction degree of fly ash was rather low with about 10% at 28 days and less than 20% after 90 days (Poon et al., 2000; Li et al., 2000). The unreacted fly ash served as fillers in cement paste. In high volume fly ash cement (fly ash content more than 50%), most fly ash remained unreacted and filling effect appeared to be dominant (Lam et al., 2000). Previous studies showed that high volume dosage of fly ash produced less permeable concrete with higher resistance to chloride ions penetration (Ramezanianpour and Malhotra, 1995). It was also found that fly ash helped improve concrete performance in exposure to sulfate attack or alkali-aggregate interaction (Berry and Malhotra, 1980).

Ground granulated blast furnace slag (GGBFS) blended cement was firstly introduced to commercially market in Germany in 1888. The glass content had critical effect on hydraulic activity of slag concrete (Pal et al., 2003). Slag blended concrete was also found reduced compressive strength in the early age. However, using of alkali activated slag as binder was reported to yield desirably increased early strength (Collins

and Sanjayan, 1999). Pore structure in slag blended cement was found much finer than in plain OPC paste. Thus diffusivity and penetration of chloride ions could be reduced (Bijen, 1996). In spite that slag cement concrete showed higher late strength and better resistance to sulfate attack and alkali silica reaction, it was noted that early curing condition played critical role on both mechanical and durability performance (Osborne, 1999).

#### 2.3. PORE STRUCTURE

Pore structure had significant effect on durability and mechanical properties of concrete. Generally in solid materials pore structure could be classified into three categories as proposed by International Union of Pure and Applied Chemistry (<u>Dubinin</u>, 1960; <u>Everett</u>, 1972): micropores (less than 2 nm), mesopores (between 2 to 50 nm) and macropores (larger than 50 nm). Pores in hardened cement paste in concrete were usually categorized in accord to formation mechanism and their effect on concrete. Pores in concrete (<u>Mehta</u>, 1986) were suggested to include gel pores (less than 3 nm), capillary pores (10 nm to 5 µm) and entrained voids (50 µm to 1 mm). It was noted that division of different pores was not distinct and might appear to be arbitrary since the spectrum of pore sizes is continuous in hardened cement paste (<u>Aligizaki</u>, 2005).

#### **2.3.1.** Gel pores

Gel pores existed in C-S-H as the latter showed colloidal amorphous structure (<u>Jennings et al., 1981</u>). It was found that gel pores had notable effect on hydration rates but contributed little to permeability of cement paste (<u>Klieger, 1994</u>). It was commonly considered to represent characteristic of C-S-H structure (<u>Powers, 1958</u>). Intensive studies were found regarding formation mechanism and microstructural models of C-S-H gel.

Early studies conducted by T. Powers and T. Brownyard proposed a layer structure for C-S-H gel. It was assumed to be composed of layered particles (Powers and Brownyard, 1946). Each particle contained gel substance and slit-shaped pores. The model was evidenced by experimental research performed on gas adsorption measurement (Hagymassy et al., 1972; Mikhail et al., 1964). It was also supported by past X-ray diffraction studies. Through studies on water in hardened cement paste F. Wittmann considered C-S-H as a three dimensional network composed of amorphous colloid gel particles (Aligizaki, 2005). Accordingly Munich model was developed and pore structure was linked with mechanical behavior of hardened cement paste through surface energy (Setzer and Wittmann, 1974; Wittmann, 1973). Another model suggested that the cement paste was packed by basic units with roughly spherical structure which was about 2 nm across with specific surface area of about 1000 m<sup>2</sup>/g (Jennings, 2000). Nitrogen adsorption studies were conducted to support the model of C-S-H structure (Jennings and Tennis, 1994; Tennis and Jennings, 2000).

#### 2.3.2. Capillary pores

Unlike gel pores which remained little effect on strength and durability (<u>Odler and Rößler, 1985</u>), capillary pores played the dominate role on mechanical and transport behavior of concrete. It accounted for most of durability related issues of concrete.

The volume and connectivity had significantly effect on permeability of cement paste and concrete (Young, 1988). Specific surface area of pore structure also showed well agreement with permeation behavior (Nyame and Illston, 1981). It was also proposed that C-S-H grew into capillary pores as needles and capillary pores were separated to smaller size as a result (Do et al., 2013).

#### 2.3.3. Entrained voids

In order to improve resistance to frost damage air void was incorporated in hardened concrete. The entrained voids, in the order of about 0.05 mm, existed in form of discrete cavities as to dilate the pressure generated during freezing process. However, concrete porosity was increased and compressive strength was reduced as side effect. More details could be found in other studies (<u>Du and Folliard, 2005</u>; <u>Sun and Scherer, 2010</u>).

#### 2.3.4. Pore structure evolution

Pore structure of the hydrated cement-based materials remained changing during the service life due to various factors such as further cement hydration, pozzolanic reaction and external deteriorations in weathering condition.

Hydration degree played critical effect on pore structure evolution. Capillary pores were reduced or separated into smaller space as C-S-H gel generated during the hydration process (Neville, 1995b). Consequently the total pore volume and pore size decreased (Chen and Wu, 2013). In blended cement, the addition of fly ash was reported to increase total porosity but decreased average pore size. Fineness of fly ash also had notable effect on pore structure. With finer fly ash added, total porosity and capillary pores were reduced while an increase amount was measured for gel pores (Chindaprasirt et al., 2005).

Hydration temperature was found notable influence on the physical structure. High temperature was inclined to increase capillary pores in plain cement paste and remain deleterious effect on concrete durability (Kjellsen et al., 1990). Curing methods were also reported to affect pore structure and permeability according to experimental studies (Poon et al., 1997).

Effect of early carbonation on pore structure remained a blank research area. Weathering carbonation effect, however, was studied quite well. Total porosity was found reduced by weathering carbonation while the volume of capillary pore increased (Ngala and Page, 1997). It was also suggested that there was increase in pore volume

corresponding to diameter of approximately  $0.1~\mu m$  and  $0.03~\mu m$  after carbonation (Lawrence et al., 2007).

## 2.3.5. Mercury intrusion porosimetry (MIP)

Firstly introduced in 1921 (Washburn, 1921), Mercury intrusion porosimetry (MIP) had been well developed to be one of most commonly used methods for pore structure characterization in porous media (Ritter and Drake, 1945). Pore size examined by MIP ranges widely from 2.5 nm to 800 μm which was able to cover most pore sizes existing in cement-based materials. Mercury was intruded with low and high pressure at approximately 3~4 kPa and up to 405 MPa, respectively. To interpret the experimental results, pores in hardened cement paste were commonly assumed cylindrical shape in geometry. The calculation of equivalent pore size corresponding to the intrusion pressure was provided by Washburn Equation. Consumptions and corrections were examined to generalize the application in cement-based materials (Cook and Hover, 1993). Surface area was also able to be acquired from the relation of applied mercury pressure versus intruded volume (Rootare and Prenzlow, 1967). Theoretical simulations were also conducted in regard to the intrusion process (Navi and Pignat, 1999).

Drying method had notable effect on test result. Primary techniques used for predrying included oven drying (high and low temperature), vacuum drying, freeze drying and solvent replacement (Gallé, 2001). Solvent replacement was proved with least damage on pore structure during water removal process (Feldman and Beaudoin, 1991; Konecny and Naqvi, 1993). Nevertheless, some researchers concerned about the chemical reaction between organic liquid and cement paste. It was found that calcium hydroxide in cement paste was vulnerable to reaction with organic liquid and forms 'carbonate-like' material (Day, 1981). It was also reported by Taylor that organic liquid (like methanol, acetone, etc.) was strongly sorbed by tricalcium silicate paste (Taylor and Turner, 1987). Beaudoin reported that surface area of calcium hydroxide was increased after immersion in methanol (Beaudoin et al., 1994). However, with various tests including thermogravimetric analysis, X-ray diffraction, infra-red spectroscopy and mercury intrusion test, Thomas suggested that organic solvent was unreactive with cement paste in room temperature (Thomas, 1989).

Another factor affecting MIP results was the dimension of testing sample which was reported of notable influence on pore size distribution but little on total porosity (Hearn and Hooton, 1992). In spite of the cylindrical shape assumption, the pore geometry, typically the 'ink-bottle' shape played important role on mercury intrusion results (Kaufmann et al., 2009). Pores with small diameter were inclined to be overestimated as a result (Moro and Böhni, 2002). This was intrinsic deviation of mercury intrusion experiment and inevitable with the testing approach.

Intensive studies were conducted as to interpret pore structure information and link them with concrete properties. The primary parameters acquired from the experimental results included pore size distribution plots (cumulative and differential curves) and total pore volume or porosity. The pore size distribution curve presented plentiful information. The critical pore diameter, which corresponded to the steepest slope in cumulative curve and the peak value in differential curve, was reported to be strongly correlated with chloride ion diffusion and permeability (Halamickova et al.,

1995). It was also believed that critical pore diameter represented the largest and most frequently existed interconnected pore size due to the maximum incremental volume of mercury intrusion (Winslow and Diamond, 1970). Peaks of differential curves were identified as 'initial' and 'rounded' indicating connected capillary pores and crushing of interposed hydration products, respectively (Cook and Hover, 1999). Another parameter quantifying the pore size was threshold diameter. It was defined as the largest diameter where significantly mercury intrusion occurred. The critical and threshold diameter were sometimes used as alternative to each other. However, the two parameters were clearly distinguished in some studies (Feldman and Beaudoin, 1991). Permeability was found more sensitive to threshold diameter comparing to other indicators on pore size distribution curve (Winslow et al., 1994; Liu and Winslow, 1995). Nevertheless, both critical and threshold pore diameter were observed to reduce as prolonged curing age and lower water to binder ratio (Zeng et al., 2012).

Concerns on the experimental results of MIP were found in several aspects. Firstly, there was an underestimation regarding measurements of pores with too small diameter or specific shape which was also referred to as 'lost porosity' in previous work. Typically the ink-bottle pores with much smaller neck entrance into a large cavity contribute hysteresis in the intrusion-extrusion curve (Liabastre and Orr, 1978; Lowell, 1980). Secondly, several studies suggested that the accuracy of MIP technique was under controversy since conditions required by the method could not be perfectly reached in cement paste (Beaudoin, 1979). Another limitation of mercury intrusion method was the application on concrete. D. Winslow and D. Liu compared the experimental results from concrete and paste and conclude that pore structure in concrete was more porous with

volume increasing of pores larger than the threshold diameter (Winslow and Liu, 1990). It was suggested that MIP was only suitable for estimation of threshold diameter and connectivity of pore structure instead of actual pore sizes present (Diamond, 2000).

### 2.3.6. Gas adsorption

Gas molecules resided on surface of a solid and the impinged volume varies as gas pressure changed. This phenomenon, also referred to as 'gas adsorption', was applied to examine microstructure of a porous media. Under certain ambient condition, the adsorbed gas molecule on solid surface started from monolayer to multilayer, and finally filled the entire porous space which formed capillary condensation. Basic assumptions were made to apply this phenomenon on pore structure characterization.

- (1) Gas molecule was not reactive with the solid and evenly distributed on surface of the porous media;
- (2) The dimension of the pore to be measured was large comparing to gas molecule;
- (3) The porous space was assumed cylindrical in geometry for the calculation of pore size distribution.

The adsorbed gas volume versus relative pressure  $(P/P_0)$  presented the adsorption isotherm. Commonly the isotherm curve contained two branches corresponding to adsorption and desorption process. The isotherm had been studied in regard to various materials and types (Rouquerol et al., 2013; Lowell and Shields, 2013).

Extensive studies were available on interpretation of adsorption isotherm. Based on different assumptions various analysis methods were developed regarding different parameters. The pore size was calculated from relative pressure according to Kelvin equation assuming monolayer of gas molecule (<u>Thomson, 1872</u>). It was only applicable on small pores with diameter less than 50 nm (<u>Diamond, 1971</u>). For extremely small pores, however, Kelvin equation was also reported limited applicability when the diameter dropped in the range smaller than 3 ~ 4 nm (<u>Kadlec and Dubinin, 1969</u>).

The pore size distribution was usually determined through Barrett-Joyner-Halenda (BJH) method based on capillary condensation measurements. The desorption branch, instead of adsorption branch, was more commonly used for the calculation since it was closer to thermodynamic equilibrium (Aligizaki, 2005). Details on the application of BJH method were discussed elsewhere (Juenger and Jennings, 2001).

Another important parameter acquired from gas adsorption experiment was specific surface area. The commonly used calculation method was to determine the volume of adsorbed gas molecules regarding the monomolecular layer. The Langmuir theory was firstly applied for the calculation based on monolayer assumption (Langmuir, 1916; Langmuir, 1918). The Langmuir theory was also introduced in analysis of cement-based materials using nitrogen gas and water vapor (Aligizaki, 2005). Nevertheless, gas molecules were found more inclined to pile up to form multilayer instead of single layer. Therefore Brunauer-Emmett-Teller (BET) theory was developed on the assumption of multilayer which appeared more realistic (Brunauer et al., 1938). Pitfalls and limits were summarized in detail by other work (Groen et al., 2003).

# 2.3.7. Comparison of various characterization methods

Mercury intrusion porosimetry was commonly used combining nitrogen adsorption in cement-based materials. Extensive research was conducted on comparison between the two methods (Zhang et al., 2013). Due to the different applicable range, MIP was usually measured higher porosity than nitrogen adsorption (Day and Marsh, 1988). The surface area was observed well correlation between MIP and nitrogen adsorption (Rootare and Prenzlow, 1967; Giesche, 2006). It was reported that desorption branch of nitrogen adsorption isotherm was closer to mercury intrusion curve and could be used equivalently to each other (Murray et al., 1999).

The ink-bottle effect remained of the most concerns on MIP results. MIP was combined with visualized characterization methods to acquire fully understanding of the realistic porous structure. The visualized methods, such as Backscattered electron (BSE) imaging (Scrivener, 2004) and Secondary electron microscopy (SEM), provided pore shape information (Lange et al., 1994) which was more realistic comparing to the interconnectivity measured by MIP (Igarashi et al., 2005).

Nuclear Magnetic Resonance (NMR) was another characterizing method on pore structure (Jehng et al., 1996) based on the phenomenon of nuclear magnetism (McDonald et al., 2005). The spin-spin relaxation was measured as an indirect indicator of specific surface area of C-S-H gel (Halperin et al., 1994). Comparison between NMR and conventional methods including mercury intrusion and nitrogen gas adsorption was illustrated in past work in detail (Faure et al., 2012).

The development of nanotechnology introduced non-destructive methods with higher accuracy on micropores characterization in cement-based materials. Modern techniques with nanotechnology include Small-angle neutron scattering (SANS), Atomic force microscopy (AFM), Quasi-elastic neutron scattering (QENS), and Nuclear resonance reaction analysis (NRRA) etc. (Jennings et al., 2007). Review of nanotechnology application on concrete could be found elsewhere (Sanchez and Sobolev, 2010; Bossa et al., 2015).

### 2.4. CORROSION

Corrosion of steel reinforcement in concrete structure were extensively studied in decades. It was widely accepted that rebar corrosion was attributed to two factors during the service life of reinforced concrete: chloride ingress and atmospheric carbonation. The two mechanisms might exist together causing more severe deterioration of steel rebar (Lee et al., 2013). Rebar subjected to corrosion lost sufficient bond with concrete and cross section was reduced in the meanwhile (Cabrera, 1996). The expansion in volume might also lead to cracking in concrete (Chen and Mahadevan, 2008). Performance of concrete, especially permeability, played a critical role in corrosion deterioration of reinforced concrete structure.

### 2.4.1. Chloride-induced corrosion

With presence of sufficient moist and oxygen, corrosion initialized as the ambient chloride content exceeded the threshold concentration (<u>Broomfield</u>, 2002). The threshold value was found to vary with the alkalinity of pore solution. Higher pH in pore solution required higher chloride concentration for steel depassivation to take place (<u>Glass and Buenfeld</u>, 1997). The concentration ratio of chloride and hydroxyl ions [Cl<sup>-</sup>]/[OH<sup>-</sup>] was used as indicator for evaluation of corrosion initialization (<u>Angst et al.</u>, 2009). It was also reported that the threshold [Cl<sup>-</sup>]/[OH<sup>-</sup>] increased as pH became higher (<u>Li and Sagues</u>, 2001).

The existence of chloride in concrete was attributed to two primary sources: internal contamination and external ingress. Chloride in the former was basically from the raw materials or water used for the mixture. The chloride ingress, however, was mainly dependent on permeability of the hardened concrete.

Chloride in cement-based materials existed in two types: binding state and free state. Commonly only free chloride, instead of total amount, was directly related to steel corrosion (Glass and Buenfeld, 2000). The content of free chloride varied according to pH, tricalcium aluminate (C<sub>3</sub>A) content and physical structure of hardened paste (Rasheeduzzafar, 1992; Arya and Xu, 1995). Different experimental methods were developed as to the measurements for individual type.

### 2.4.2. Carbonation-induced corrosion

Pore solution of hydrated cement was highly alkaline allowing the passivation film on steel surface remaining stable. During concrete service life, atmospheric carbon dioxide reacted with hydration products (mainly calcium hydroxide and C-S-H). Consequently pH reduced in the pore solution (Tuutti, 1982). The threshold value of pore solution pH from past studies was summarized in Table 2.1. Besides the depassivation due to carbonation, the loss of alkalinity in pore solution also reduced the threshold for chloride-induced corrosion, which led to more severe situation for corrosion deterioration (Neville, 1995a).

Table 2.1. pH threshold of carbonation corrosion

Reference	pH threshold	Details	
(Ahmad, 2003; Berkeley and	9.5	Corrosion commencement	
Pathmanaban, 1990)	8	Passive film disappears	
	below 7	Catastrophic corrosion occurs	
( <u>Parrott, 1990</u> )	11	Corrosion initiates	
( <u>Jung et al., 2003</u> )	11~11.5	Corrosion occurs	
(Bertolini et al., 2013)	9	Depassivation	
(Krajei and Janotka, 2000)	11.5	Corrosion initiates	
( <u>Böhni, 2005</u> )	11	Corrosion initiates	

### **2.5. SUMMARY**

Literature review on topics related to this thesis was briefly summarized. It involved state-of-art, theoretical basis and experimental techniques to be used in this research. According to this review it was recognized that there were still technical challenges for promoting the early carbonation technology to wider application in

reinforced concrete production. Four tasks were proposed and the thesis was composed of four major chapters dealing with the challenges.

- (1) Task 1 was to develop the carbonation process for wet-mix concrete. As the most used type of precast products, wet-mix concrete was intentionally designed sufficient workability and viscosity. Unlike dry-mix, research on processing of wet-mix concrete was scarce. Primary challenge located on the extra liquid, either as water or as chemical admixture, which impeded penetration of carbon dioxide gas.
- (2) Task 2 was to examine early carbonation curing on concrete incorporated with supplementary cementitious materials (SCMs). Modern concrete were using increasing amount of SCMs such as fly ash, slag and silica fume to improve the performance. Since pozzolanic reaction might be competing with carbonation reaction it was necessary to elucidate their interaction as well as the resulted effect on both short and long term performance.
- (3) Task 3 was to study the pore structure which affected concrete performance in vast means. The improved durability of carbonated concrete was also to be interpreted from the prospect of physical pore structure.
- (4) Task 4 was to investigate the corrosion potential due to chloride attack. Instead of accelerated tests which remained controversial, natural simulations of service environment for reinforced concrete were to be conducted.

These four tasks were intended to address the primary concerns on the suitability of early carbonation process in the following individual chapters.

### REFERENCES

- AHMAD, S. 2003. Reinforcement corrosion in concrete structures, its monitoring and service life prediction—a review. *Cement and Concrete Composites*, 25, 459-471.
- ALIGIZAKI, K. K. 2005. Pore structure of cement-based materials: testing, interpretation and requirements, CRC Press.
- ANGST, U., ELSENER, B., LARSEN, C. K. & VENNESLAND, Ø. 2009. Critical chloride content in reinforced concrete—a review. *Cement and Concrete Research*, 39, 1122-1138.
- ANSTICE, D., PAGE, C. & PAGE, M. 2005. The pore solution phase of carbonated cement pastes. *Cement and Concrete Research*, 35, 377-383.
- ARANDIGOYEN, M., BICER-SIMSIR, B., ALVAREZ, J. I. & LANGE, D. A. 2006. Variation of microstructure with carbonation in lime and blended pastes. *Applied surface science*, 252, 7562-7571.
- ARYA, C. & XU, Y. 1995. Effect of cement type on chloride binding and corrosion of steel in concrete. *Cement and Concrete Research*, 25, 893-902.
- BEAUDOIN, J., FELDMAN, R. & TUMIDAJSKI, P. 1994. Pore structure of hardened Portland cement pastes and its influence on properties. *Advanced Cement Based Materials*, 1, 224-236.
- BEAUDOIN, J. J. 1979. Porosity measurement of some hydrated cementitious systems by high pressure mercury intrusion-microstructural limitations. *Cement and Concrete Research*, 9, 771-781.
- BERGER, R., YOUNG, J. & LEUNG, K. 1972. Acceleration of hydration of calcium silicates by carbon dioxide treatment. *Nature*, 240, 16-18.
- BERKELEY, K. & PATHMANABAN, S. 1990. Cathodic protection of reinforcement steel in concrete.
- BERRY, E. & MALHOTRA, V. M. Fly ash for use in concrete-a critical review. ACI Journal Proceedings, 1980. ACI.

- BERTOLINI, L., ELSENER, B., PEDEFERRI, P., REDAELLI, E. & POLDER, R. B. 2013. Corrosion of steel in concrete: prevention, diagnosis, repair, John Wiley & Sons.
- BIJEN, J. 1996. Benefits of slag and fly ash. Construction and Building Materials, 10, 309-314.
- BÖHNI, H. 2005. Corrosion in reinforced concrete structures, Elsevier.
- BOSSA, N., CHAURAND, P., VICENTE, J., BORSCHNECK, D., LEVARD, C., AGUERRE-CHARIOL, O. & ROSE, J. 2015. Micro-and nano-X-ray computed-tomography: A step forward in the characterization of the pore network of a leached cement paste. *Cement and Concrete Research*, 67, 138-147.
- BROOMFIELD, J. P. 2002. Corrosion of steel in concrete: understanding, investigation and repair, CRC Press.
- BRUNAUER, S., EMMETT, P. H. & TELLER, E. 1938. Adsorption of gases in multimolecular layers. *Journal of the American chemical society*, 60, 309-319.
- CABRERA, J. 1996. Deterioration of concrete due to reinforcement steel corrosion. *Cement and concrete composites*, 18, 47-59.
- CASTRO, P., MORENO, E. & GENESCÁ, J. 2000. Influence of marine micro-climates on carbonation of reinforced concrete buildings. *Cement and Concrete Research*, 30, 1565-1571.
- CHANG, C.-F. & CHEN, J.-W. 2006. The experimental investigation of concrete carbonation depth. *Cement and Concrete Research*, 36, 1760-1767.
- CHEN, D. & MAHADEVAN, S. 2008. Chloride-induced reinforcement corrosion and concrete cracking simulation. *Cement and Concrete Composites*, 30, 227-238.
- CHEN, J. J., THOMAS, J. J. & JENNINGS, H. M. 2006. Decalcification shrinkage of cement paste. *Cement and concrete research*, 36, 801-809.
- CHEN, X. & WU, S. 2013. Influence of water-to-cement ratio and curing period on pore structure of cement mortar. *Construction and Building Materials*, 38, 804-812.
- CHINDAPRASIRT, P., JATURAPITAKKUL, C. & SINSIRI, T. 2005. Effect of fly ash fineness on compressive strength and pore size of blended cement paste. *Cement and Concrete Composites*, 27, 425-428.

- CIZER, Ö., VAN BALEN, K., ELSEN, J. & VAN GEMERT, D. Crystal morphology of the precipitated calcite crystals from accelerated carbonation of lime binders. 2nd International Conference on Accelerated Carbonation for Environmental and Materials Engineering, 2008. University of Rome" La Sapienza", 149-158.
- COLLINS, F. & SANJAYAN, J. 1999. Workability and mechanical properties of alkali activated slag concrete. *Cement and concrete research*, 29, 455-458.
- COOK, R. A. & HOVER, K. C. 1993. Mercury porosimetry of cement-based materials and associated correction factors. *Construction and Building Materials*, 7, 231-240.
- COOK, R. A. & HOVER, K. C. 1999. Mercury porosimetry of hardened cement pastes. *Cement and Concrete research*, 29, 933-943.
- DAY, R. 1981. Reactions between methanol and Portland cement paste. *Cement and Concrete Research*, 11, 341-349.
- DAY, R. L. & MARSH, B. K. 1988. Measurement of porosity in blended cement pastes. *Cement and Concrete Research*, 18, 63-73.
- DIAMOND, S. 1971. A critical comparison of mercury porosimetry and capillary condensation pore size distributions of portland cement pastes. *Cement and concrete research*, 1, 531-545.
- DIAMOND, S. 2000. Mercury porosimetry: an inappropriate method for the measurement of pore size distributions in cement-based materials. *Cement and concrete research*, 30, 1517-1525.
- DO, Q., BISHNOI, S. & SCRIVENER, K. 2013. Numerical simulation of porosity in cements. *Transport in porous media*, 99, 101-117.
- DOTTO, J., DE ABREU, A., DAL MOLIN, D. & MÜLLER, I. 2004. Influence of silica fume addition on concretes physical properties and on corrosion behaviour of reinforcement bars. *cement and concrete composites*, 26, 31-39.
- DU, L. & FOLLIARD, K. J. 2005. Mechanisms of air entrainment in concrete. *Cement and concrete research*, 35, 1463-1471.
- DUBININ, M. 1960. The potential theory of adsorption of gases and vapors for adsorbents with energetically nonuniform surfaces. *Chemical Reviews*, 60, 235-241.

- DUVAL, R. & KADRI, E. 1998. Influence of silica fume on the workability and the compressive strength of high-performance concretes. *Cement and concrete Research*, 28, 533-547.
- EL-HASSAN, H., SHAO, Y. & GHOULEH, Z. 2013. Effect of initial curing on carbonation of lightweight concrete masonry units. *ACI Materials Journal*, 110, 441-450.
- EVERETT, D. 1972. Manual of symbols and terminology for physicochemical quantities and units, appendix II: Definitions, terminology and symbols in colloid and surface chemistry. *Pure and Applied Chemistry*, 31, 577-638.
- FAURE, P. F., CARÉ, S., MAGAT, J. & CHAUSSADENT, T. 2012. Drying effect on cement paste porosity at early age observed by NMR methods. *Construction and Building materials*, 29, 496-503.
- FELDMAN, R. F. & BEAUDOIN, J. J. 1991. Pretreatment of hardened hydrated cement pastes for mercury intrusion measurements. *Cement and Concrete Research*, 21, 297-308.
- GALLÉ, C. 2001. Effect of drying on cement-based materials pore structure as identified by mercury intrusion porosimetry: a comparative study between oven-, vacuum-, and freezedrying. *Cement and Concrete Research*, 31, 1467-1477.
- GIESCHE, H. 2006. Mercury porosimetry: a general (practical) overview. *Particle & particle systems characterization*, 23, 9-19.
- GLASS, G. & BUENFELD, N. 1997. The presentation of the chloride threshold level for corrosion of steel in concrete. *Corrosion Science*, 39, 1001-1013.
- GLASS, G. & BUENFELD, N. 2000. The influence of chloride binding on the chloride induced corrosion risk in reinforced concrete. *Corrosion Science*, 42, 329-344.
- GOODBRAKE, C. J., YOUNG, J. F. & BERGER, R. L. 1979. Reaction of Beta-Dicalcium Silicate and Tricalcium Silicate with Carbon Dioxide and Water Vapor. *Journal of the American Ceramic Society*, 62, 168-171.
- GOTO, S., SUENAGA, K., KADO, T. & FUKUHARA, M. 1995. Calcium silicate carbonation products. *Journal of the American Ceramic Society*, 78, 2867-2872.
- GROEN, J. C., PEFFER, L. A. & PÉREZ-RAMÍREZ, J. 2003. Pore size determination in modified micro-and mesoporous materials. Pitfalls and limitations in gas adsorption data analysis. *Microporous and Mesoporous Materials*, 60, 1-17.

- GROVES, G. W., BROUGH, A., RICHARDSON, I. G. & DOBSON, C. M. 1991. Progressive changes in the structure of hardened C3S cement pastes due to carbonation. *Journal of the American Ceramic Society*, 74, 2891-2896.
- HAGYMASSY, J., ODLER, I., YUDENFREUND, M., SKALNY, J. & BRUNAUER, S. 1972. Pore structure analysis by water vapor adsorption. III. Analysis of hydrated calcium silicates and portland cements. *Journal of Colloid and Interface Science*, 38, 20-34.
- HALAMICKOVA, P., DETWILER, R. J., BENTZ, D. P. & GARBOCZI, E. J. 1995. Water permeability and chloride ion diffusion in Portland cement mortars: relationship to sand content and critical pore diameter. *Cement and Concrete Research*, 25, 790-802.
- HALPERIN, W. P., JEHNG, J.-Y. & SONG, Y.-Q. 1994. Application of spin-spin relaxation to measurement of surface area and pore size distributions in a hydrating cement paste. *Magnetic Resonance Imaging*, 12, 169-173.
- HEARN, N. & HOOTON, R. 1992. Sample mass and dimension effects on mercury intrusion porosimetry results. *Cement and concrete research*, 22, 970-980.
- IGARASHI, S.-I., WATANABE, A. & KAWAMURA, M. 2005. Evaluation of capillary pore size characteristics in high-strength concrete at early ages. *Cement and Concrete Research*, 35, 513-519.
- JEHNG, J.-Y., SPRAGUE, D. & HALPERIN, W. 1996. Pore structure of hydrating cement paste by magnetic resonance relaxation analysis and freezing. *Magnetic Resonance Imaging*, 14, 785-791.
- JENNINGS, H., DALGLEISH, B. & PRATT, P. 1981. Morphological development of hydrating tricalcium silicate as examined by electron microscopy techniques. *Journal of the American Ceramic Society*, 64, 567-572.
- JENNINGS, H. M. 2000. A model for the microstructure of calcium silicate hydrate in cement paste. *Cement and Concrete Research*, 30, 101-116.
- JENNINGS, H. M. & TENNIS, P. D. 1994. Model for the developing microstructure in Portland cement pastes. *Journal of the American Ceramic Society*, 77, 3161-3172.

- JENNINGS, H. M., THOMAS, J. J., GEVRENOV, J. S., CONSTANTINIDES, G. & ULM, F.-J. 2007. A multi-technique investigation of the nanoporosity of cement paste. *Cement and Concrete Research*, 37, 329-336.
- JUENGER, M. C. G. & JENNINGS, H. M. 2001. The use of nitrogen adsorption to assess the microstructure of cement paste. *Cement and Concrete Research*, 31, 883-892.
- JUNG, W.-Y., YOON, Y.-S. & SOHN, Y.-M. 2003. Predicting the remaining service life of land concrete by steel corrosion. *Cement and concrete research*, 33, 663-677.
- JUSTNES, H., MELAND, I., BJOERGUM, J., KRANE, J. & SKJETNE, T. 1990. Nuclear magnetic resonance (NMR)—a powerful tool in cement and concrete research. *Advances in Cement Research*, 3, 105-110.
- KADLEC, O. & DUBININ, M. 1969. Comments on the limits of applicability of the mechanism of capillary condensation. *Journal of Colloid and Interface Science*, 31, 479-489.
- KAUFMANN, J., LOSER, R. & LEEMANN, A. 2009. Analysis of cement-bonded materials by multi-cycle mercury intrusion and nitrogen sorption. *Journal of colloid and interface science*, 336, 730-737.
- KJELLSEN, K. O., DETWILER, R. J. & GJØRV, O. E. 1990. Pore structure of plain cement pastes hydrated at different temperatures. *Cement and concrete research*, 20, 927-933.
- KLIEGER, P. 1994. Significance of tests and properties of concrete and concrete-making materials, ASTM International.
- KOBAYASHI, K., SUZUKI, K. & UNO, Y. 1994. Carbonation of concrete structures and decomposition of C-S-H. *Cement and Concrete Research*, 24, 55-61.
- KONECNY, L. & NAQVI, S. 1993. The effect of different drying techniques on the pore size distribution of blended cement mortars. *Cement and concrete research*, 23, 1223-1228.
- KRAJEI, L. & JANOTKA, I. 2000. Measurement techniques for rapid assessment of carbonation in concrete. *ACI Materials Journal*, 97.
- LAM, L., WONG, Y. & POON, C. 2000. Degree of hydration and gel/space ratio of high-volume fly ash/cement systems. *Cement and Concrete Research*, 30, 747-756.

- LANGE, D. A., JENNINGS, H. M. & SHAH, S. P. 1994. Image analysis techniques for characterization of pore structure of cement-based materials. *Cement and Concrete Research*, 24, 841-853.
- LANGMUIR, I. 1916. THE CONSTITUTION AND FUNDAMENTAL PROPERTIES OF SOLIDS AND LIQUIDS. PART I. SOLIDS. *Journal of the American Chemical Society*, 38, 2221-2295.
- LANGMUIR, I. 1918. The adsorption of gases on plane surfaces of glass, mica and platinum. *Journal of the American Chemical society*, 40, 1361-1403.
- LAWRENCE, R. M., MAYS, T. J., RIGBY, S. P., WALKER, P. & D'AYALA, D. 2007. Effects of carbonation on the pore structure of non-hydraulic lime mortars. *Cement and Concrete Research*, 37, 1059-1069.
- LEE, M. K., JUNG, S. H. & OH, B. H. 2013. Effects of carbonation on chloride penetration in concrete. *ACI Materials Journal*, 110.
- LI, D., CHEN, Y., SHEN, J., SU, J. & WU, X. 2000. The influence of alkalinity on activation and microstructure of fly ash. *Cement and Concrete Research*, 30, 881-886.
- LI, L. & SAGUES, A. 2001. Chloride corrosion threshold of reinforcing steel in alkaline solutions-Open-circuit immersion tests. *Corrosion*, 57, 19-28.
- LIABASTRE, A. A. & ORR, C. 1978. An evaluation of pore structure by mercury penetration. *Journal of Colloid and Interface Science*, 64, 1-18.
- LIU, Z. & WINSLOW, D. 1995. Sub-distributions of pore size: a new approach to correlate pore structure with permeability. *Cement and concrete research*, 25, 769-778.
- LOWELL, S. 1980. Continuous scan mercury porosimetry and the pore potential as a factor in porosimetry hysteresis. *Powder Technology*, 25, 37-43.
- LOWELL, S. & SHIELDS, J. E. 2013. *Powder surface area and porosity*, Springer Science & Business Media.
- MAZLOOM, M., RAMEZANIANPOUR, A. & BROOKS, J. 2004. Effect of silica fume on mechanical properties of high-strength concrete. *Cement and Concrete Composites*, 26, 347-357.

- MCDONALD, P., KORB, J.-P., MITCHELL, J. & MONTEILHET, L. 2005. Surface relaxation and chemical exchange in hydrating cement pastes: a two-dimensional NMR relaxation study. *Physical Review E*, 72, 011409.
- MEHTA, P. & GJØRV, O. 1982. Properties of portland cement concrete containing fly ash and condensed silica-fume. *Cement and Concrete Research*, 12, 587-595.
- MEHTA, P. K. 1986. Concrete. Structure, properties and materials, Prentice-Hall.
- MIKHAIL, R. S., COPELAND, L. E. & BRUNAUER, S. 1964. Pore structures and surface areas of hardened Portland cement pastes by nitrogen adsorption. *Canadian Journal of Chemistry*, 42, 426-438.
- MONKMAN, S. & SHAO, Y. 2009. Carbonation curing of slag-cement concrete for binding CO<sub>2</sub> and improving performance. *Journal of Materials in Civil Engineering*, 22, 296-304.
- MONKMAN, S. & SHAO, Y. 2010. Integration of carbon sequestration into curing process of precast concrete. *Canadian Journal of Civil Engineering*, 37, 302-310.
- MOOREHEAD, D. 1986. Cementation by the carbonation of hydrated lime. *Cement and Concrete Research*, 16, 700-708.
- MORANDEAU, A., THIERY, M. & DANGLA, P. 2014. Investigation of the carbonation mechanism of CH and C-S-H in terms of kinetics, microstructure changes and moisture properties. *Cement and Concrete Research*, 56, 153-170.
- MORO, F. & BÖHNI, H. 2002. Ink-bottle effect in mercury intrusion porosimetry of cement-based materials. *Journal of Colloid and Interface Science*, 246, 135-149.
- MORSE, J. W., ARVIDSON, R. S. & LÜTTGE, A. 2007. Calcium carbonate formation and dissolution. *Chemical reviews*, 107, 342-381.
- MURRAY, K., SEATON, N. & DAY, M. 1999. Use of mercury intrusion data, combined with nitrogen adsorption measurements, as a probe of pore network connectivity. *Langmuir*, 15, 8155-8160.
- NAVI, P. & PIGNAT, C. 1999. Three-dimensional characterization of the pore structure of a simulated cement paste. *Cement and Concrete Research*, 29, 507-514.

- NEVILLE, A. 1995a. Chloride attack of reinforced concrete: an overview. *Materials and Structures*, 28, 63-70.
- NEVILLE, A. M. 1995b. Properties of concrete, Longman Group UK Limited.
- NGALA, V. & PAGE, C. 1997. Effects of carbonation on pore structure and diffusional properties of hydrated cement pastes. *Cement and Concrete Research*, 27, 995-1007.
- NISHIKAWA, T., SUZUKI, K., ITO, S., SATO, K. & TAKEBE, T. 1992. Decomposition of synthesized ettringite by carbonation. *Cement and Concrete Research*, 22, 6-14.
- NYAME, B. & ILLSTON, J. 1981. Relationships between permeability and pore structure of hardened cement paste. *Magazine of Concrete Research*, 33, 139-146.
- ODLER, I. & RÖßLER, M. 1985. Investigations on the relationship between porosity, structure and strength of hydrated Portland cement pastes. II. Effect of pore structure and of degree of hydration. *Cement and Concrete Research*, 15, 401-410.
- OSBORNE, G. 1999. Durability of Portland blast-furnace slag cement concrete. *Cement and Concrete Composites*, 21, 11-21.
- PAL, S., MUKHERJEE, A. & PATHAK, S. 2003. Investigation of hydraulic activity of ground granulated blast furnace slag in concrete. *Cement and Concrete Research*, 33, 1481-1486.
- PARROTT, L. 1990. Damage caused by carbonation of reinforced concrete. *Materials and Structures*, 23, 230-234.
- PERSSON, B. 1998. Experimental studies on shrinkage of high-performance concrete. *Cement and Concrete Research*, 28, 1023-1036.
- POON, C., LAM, L. & WONG, Y. 2000. A study on high strength concrete prepared with large volumes of low calcium fly ash. *Cement and Concrete Research*, 30, 447-455.
- POON, C., WONG, Y. & LAM, L. 1997. The influence of different curing conditions on he pore structure and related properties of fly-ash cement pastes and mortars. *Construction and Building Materials*, 11, 383-393.
- POWERS, T. C. 1958. Structure and physical properties of hardened Portland cement paste. *Journal of the American Ceramic Society*, 41, 1-6.

- POWERS, T. C. & BROWNYARD, T. L. Studies of the physical properties of hardened Portland cement paste. ACI Journal Proceedings, 1946. ACI.
- RAMEZANIANPOUR, A. & MALHOTRA, V. 1995. Effect of curing on the compressive strength, resistance to chloride-ion penetration and porosity of concretes incorporating slag, fly ash or silica fume. *Cement and concrete composites*, 17, 125-133.
- RASHEEDUZZAFAR 1992. Influence of cement composition on concrete durability. *ACI Materials Journal*, 89.
- RITTER, H. & DRAKE, L. 1945. Pressure porosimeter and determination of complete macropore-size distributions. Pressure porosimeter and determination of complete macropore-size distributions. *Industrial & Engineering Chemistry Analytical Edition*, 17, 782-786.
- ROOTARE, H. M. & PRENZLOW, C. F. 1967. Surface areas from mercury porosimeter measurements. *The Journal of physical chemistry*, 71, 2733-2736.
- ROSTAMI, V., SHAO, Y. & BOYD, A. J. 2011a. Carbonation curing versus steam curing for precast concrete production. *Journal of Materials in Civil Engineering*, 24, 1221-1229.
- ROSTAMI, V., SHAO, Y. & BOYD, A. J. 2011b. Durability of concrete pipes subjected to combined steam and carbonation curing. *Construction and Building Materials*, 25, 3345-3355.
- ROUQUEROL, J., ROUQUEROL, F., LLEWELLYN, P., MAURIN, G. & SING, K. S. 2013.

  Adsorption by powders and porous solids: principles, methodology and applications,

  Academic press.
- SABIR, B. 1997. Mechanical properties and frost resistance of silica fume concrete. *Cement and Concrete Composites*, 19, 285-294.
- SANCHEZ, F. & SOBOLEV, K. 2010. Nanotechnology in concrete—a review. *Construction and Building Materials*, 24, 2060-2071.
- SCRIVENER, K. L. 2004. Backscattered electron imaging of cementitious microstructures: understanding and quantification. *Cement and Concrete Composites*, 26, 935-945.
- SETZER, M. & WITTMANN, F. 1974. Surface energy and mechanical behaviour of hardened cement paste. *Applied physics*, 3, 403-409.

- SUN, Z. & SCHERER, G. W. 2010. Effect of air voids on salt scaling and internal freezing. *Cement and Concrete Research*, 40, 260-270.
- TAYLOR, H. F. W. & TURNER, A. 1987. Reactions of tricalcium silicate paste with organic liquids. *Cement and Concrete Research*, 17, 613-623.
- TENNIS, P. D. & JENNINGS, H. M. 2000. A model for two types of calcium silicate hydrate in the microstructure of Portland cement pastes. *Cement and Concrete Research*, 30, 855-863.
- THOMAS, M. 1989. The suitability of solvent exchange techniques for studying the pore structure of hardened cement paste. *Advances in Cement Research*, 2, 29-34.
- THOMSON, W. 1872. On the Equilibrium of Vapour at a Curved Surface of Liquid. *Proceedings* of the Royal Society of Edinburgh, 7, 63-68.
- TOUTANJI, H., DELATTE, N., AGGOUN, S., DUVAL, R. & DANSON, A. 2004. Effect of supplementary cementitious materials on the compressive strength and durability of short-term cured concrete. *Cement and Concrete Research*, 34, 311-319.
- TUUTTI, K. 1982. Corrosion of steel in concrete. Swedish Cement and Concrete Institute.
- VENHUIS, M. A. & REARDON, E. J. 2001. Vacuum method for carbonation of cementitious wasteforms. *Environmental science & technology*, 35, 4120-4125.
- VILLAIN, G., THIERY, M. & PLATRET, G. 2007. Measurement methods of carbonation profiles in concrete: thermogravimetry, chemical analysis and gammadensimetry. *Cement and Concrete Research*, 37, 1182-1192.
- WASHBURN, E. W. 1921. Note on a method of determining the distribution of pore sizes in a porous material. *Proceedings of the National Academy of Sciences of the United States of America*, 115-116.
- WINSLOW, D. & LIU, D. 1990. The pore structure of paste in concrete. *Cement and concrete research*, 20, 227-235.
- WINSLOW, D. N., COHEN, M. D., BENTZ, D. P., SNYDER, K. A. & GARBOCZI, E. J. 1994.

  Percolation and pore structure in mortars and concrete. *Cement and concrete research*,
  24, 25-37.

- WINSLOW, D. N. & DIAMOND, S. 1970. A MERCURY POROSIMETRY STUDY OF THE POROSITY IN PORTLAND CEMENT. *Journal of Materials*, 5, 564-585.
- WITTMANN, F. 1973. Interaction of hardened cement paste and water. *Journal of the American ceramic society*, 56, 409-415.
- YOUNG, J. 1988. Review of the Pore Structure of Cement Paste and Concrete and its Influence on Permeability. *ACI Special Publication*, 108.
- YOUNG, J., BERGER, R. & BREESE, J. 1974. Accelerated curing of compacted calcium silicate mortars on exposure to CO<sub>2</sub>. *Journal of the american ceramic society*, 57, 394-397.
- ZENG, Q., LI, K., FEN-CHONG, T. & DANGLA, P. 2012. Pore structure characterization of cement pastes blended with high-volume fly-ash. *Cement and Concrete Research*, 42, 194-204.
- ZHANG, Q., YE, G. & KOENDERS, E. 2013. Investigation of the structure of heated Portland cement paste by using various techniques. *Construction and Building Materials*, 38, 1040-1050.

# **CHAPTER 3**

\_

### EARLY AGE CARBONATION CURING FOR PRECAST REINFORCED CONCRETES

#### **PREFACE**

This chapter presented experimental study on unique process developed for early age carbonation curing of precast reinforced concrete to maximize performance improvement and utilization capacity of carbon dioxide. The process included vibration casting, in-mold curing, off-mold preconditioning, carbonation curing and subsequent hydration. It was found that carbon dioxide uptake of 16% based on cement content could reduce concrete pH to 9.2 on surface and maintain pH of 13.0 at core immediately after 12 hours carbonation. The subsequent hydration was able to increase the pH on surface to over 12.3 as comparable to hydration reference. The carbonated concrete showed enhanced resistance to permeation by forming denser surface with higher electrical resistivity. The off-mold preconditioning in open air measured no shrinkage cracking owing to the controlled evaporation rate. The process created concrete sandwich structure with carbonate-rich surface which was responsible for strength gain, carbon dioxide utilization and durability enhancement and was proved suitable for precast reinforced concrete production.

# 3.1. Introduction

Precast concrete accounted for 20-30% of total concrete market including both dry- and wet-mix products (Glass et al., 2000). The dry-mix concretes, such as concrete blocks, pavers and hollow core slabs, were of typical zero-slump mixture with low cement content. They were consolidated by special vibration compaction and were able to be demolded immediately after casting. Wet-mix concretes constituted the majority of precast products which were formed using superplasticizer and internal vibrator. The wet-mix concretes usually required several hours proper curing before the mold removed.

Recent research showed that dry-mix concrete could be treated with carbonation curing at early age for accelerated strength gain and improved durability (Rostami et al., 2011b). Carbonation curing were applied successfully to production of concrete masonry unit (El-Hassan et al., 2013a) and hollow core slab (Shao and Morshed, 2015). However, early age carbonation curing of wet-mix concrete was not investigated. The challenge was the wet-mix concrete contained higher liquid including water and superplasticizer which might impede penetration of carbon dioxide. In addition, the wet-mix concretes were usually reinforced with steel bars. There was concern on the reduction of alkalinity in concrete due to the early carbonation which was able to initiate corrosion of reinforcing steel.

Carbonation corrosion of concrete subjected to weathering carbonation was well studied. The progressive weathering carbonation took place as matured concrete reacted with atmospheric carbon dioxide. The progressive reaction reduced pH value of concrete and was detrimental to the long term performance. It was believed that steel remained in

passive state in alkaline environment provided by concrete pore solution. Reduction of pH to 11.0 destroyed passivation film on steel surface and thus initiated corrosion (Tuutti, 1982). Transition from passive to active corrosion of mild steel bars was found to happen as pH varying between 9.4 and 10 (Huet et al., 2005). It was also reported by X-ray photoelectron spectroscopy (XPS) that passivation of mild steel were achieved as pH ranged from 10 to 13 (Huet et al., 2005). The pH value of concrete became critical indicator for carbonation corrosion.

Carbonation curing at concrete early age was different from weathering carbonation. It was introduced to fresh mixture within 24 hours after casting. Therefore the subsequent hydration took place afterwards. Two approaches were reported on early age carbonation. If performed immediately after casting, the reaction occurred between C<sub>3</sub>S or C<sub>2</sub>S and carbon dioxide. The governing equations were given in Eqs. 3.1-3.2 (Young et al., 1974). Another approach was to apply the technique after a short period of initial hydration which prompted carbonation of both anhydrous (C<sub>3</sub>S and C<sub>2</sub>S) and hydrous (Ca(OH)<sub>2</sub>, C-S-H) phases. The corresponding reactions were governed by Eqs. 3.1-3.4. In either case, the reaction products were found hybrid of hydrates and carbonates. The reaction kinetics was studied through mathematical modelling (Kashef-Haghighi et al., 2015).

$$C_3S + (3-x)CO_2 + yH_2O \rightarrow C_xSH_y + (3-x)CaCO_3$$
 (3.1)

$$C_2S + (2-x)CO_2 + yH_2O \rightarrow C_xSH_y + (2-x)CaCO_3$$
 (3.2)

$$Ca(OH)_2 + CO_2 \rightarrow CaCO_3 + H_2O$$
 (3.3)

$$C-S-H + 2CO2 \rightarrow SiO2 + 2CaCO3 + H2O$$
(3.4)

Eqs. 3.1-3.4 also indicated that carbonation curing was a process of carbon uptake. Gaseous carbon dioxide was converted to solid carbonates and permanently stored in concrete for emission reduction (El-Hassan et al., 2013b). To maximize the benefits of the process and promote its application in wet-mix precast concrete with reinforcing steel, the effect of early carbonation curing on pH value of concrete should be examined. In addition, special process was needed for carbonation of wet-mix concrete with high slump.

The purpose of this study was to develop the early carbonation curing process for wet-mix precast concrete with high slump. It included in-mold hydration curing, off-mold preconditioning, carbonation curing and subsequent hydration. To maximize the reaction extent and its related carbon dioxide utilization, process parameters such as water content and carbonation duration were studied. The concrete performance was evaluated by carbon dioxide uptake, strength gain, permeability, pH distribution, weathering carbonation depth and preconditioning shrinkage.

#### 3.2. EXPERIMENTAL PROGRAM

# 3.2.1. Materials and mixture proportions

Precast concrete was proportioned for general use. Ordinary Portland Cement (OPC) and granite aggregates were chosen. The use of granite was to eliminate the effect of carbon content in aggregate on thermal analysis of concrete. The water absorption of fine and coarse aggregate was about 4.3% and 1.6%, respectively. Fineness modulus of

fine granite was 3.0 and the maximum aggregate size was 12 mm. Sieve analysis was performed and is presented in Fig. 3.1. The gradation was selected following Fuller equation for maximum packing density.

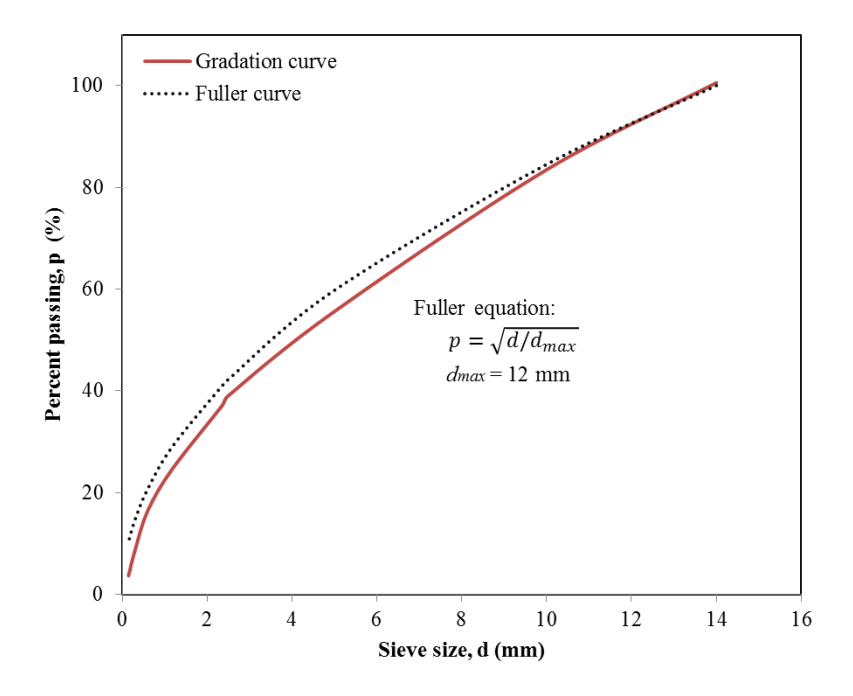


Fig. 3.1. Sieve analysis of aggregate

Two mixture proportions were examined and the details are presented in Table 3.1. Mix A was developed for carbonation with water to cement ratio (w/c) of 0.4 while Mix B was for w/c of 0.3. Mix B concrete was commonly used in high performance precast concrete (Mehta and Aietcin, 1990) such as railway crosstie production. Superplasticizer was used to achieve a slump of about 160 mm. It was intended to examine if carbonation could produce equivalent compressive strength with less cement usage. To maintain the same slump, Mix B employed three times higher dosage of superplasticizer than Mix A. Superplasticizer was provided by W. R. Grace (AVDA Cast

575). Concrete was cast in 100 mm cubes and consolidated by 30-second vibration on vibration table.

Table 3.1. Mixture proportions of concrete

	Mix A	Mix B
Cement (c), kg/m <sup>3</sup>	452	526
Water (w), kg/m³	181	158
Coarse granite, kg/m <sup>3</sup>	1060	1060
Fine granite, kg/m <sup>3</sup>	680	680
Concrete, kg/m³	2375	2431
Superplasticizer (sp), mL/m <sup>3</sup>	2055	7173
w/c	0.4	0.3
SP/c, %	0.5	1.5
Slump, mm	158	151

## 3.2.2. Carbonation curing procedure

Carbonation procedure was established for wet-mix concrete. Four steps were involved as shown in Fig. 3.2: (1) in-mold curing, (2) off-mold preconditioning, (3) carbonation curing and (4) subsequent hydration.

Since wet-mix mixture presented higher slump, it was not possible to demold right after casting. Initial hydration in mold was necessary which was accomplished by Step 1. The time required for this step was dependent on mixture proportion. For Mix A and B, it took approximately 5 hours to reach initial set at ambient condition (25 °C and 60% relative humidity) in open air. This was also intended to naturally evaporate portion of the mixing water. After initial set, the four side plates were removed and samples were left on bottom plates. Off-mold preconditioning by fan drying was then performed. It was accomplished at wind speed of 1 m/s in condition of 25 °C and 50  $\pm$  5 % relative

humidity. Step 2 was critically important. The preconditioning further removed part of the free water and evacuated more space for carbon dioxide to penetrate. To remove 40% free water, it took about 5 hours. In step 3, the conditioned concrete was carbonated in pressure chamber with CO<sub>2</sub> gas of 99.8% purity and at varied durations and pressures. After carbonation, the concrete cubes were placed in moisture room (25 °C, 95% RH) for another 27 days subsequent hydration. Hydration references were prepared as well. Fwere cured in sealed mold within the first 24 hours and then demolded and further cured in the same moisture room for 27 days.

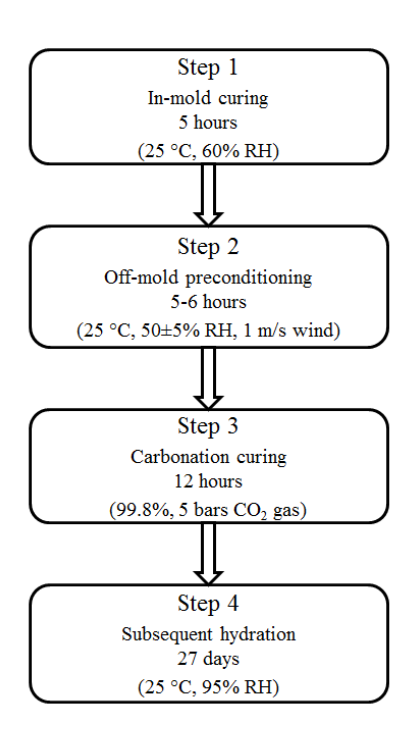


Fig. 3.2. Carbonation curing procedure for wet-mix concrete

The setup for carbonation curing is shown in Fig. 3.3. Carbon dioxide gas was injected into the chamber till constant pressure. The chamber was placed on digital

balance to obtain the CO<sub>2</sub> uptake through mass curve measurement. To enhance the degree of early carbonation for strength gain and carbon dioxide utilization, parametric study was conducted regarding the carbonation process. It included percent water removal by preconditioning, gas pressure and carbonation duration. Degree of carbonation was assessed by CO<sub>2</sub> uptake of the concrete.

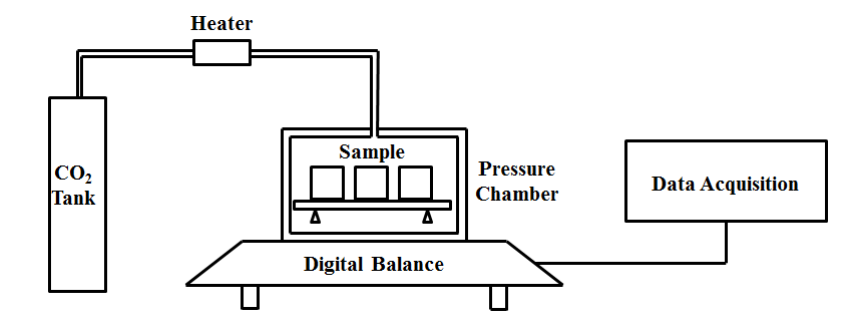


Fig. 3.3. Schematic of carbonation curing setup

# 3.2.3. CO<sub>2</sub> uptake estimation

 $CO_2$  uptake was estimated by two methods: mass gain and mass curve. The former calculated  $CO_2$  uptake in concrete by comparing mass change of samples during carbonation as shown in Eq. 3.5, in which  $m_1$  and  $m_2$  represented sample mass before and after the reaction, respectively. Carbonation-induced water loss ( $m_{\text{water}}$ ) was collected by absorbent paper and added to final mass ( $m_2$ ). By treating the system as enclosed, it was imperative to include the evaporated water, which was initially inside the samples prior to carbonation. Percent  $CO_2$  uptake was expressed with reference to the anhydrous cement mass ( $m_{\text{cement}}$ ).

$$CO_2 \text{ uptake}(\%) = \frac{m_2 + m_{water} - m_1}{m_{cement}} \times 100\%$$
 (3.5)

Mass curve method estimated the  $CO_2$  uptake through digitally recorded mass. The gas was injected to the specified pressure and the mass increase was recorded as time function. Since the pressure was maintained constantly, the increase in mass of the system was solely due to the  $CO_2$  uptake by concrete. At the end of curing at which time  $CO_2$  was released and the residual mass, M, was measured. The system was calibrated by repeating the tests using  $CO_2$ -insensitive styrofoam samples of the same volume to obtain second residual mass, m. The difference between M and m represented the  $CO_2$  mass in concrete (Eq. 3.6). Data collected by mass gain and mass curve methods were two simultaneous measurements from the same process and therefore should be comparable. They were also independent from any carbon dioxide content existing before carbonation.

$$CO_2 \text{ uptake(\%)} = \frac{M - m}{mass of cement} \times 100\%$$
(3.6)

### 3.2.4. Performance evaluation

Compressive strength test was performed on 1 day and 28 days after casting in accord to ASTM C140-03. Three samples were tested and the average was presented with deviation. To evaluate transport performance of carbonated concrete, surface resistivity measurement was conducted on the same samples. Samples in condition of saturated surface dry were measured surface resistivity through Proceq Resipod Resistivity Meter

with four probes. Electric current was induced between outer two probes and detected by inner ones for calculation of resistivity. Three measurements were taken and average was used. The microstructure of carbonated concrete was examined by scanning electron microscope (SEM) Hitachi SU3500 equipped with Energy-dispersive X-ray spectroscopy (EDS) for element analysis.

To evaluate pH values of carbonated concrete, pH meter (Extech PH110) with flat head of 6 mm in diameter was used at different depths (every 10 mm from surface). The concrete cube was split and pH measurement was carried out on the freshly exposed cross section. The measuring spot was covered by small piece of absorptive paper ( $10 \times 10$  mm) which was soaked with  $100 \, \mu$ L deionized water. Equilibrium of ions was reached in 15 minutes by diffusion mechanism (Heng and Murata, 2004). The pH probe measured pH value of the extracted pore solution through absorptive paper. PH of reference hydration concrete at different ages was in a range of 12.7 to 13.0. The advantage of using the pH meter was the non-destructive features and instant measurement at any ages.

Another method to access pH value was the phenolphthalein solution spray following RILEM approach (RILEM, 1988). It was commonly used to identify depth of carbonation. The indicator showed colorless as pH dropped below 9.5. Otherwise, purple red was observed for pH higher than 10 (Dean, 1985).

To quantify CO<sub>2</sub> content at different depth and its correlation with pH, thermal analysis was executed. Thermogravimetric analysis (TGA) was found difficult to determine CO<sub>2</sub> content because of the impact of aggregates in concrete samples. Therefore electrical furnace was employed for pyrolysis analysis of concrete collected

from different depths. Concrete samples of 100g for each were heated up to 105, 550 and 950  $^{\circ}$ C and the mass at each temperature was measured. The mass loss between 550 and 950  $^{\circ}$ C was assumed the loss of carbon dioxide due to decomposition of calcium carbonate. The CO<sub>2</sub> content was estimated by Eq. 3.7.

$$CO_2$$
 uptake (%) =  $\frac{sample\ mass\ at\ 550^{\circ}C - sample\ mass\ at\ 1000^{\circ}C}{cement\ mass\ in\ original\ sample} \times 100\%$  (3.7)

### 3.2.5. Accelerated weathering carbonation test

It was reported that carbonation curing reduced calcium hydroxide (Rostami et al., 2011a). This was usually beneficial to durability improvement such as resistance to sulphate attack and efflorescence. However, there was concern that the reduced calcium hydroxide content might promote more carbonation depth due to weathering carbonation (Papadakis et al., 1991). Therefore accelerated weathering carbonation test was conducted in the laboratory for 25 weeks' period using Mix A concrete. Both carbonation cured and hydrated concrete cubes were prepared. After initial curing and 27 days subsequent hydration, concrete cubes were coated on four sides by epoxy, leaving only two sides exposed. The epoxy coating assured one-dimensional diffusion which was used to estimate the  $CO_2$  diffusion coefficient. The concrete cubes were then placed in weathering carbonation chamber with RH of  $65 \pm 5\%$  and temperature of  $25 \pm 3$  °C.  $CO_2$  concentration was controlled within the range of  $25 \pm 5\%$ . At 10, 15. 20, 25 weeks, concrete cubes were split to expose the cross section and carbonation depth was measured by phenolphthalein indicator. Carbonation depth was defined as colorless regime and

measured within 24 hours. At least 10 measurements, 5 on each exposed side, were taken and averaged. Meanwhile, pH values on the surface and at 25 mm depth were recorded. Two samples were averaged for one measurement.

### 3.2.6. Preconditioning shrinkage of reinforced concrete beam

The preconditioning raised concern on shrinkage and cracking in concrete. It was necessary to remove certain amount of free water at fresh state to facilitate carbonation reaction. At the same time the process possibly generated shrinkage cracking, especially in restrained condition such as reinforced concrete. To assure feasibility of the developed process carbonation curing was applied on reinforced beam. The dimension of the beam was shown in Fig. 3.4. It was 800 mm in length with 100 mm square section. The optimized process parameters obtained from cube tests were applied to the beam production. The beam was cast with Mix A concrete of w/c=0.4 and weight of 19 kg. Four straight bars ( $\phi$  5 mm) and three stirrups ( $\phi$  3 mm) were used as steel reinforcement in the beam. The cover thickness was 25 mm. Vibration table was used for compaction to simulate wet-mix process. The carbonation procedure given in Fig. 3.2 was followed. After 5 hours in-mold curing, the beam was demolded and LVDT was installed to measure the shrinkage strain due to fan drying. The setup of measuring apparatus is also shown in Fig. 3.4. Two steel plates were embedded in concrete during casting as measuring spots without touching steel bars or the bottom of the mold. Distance between two measuring spots was 600 mm. LVDT was installed with a rigid bar set between the two measuring spots. Displacement was recorded by data acquisition every 10 seconds.

The beam was placed on digital balance with mass recording every 30 seconds. The preconditioning by fan drying took approximately 5 hours to reach the desired water removal. The beam was then placed in large chamber of 840 mm in depth and 660 mm in diameter for carbonation curing. Concrete surface was inspected for cracks after fan drying and carbonation curing using alcohol spray. For hairline cracks with width larger than 0.1 mm, alcohol penetrates forming dark lines. This was an easy approach to examine the cracks in large area. After carbonation, the pH values and carbon content were measured. The beam was surface water spray to compensate water loss in preconditioning and wrapped with plastic sheet for further hydration. The pH values and carbon content were measured again at 28 days. Two beams were repeated for average.

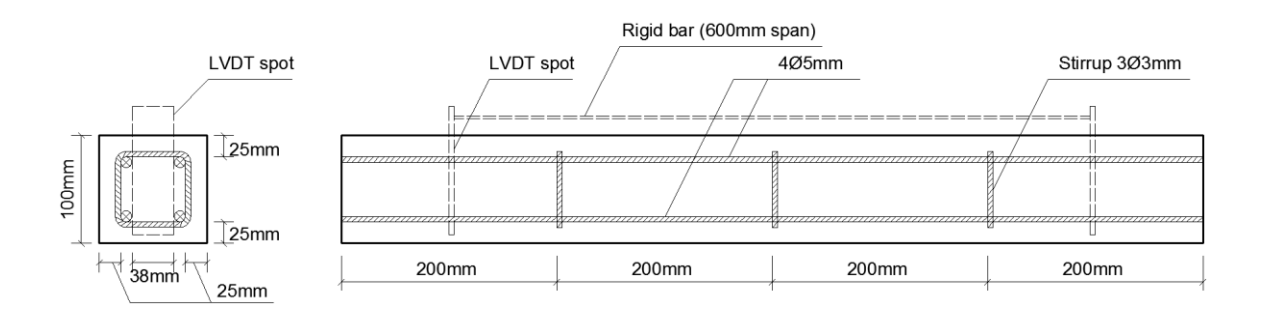


Fig. 3.4. Schematic of reinforced concrete beam

#### 3.3. RESULTS AND DISCUSSIONS

#### 3.3.1. Carbonation curing of wet-mix concrete

To maximize the extent of carbonation on wet-mix concrete, the effect of process parameters was examined. The parameters included the water removal by fan drying conditioning, the carbonation duration and carbonation pressure. They were evaluated in

terms of CO<sub>2</sub> uptake. Fig. 3.5 shows the effect of percent water removal on the CO<sub>2</sub> uptake by concrete in 30 min carbonation reaction. The preconditioning was conducted after 5 hours in-mold curing. CO<sub>2</sub> uptake was determined by mass gain method. It was apparent that the maximum uptake was observed at water removal of 40% to 45% in both concretes. This percent water removal was based on initial water content, indicating that about 40-45% of mixing water should be removed to maximize the degree of carbonation. For the w/c ratio of 0.3 and 0.4, it was accomplished by 5 hours fan drying. It seemed that too little of the water reduced carbonation efficiency since water was one of the essential reactants. Nevertheless, excessive free water stopped CO<sub>2</sub> gas penetration. For different water to cement ratios, the maximum CO<sub>2</sub> uptake appears approximately at 40% water removal, independent from w/c ratio used.

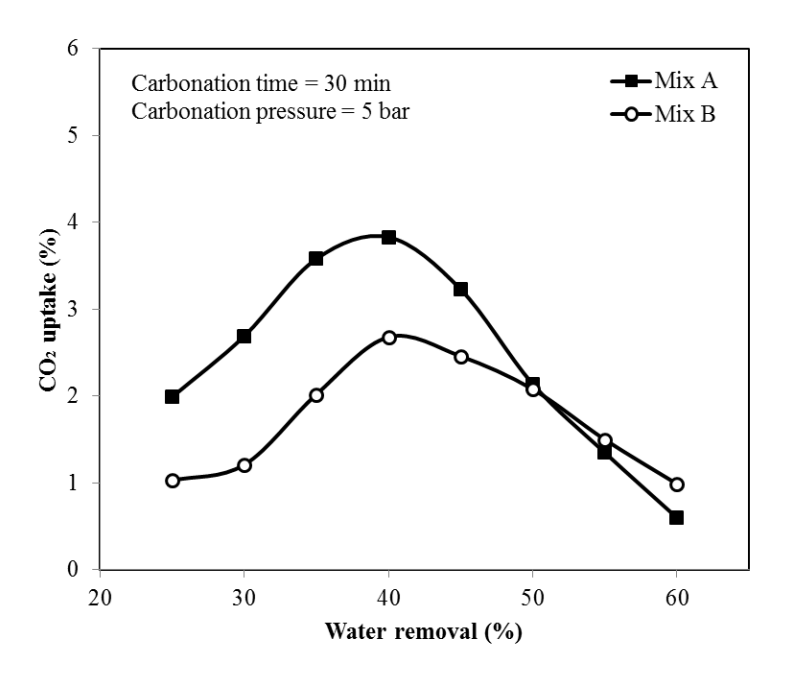


Fig. 3.5. Effect of water removal on CO<sub>2</sub> uptake

Table 3.2. CO<sub>2</sub> uptake of concrete (12 hours carbonation)

Concrete mix	Mass gain method	Mass curve method
Mix A, (%)	15.81	16.69
Mix B, (%)	10.13	11.33

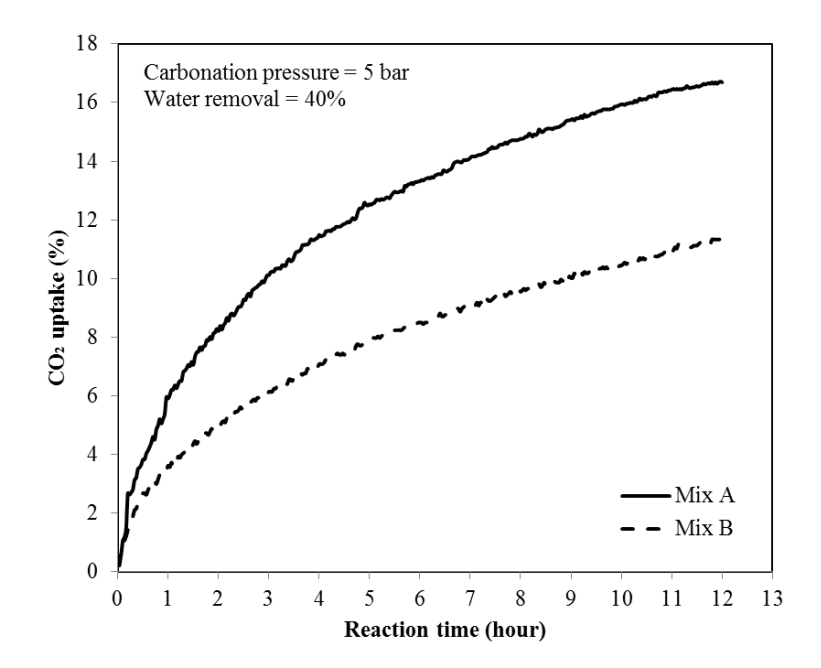


Fig. 3.6. Effect of carbonation time on CO<sub>2</sub> uptake

The effect of carbonation duration was examined as shown in Fig. 3.6. Mass curves of the two concretes were recorded by digital balance as time function up to 12 hours. The test was stopped at 12 hours to assure the process to be completed within 24 hours. CO<sub>2</sub> uptake at 12 hours is summarized in Table 3.2 by both mass curve and mass gain methods. Uptake by mass gain method seemed slightly lower since water evaporation due to carbonation could not be fully collected in Eq. 3.5. In average, Mix A reached uptake of 16.2% and Mix B of 10.7%, based on respective cement content. Mix A was more carbon dioxide reactive than Mix B although the former had lower cement

content. It was the free space generated by preconditioning that played critical role in improving reaction efficiency. Fig. 3.6 also indicates that CO<sub>2</sub> uptake was positively correlated to reaction time. Carbonation curing seemed rate-reducing reaction. With reference to uptake at 12 hours carbonation the reaction was fast in first three hours in which period 60% of reaction was complete. The reduction of reaction rate was likely caused by the build-up of reaction products and the consumption of calcium silicate reactants on surface.

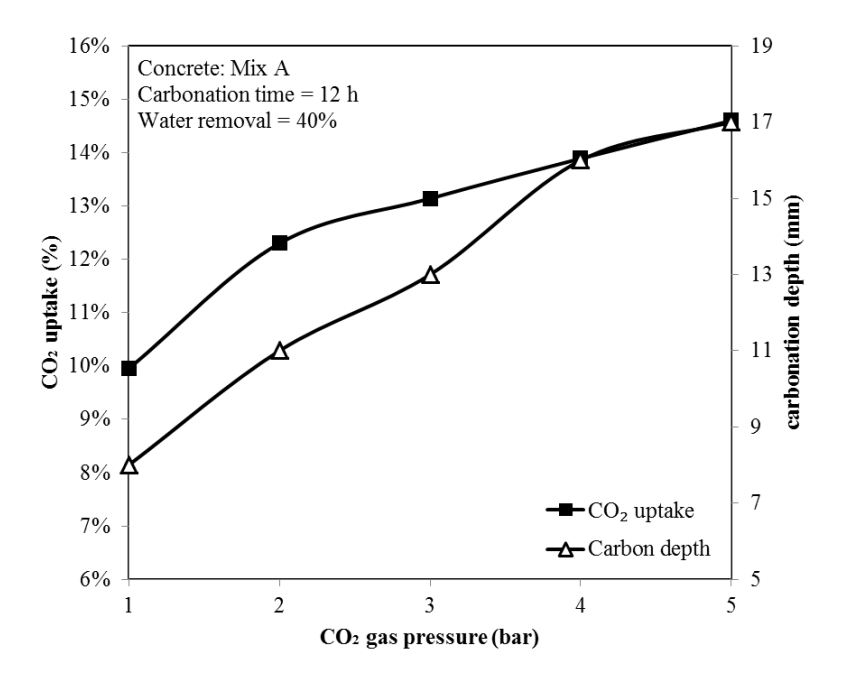


Fig. 3.7. Effect of gas pressure on CO<sub>2</sub> uptake

The effect of carbonation pressure was studied with Mix A concrete. The CO<sub>2</sub> uptakes and the corresponding carbonation depths are presented in Fig. 3.7. CO<sub>2</sub> uptakes were measured by mass gain method. It was obvious that higher gas pressure promoted higher degree of carbonation as well as deeper penetration of carbon dioxide. From 1 to 5

bar CO<sub>2</sub> uptake was increased from 9.95% to 14.60%. The increasing rate, however, was not constant according to different gas pressures. It was faster when pressure changed from 1 bar to 2 bar and slowed down afterwards. The corresponding carbonation depth was measured by phenolphthalein indicator.

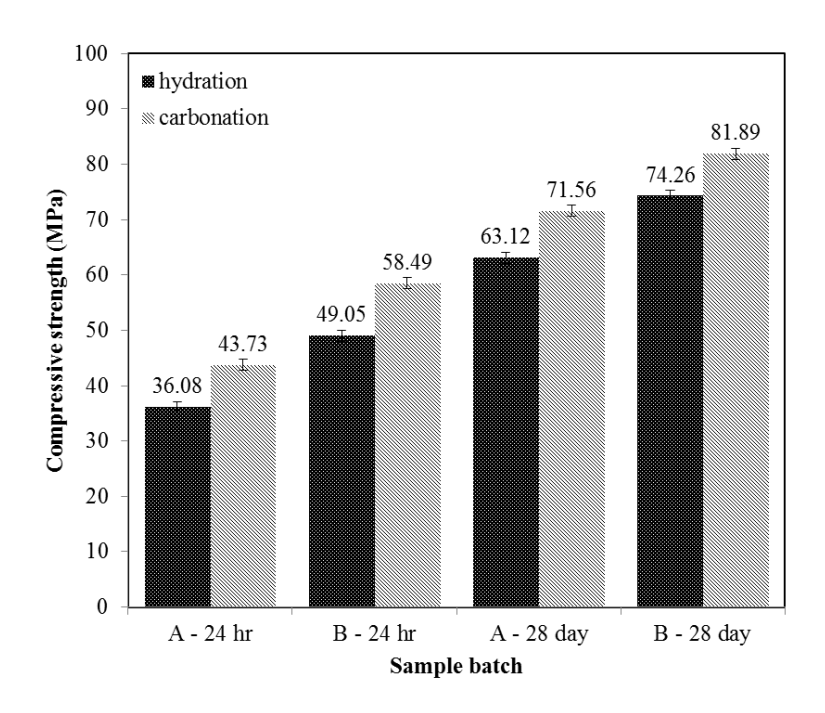


Fig. 3.8. Compressive strength of concrete

It seemed that degree of concrete carbonation was maximized with water removal of 40% based on total mixing water, 12-hour duration and 5 bar pressure. The compressive strength of the concretes processed by the maximized reaction is summarized in Fig. 3.8. Both concretes were in-mold cured for 5 hours and conditioned by fan drying another 5 hours to remove 40% of free water followed by carbonation curing at 5 bar for 12 hours. Concrete strength was tested at the age of 24 hours and 27 days subsequent hydration in moisture room. For both concretes, the 24-hour strength

was considerably increased by the 12 hours carbonation. With reference to hydration strength, this increase was 21% in Mix A and 19% in Mix B. Despite that Mix A contained 14% less cement and 33% more water comparing to Mix B, carbonation strength of Mix A (43.7 MPa) at 24 hours had reached 90% of hydration strength of Mix B (49.1 MPa). In other words, carbonation curing showed the potential to produce equivalent early age hydration strength in concrete with less cement.

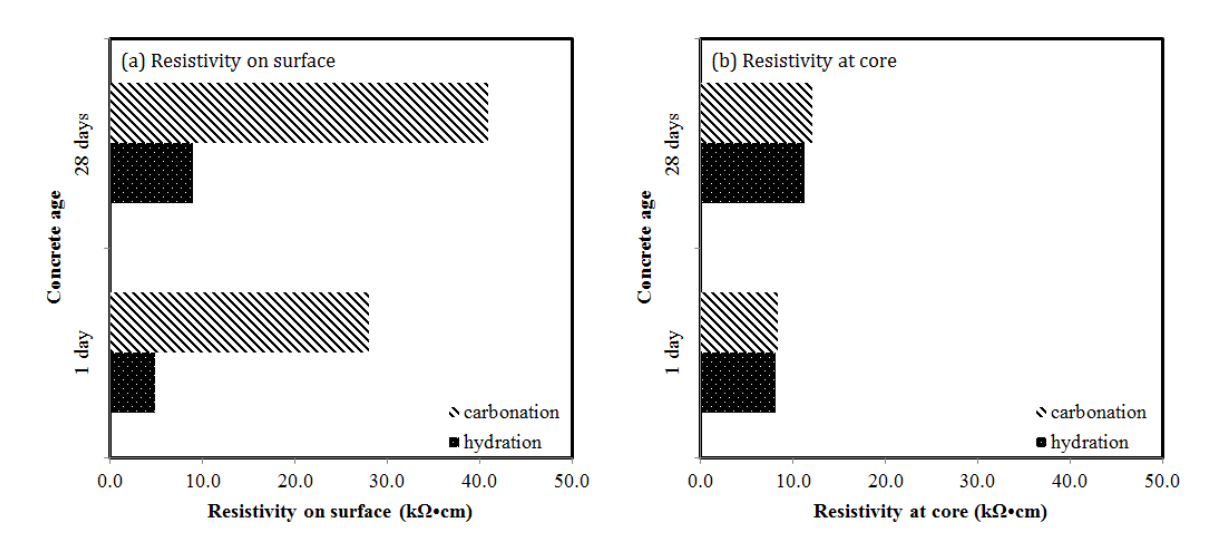


Fig. 3.9. Electrical resistivity in wet cast concrete after carbonation curing

Compressive strength of concretes with 27 days subsequent hydration is also compared in Fig. 3.8. Carbonated concretes had shown higher compressive strength than the hydration reference. However, the increase rate was reduced comparing to that of 24-hour strength. The strength increase due to carbonation curing was 13% in Mix A and 10% in Mix B concrete. It was interesting to notice that the carbonation strength of Mix A concrete had reached 96% of hydration strength of Mix B concrete. It was evident that carbonation was able to produce high strength concrete with lower cement content.

Higher uptake of carbon dioxide was beneficial to strength gain. Higher water content seemed helpful to maximize the degree of carbonation. Water removal by fan drying was able to create more free space for carbonate precipitation.

To examine the impact of carbonation curing on concrete permeability electrical resistivity tests were performed. As direct permeability tests were difficult especially for high strength concrete, electrical resistivity test was developed to indirectly determine the pore structure (AASHTO, 2011). The higher resistivity reading on concrete usually indicated less connected pore structure and thus less permeable material (Tanesi and Ardani, 2012). Resistivity test was also non-destructive in comparison to rapid chloride penetration tests (Rupnow and Icenogle, 2012). Resistivity values of Mix A concrete on surface and at core are compared in Fig. 3.9. It was clear in Fig. 3.9(a) that surface resistivity was significantly improved after carbonation curing. The resistivity value at 1 day, for instance, was 4.8 k $\Omega$ •cm for normal hydration versus 28 k $\Omega$ •cm for early carbonation. This advantage remained after 27 days subsequent hydration. It was suggested that the surface of carbonated concrete was seemingly densified by carbonate precipitates. Fig. 3.9(b) compares the core region. There was no obvious difference between hydrated and carbonated concretes. It was likely that influence of carbonation was mainly on the surface and the resistivity was much higher on surface than in the core of carbonated concrete.

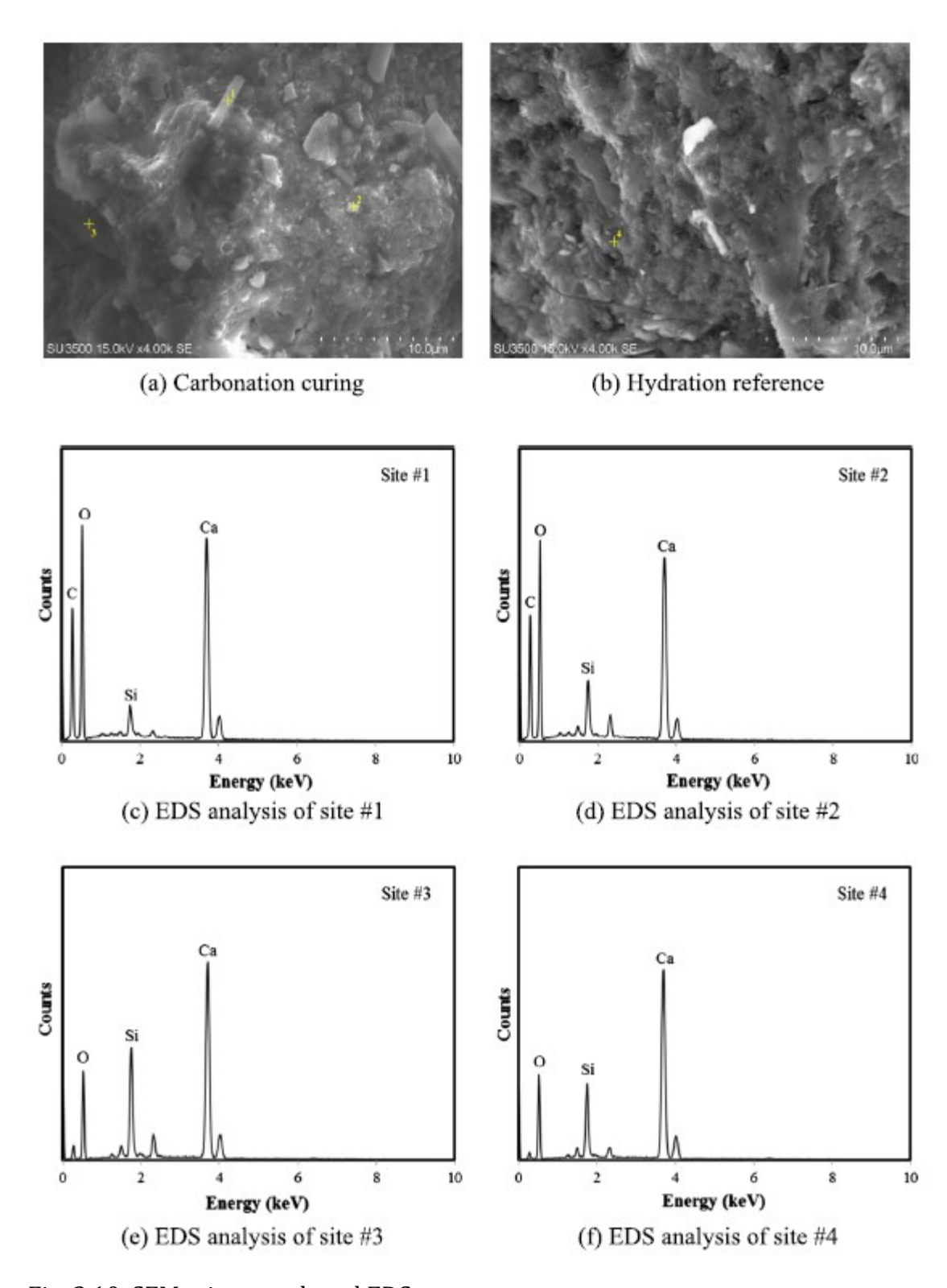
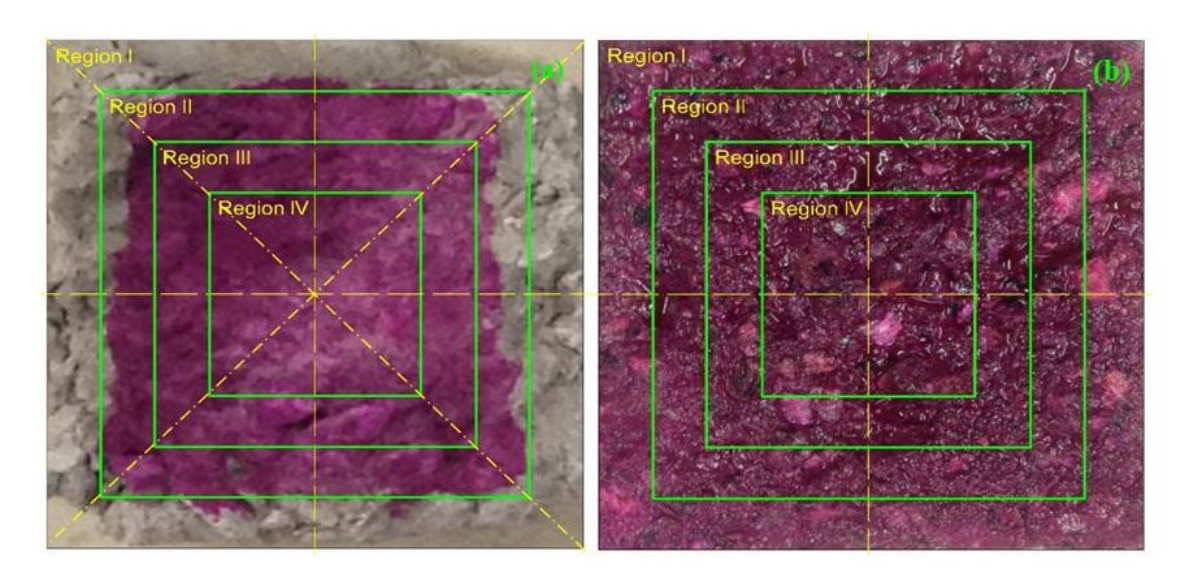


Fig. 3.10. SEM micrograph and EDS spectrum

Scanning electron microscope (SEM) test was performed on fractured surface of concrete to investigate the effect of carbonation curing on morphology. Fig. 3.10 compares the microphotograph and element composition of Mix A concrete at 28 days. As shown in Fig. 3.10(a), two types of crystals were distinguished in concrete subject to carbonation curing (Site #1 and #2). EDS point analysis in Fig. 3.10(c) and (d) showed high content of calcium and carbon but low in silicon. It was indicative that crystals of calcium carbonate were formed. According to SEM, the appearance of the calcium carbonate could be grains smaller than 1 µm as displayed on Site #2, or prism-like shape represented by Site #1. Amorphous C-S-H was also found in concrete after carbonation curing (Site #3). It seemed that calcium carbonate crystals and C-S-H were closely intermingled to form a composite binder. In comparison, hydrated concrete in Fig. 3.10(b) showed more amorphous structure. The precipitation of calcium carbonate contributed to the improved resistance to permeability.



(a) after 12 hours carbonation curing (b) after 27 days subsequent hydration Fig. 3.11. Carbonation depth after early age carbonation curing

# 3.3.2. Effect of carbonation curing on pH of concrete

Carbonation curing produced significant carbonation depth within the 24-hour process. It was necessary to investigate if the carbonation depth would maintain after 27 days subsequent hydration. Mix A concrete processed by 12 hours carbonation at 5 bar following 40% water removal was used to study the layer structure of carbonated concrete.

Table 3.3. pH and carbon content distribution in concrete by 12 hours carbonation

Region	Depth, (mm)	Details	After 12 hours carbonation		After 27 days subsequent h	· 27 days equent hydration	
			CO <sub>2</sub> content	рН	CO <sub>2</sub> content	рН	
I	0~10	Carbonated	27.20%	9.2 ± 0.1	26.50%	12.3 ± 0.2	
II	10~20	Carbonated	10.60%	$9.9 \pm 0.4$	12.10%	$12.4 \pm 0.1$	
III	20~30	Lightly- carbonated	2.60%	$12.0 \pm 0.8$	3.90%	12.5 ± 0.2	
IV	30~50	Non- carbonated	0.50%	13.0 ± 0.1	1.10%	12.9 ± 0.1	

Hydrated concrete reference: pH=12.7-13.0

Fig. 3.11(a) shows the typical cross section sprayed by phenolphthalein solution right after 24 hours curing. Carbonation depth was defined by the colorless front. A gradual transition region was observed between carbonated and non-carbonated area. The cross section was divided into four regions. PH distribution was also measured along the centerline and is listed in Table 3.3. Surface layer, labelled as Region I, was considered as fully carbonated in which pH dropped to the level of 9.1~9.3. The unaffected core region (Region IV) was non-carbonated since the pH remained as high as 12.9~13.1 which was comparable to pH in normally hydrated concrete. Between surface and core there was

transition area from fully carbonation to non-carbonation. Fig. 3.11(b) shows the cross section after 12 hours carbonation and 27 days subsequent hydration. The carbonation depth disappeared and the pH value in first 20 mm thick layer was increased to 12.3~12.4 which was of close to that at core. In this period of subsequent hydration, strength was increased at the same rate in both hydrated and carbonated concrete (Fig. 3.8), indicating the early carbonation did not hinder subsequent hydration. PH values are also summarized in Table 3.3 including CO<sub>2</sub> uptake by each layer due to carbonation curing. Surface 10-mm layer was heavily carbonated with 26 to 27% carbon dioxide uptake. The second region contained less CO<sub>2</sub>. However, the effect of carbonation curing on pH in that layer was still considerable. Effect of carbonation on Region III was minimal. This was 25 mm from the surface and might be designed the location of reinforcing steel. It seemed that the carbonation curing were applicable to concrete with reinforcing steel.

Table 3.4. Effect of early carbonation on weathering carbonation (mix A)

Testing time, weeks	time, depth, mm		pH on surface		pH at 25 mm depth	
	hydration	carbonation	hydration	carbonation	hydration	carbonation
0	0.0	0.0	13.0 ± 0.2	$12.5 \pm 0.3$	12.7 ± 0.2	12.8 ± 0.3
10	2.2	2.4	$10.2 \pm 0.2$	$10.3 \pm 0.3$	$12.8 \pm 0.5$	$13.0 \pm 0.1$
15	3.0	2.9	$10.0 \pm 0.6$	$9.8 \pm 0.3$	$12.7 \pm 0.3$	$12.7 \pm 0.1$
20	3.6	3.4	$9.5 \pm 0.3$	$9.6 \pm 0.4$	$12.6 \pm 0.4$	12.9 ± 0.5
25	3.9	4.0	$9.1 \pm 0.3$	$9.3 \pm 0.5$	$12.8 \pm 0.1$	$12.7 \pm 0.3$

### 3.3.3. Effect of early carbonation on weathering carbonation

Weathering carbonation depth was measured by phenolphthalein solution spray on split cross section and pH was measured on surface and at depth of 25 mm,

respectively. Samples were tested every 5 weeks and results are listed in Table 3.4. It was shown that carbonation depth was rather small due to high strength mixture and high content of cement. Nevertheless, the carbonation depths were of the same order of magnitude between normally hydrated and early carbonated concretes. The carbonation depth after 25 weeks was 3.9 mm in normal hydration and 4.0 mm in early carbonation which made no substantial difference between the two curing methods. The early carbonation curing did not generate more carbonation depth in weathering carbonation. The carbonation depth was plotted against weathering time in Fig. 3.12 to determine the carbonation coefficient *A* in Eq. 3.8 (Sulapha et al., 2003).

$$x = A(t)^{0.5} (3.8)$$

In which x is the carbonation depth (<u>RILEM</u>, 1988), t is the time (week) and A is the carbonation coefficient (mm/(week)<sup>0.5</sup>).

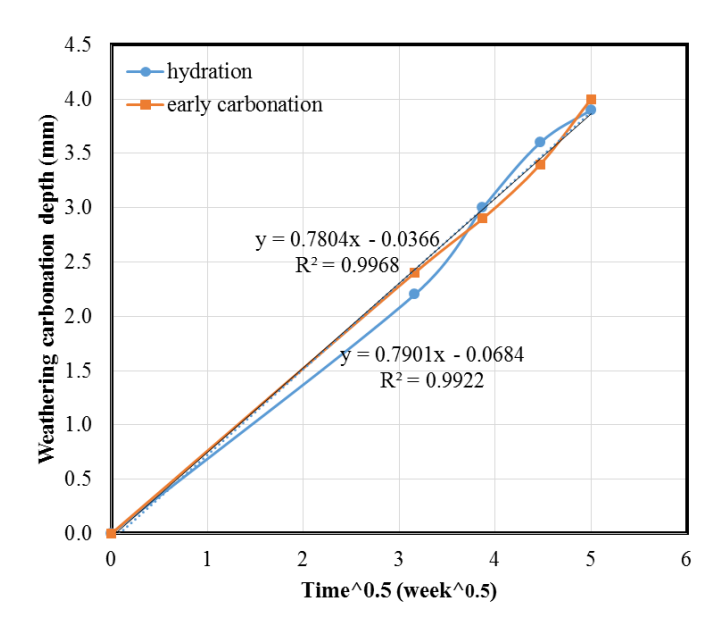


Fig. 3.12. Carbonation depth in weathering carbonation

The linear regression yielded carbonation coefficient of 0.79 mm/(week)<sup>0.5</sup> for carbonated concrete and 0.78 mm/(week)<sup>0.5</sup> for hydrated concrete. They were again of closed value which was close to the coefficient reported on concrete of 0.4 water to cement ratio (Sulapha et al., 2003).

PH values on concrete surface and at 25 mm depth were also compared in weathering carbonation. It was shown that surface pH reduced in both batches. Surface pH in normally hydrated concrete was slightly higher at start point but appeared close to early carbonated sample after 10 weeks. This indicated that weathering carbonation reaction kept the same pace between hydrated and carbonated concretes. The pH at 25 mm depth, however, remained higher than 12.5 indicating that carbonation reaction failed to reach this area.

# 3.3.4. Preconditioning shrinkage of reinforced concrete beams

To maximize the degree of carbonation curing fan drying conditioning to remove about 40% free water seemed necessary. The effect of fan drying at fresh state on shrinkage cracking, especially in restrained condition with internal reinforcement, was examined with the 800-mm long reinforced concrete beam shown in Fig. 3.4. The beam was cured in mold in the open air at 25 °C and  $55 \pm 5\%$  RH for 5 hours and then preconditioned by 5.5 hours fan drying after demolding. The water evaporation was monitored on digital balance. The water loss was approximately 13% during in-mold curing and 25% during fan drying conditioning. Total water removed was approximately 38% based on mixing water used for the beam. The water evaporation curve and the

corresponding shrinkage curve during fan drying conditioning are plotted in Fig. 3.13. Evaporation rate was higher in first two hours and gradually reduced afterwards. After 5.5 hours preconditioning, preconditioning-induced water loss reached 25%. The corresponding shrinkage was approximately 40 micro-strains. Alcohol solution spray was used to assess the hairline cracks due to restrained shrinkage. No obvious cracks were detected on surface.

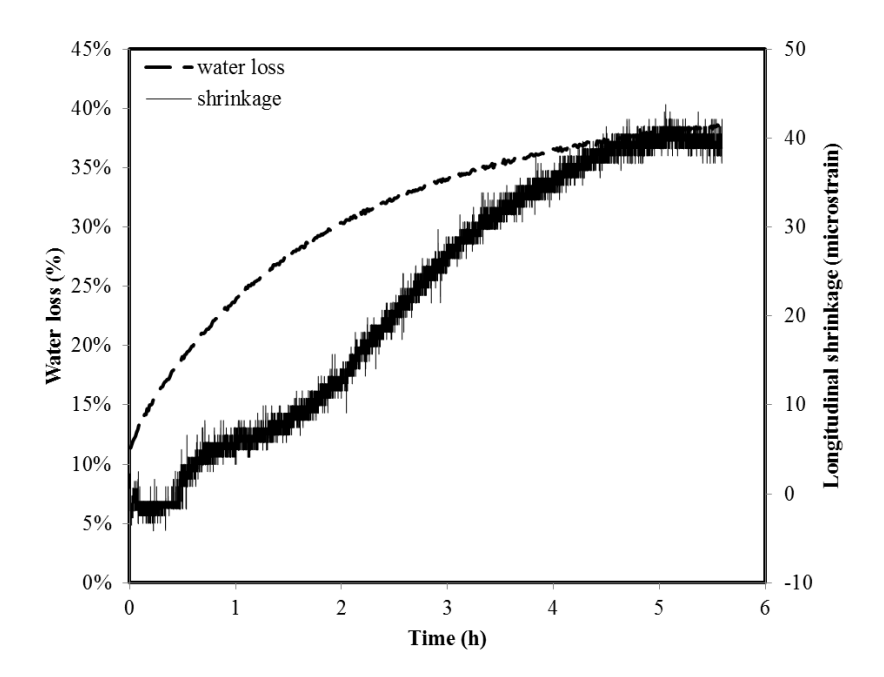
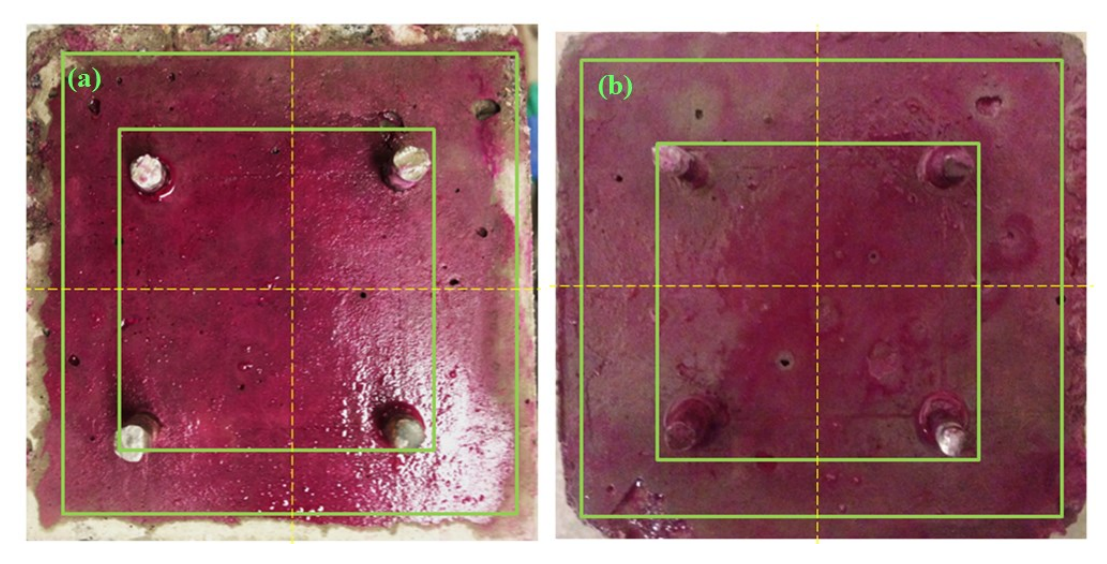


Fig. 3.13. Shrinkage of reinforced concrete beam due to fan drying conditioning

The shrinkage cracking of fresh concrete was highly dependent on water evaporation rate (Almusallam et al., 1998) which were calculated through Eq. 3.9.

$$Evaporation \ rate = \frac{water \ removal \ mass}{area \times time}$$
 (3.9)

For the 800-mm beam shown in Fig. 3.4 using Mix A concrete proportion, the water required for one beam was 1.448 kg. The water evaporation rate was 0.47 kg/m²/h for 5 hours during in-mold curing and 0.19 kg/m²/h for 5.5 hours by fan drying conditioning. To prevent shrinkage cracking, ACI suggested the evaporation rate of fresh concrete to be limited in 1 kg/m²/h. Concrete experienced with higher evaporation rate due to early age drying was vulnerable to plastic shrinkage cracking (Uno, 1998).



(a) immediately after carbonation

(b) after 27 days subsequent hydration

Fig. 3.14. Carbonation depth in reinforced concrete beam due to carbonation curing

Table 3.5. Early carbonation of reinforced concrete beam

Sample	Sample location	рН	CO <sub>2</sub> uptake	CO <sub>2</sub> uptake
			Mass gain	Thermal analysis
24 hours after	0-10mm	$9.6 \pm 0.3$	9.600/	23.70%
carbonation	Steel bar, 20-30mm	$13.0 \pm 0.1$	8.60%	0.46%
27 days subsequent	0-10mm	$12.6 \pm 0.1$	-	24.57%
hydration	Steel bar, 20-30mm	$12.7 \pm 0.2$	-	0.04%
28 days hydration	Hydration reference	$12.9 \pm 0.2$	-	0

After 10.5 hours initial curing, the beam was placed in pressure chamber for 12 hours carbonation curing. Fig. 3.14 shows carbonation depth of the cross section characterized by phenolphthalein solution immediately after carbonation treatment and after 27 days subsequent hydration. The results are summarized in Table 3.5. The CO<sub>2</sub> uptake by the beam was calculated through mass gain method. It was about 8.6% based on mass of the anhydrous cement. It was shown that immediately after carbonation pH value on surface was reduced to 9.6 while remained at 13.0 near the steel bars. After 27 days subsequent hydration pH on concrete surface and at core both reached the value of 12.6-12.7, which was of close to the hydration reference of 12.9. Pyrolysis analysis of concrete was also performed to obtain carbon content from surface 10 mm layer and at steel bars (20-30 mm from surface). It was 27.2% at surface layer and 4% at steel bar. The hydration reference concrete showed carbon dioxide content of 3.5% which was mainly attributed to the limestone addition in cement. The initial carbon content due to limestone addition was subtracted from that of carbonated concrete. The final CO<sub>2</sub> uptake due to carbonation curing was calculated and is also shown in Table 3.5. Obviously carbonation occurred mainly on the surface 10 mm. Assuming that the surface 10-mm layer took 23.7% carbon dioxide and the rest was negligible, the CO<sub>2</sub> uptake by carbonation was about 8.5% which was close to 8.6%, the value by mass gain method. At steel bars (25 mm from surface), carbonation effect was negligible. The result was also suggestive that there was size effect on carbonation. Beam was designed the same cross section as cubes but displayed much reduced degree of carbonation. The effect of carbonation degree on compressive strength was examined. Concrete cubes of Mix A carbonated by 2 hours at 5 bar could gain CO<sub>2</sub> uptake of 8.2% (Fig. 3.6). The resulted

average compressive strength was 40.1 MPa at 24 hours and 67.8 MPa after 28 days. The same concrete cubes carbonated by 12 hours under the same condition obtained compressive strength of 43.7 MPa in 24 hours and 71.5 MPa after 28 days (Fig. 3.8). It was likely the compressive strength of the concrete was not linearly proportional to the degree of carbonation curing. Even the carbon dioxide uptake was only half in 2-hour carbonation in comparison to the 12 hour process strength produced was of close value. Therefore a limit existed on the strength gain by carbonation. Increase in duration of carbonation over 2 hours observed little effect on strength gain. However, it was beneficial to carbon dioxide utilization and durability improvement by creating carbonate-rich surface layer.

## 3.3.5. Utilization capacity of carbon dioxide and cost analysis

Early age carbonation curing is carbon dioxide sequestration process. Precast concrete products could be used to permanently convert carbon dioxide as stable carbonates. In concrete railway crosstie application, the typical product has the dimension of  $2.5 \text{ m} \times 0.25 \text{ m} \times 0.25 \text{ m}$ . If carbonation curing could be used to replace the steam and carbonation occurs only 10 mm on surface, the volume of fully carbonated surface area is  $0.024 \text{ m}^3$ . With 25% carbon dioxide uptake in this area there would be 2.8 kg of carbon dioxide sequestrated. Assuming 3000 railway ties are required per Kilometer as average, early carbonation curing is able to utilize 8.4 tons of carbon dioxide and permanently convert it in concrete railway ties per km.

Industrial scale operation of carbonation curing requires system network including carbon supplement and concrete preconditioning. Currently there is no commercial production using carbonation curing because of the high price of the gas. However, large quantities of high purity and low cost carbon dioxide could soon be available as regulations requiring reductions in CO<sub>2</sub> emissions may be developed. In that case carbon dioxide may be free for concrete production utilization. Concrete producers may even obtain carbon credits by using concrete products as carbon sink. In this scenario, the only cost of carbonation curing is the fan drying conditioning. Based on laboratory set up, the preconditioning took 5~6 hours to reach the required water removal and consumed 28 kWh per cubic meter of concrete. Assuming the electricity price is \$0.06 for 1 kWh, 6 hours preconditioning would cost \$1.69 per cubic meter. The energy consumption of steam curing for one cubic meter concrete is 164 kWh and costs \$9.84 (Kawai et al., 2005). Carbonation curing could have advantage over price in comparison to conventional steam curing.

#### 3.4. CONCLUSIONS

Unique process of carbonation curing of precast reinforced concrete was developed to maximize the degree of carbonation and improve performance of the concrete. The following conclusions were drawn.

1. For wet-mix concrete carbonation curing, the four-step process, including inmold curing, off-mold preconditioning, carbonation curing and subsequent hydration, was necessary to maximize the strength gain and carbon dioxide uptake. The process took less than 24 hours and was able to be scaled up for full production.

- 2. The in-mold curing and off-mold preconditioning were carried out to remove portion of free water which was of critical importance for concrete to reach maximized degree of carbonation. The ideal water removal was approximately 40% of initial water content. The water removal at early age did not generate shrinkage cracking and could be compensated by subsequent hydration. The resistivity of carbonated concrete was higher than that of the hydrated reference, indicating that permeability of concrete was reduced by carbonation curing.
- 3. Immediately after carbonation, pH value of concrete was reduced to 9.2-9.9 on surface of 20 mm thick layer, but remained above 12 near the location of steel reinforcement. With subsequent hydration, both surface and core gained pH higher than 12. Carbonation curing created a sandwich structure in concrete with carbonate-rich surface.
- 4. The carbonated concrete was not more vulnerable to weathering carbonation.

  The carbonation depth and the carbonation coefficients measured in accelerated weathering carbonation were comparable to those of reference concrete.
- 5. Size effect existed on degree of carbonation. With the same process parameters, concrete cubes gained higher carbon dioxide uptake than concrete beams. However, the strength gain due to carbonation was not proportional to carbon dioxide uptake. There existed uptake threshold over which more carbonation reaction failed to enhance the strength gain. Nevertheless, higher degree of carbonation promoted higher capacity of

carbon dioxide utilization and improved durability of concrete by creating the carbonaterich surface layer.

## **ACKNOWLEDGEMENT**

The financial supports by Natural Sciences and Engineering Research Council (NSERC) of Canada and by Climate Change and Emissions Management Corporation (CCEMC) of Alberta are gratefully acknowledged.

#### REFERENCES

- AASHTO, T. 2011. 95-11 "Standard Method of Test for Surface Resistivity Indication of Concrete's Ability to Resist Chloride Ion Penetration.". *AASHTO Provisional Standards*, 2011 Edition.
- ALMUSALLAM, A., MASLEHUDDIN, M., ABDUL-WARIS, M. & KHAN, M. 1998. Effect of mix proportions on plastic shrinkage cracking of concrete in hot environments. *Construction and Building Materials*, 12, 353-358.
- DEAN, J. A. 1985. Lange's handbook of chemistry, New York, McGraw Hill Book Co.
- EL-HASSAN, H., SHAO, Y. & GHOULEH, Z. 2013a. Effect of initial curing on carbonation of lightweight concrete masonry units. *ACI Materials Journal*, 110, 441-450.
- EL-HASSAN, H., SHAO, Y. & GHOULEH, Z. 2013b. Reaction Products in Carbonation-Cured Lightweight Concrete. *Journal of Materials in Civil Engineering*, 25, 799-809.
- GLASS, J., FEDERATION, B. P. C. & ASSOCIATION, B. C. 2000. *The future for precast concrete in low-rise housing*, British Precast Concrete Federation Leicester.
- HENG, M. & MURATA, K. 2004. Aging of concrete buildings and determining the pH value on the surface of concrete by using a handy semi-conductive pH meter. *Analytical sciences*, 20, 1087-1090.
- HUET, B., L'HOSTIS, V., MISERQUE, F. & IDRISSI, H. 2005. Electrochemical behavior of mild steel in concrete: Influence of pH and carbonate content of concrete pore solution. *Electrochimica Acta*, 51, 172-180.
- KASHEF-HAGHIGHI, S., SHAO, Y. & GHOSHAL, S. 2015. Mathematical modeling of CO<sub>2</sub> uptake by concrete during accelerated carbonation curing. *Cement and Concrete Research*, 67, 1-10.
- KAWAI, K., SUGIYAMA, T., KOBAYASHI, K. & SANO, S. 2005. Inventory data and case studies for environmental performance evaluation of concrete structure construction. *Journal of Advanced Concrete Technology*, 3, 435-456.
- MEHTA, P. K. & AIETCIN, P.-C. 1990. Principles underlying production of high-performance concrete. *Cement, concrete and aggregates,* 12, 70-78.

- PAPADAKIS, V. G., VAYENAS, C. G. & FARDIS, M. N. 1991. Experimental investigation and mathematical modeling of the concrete carbonation problem. *Chemical Engineering Science*, 46, 1333-1338.
- RILEM, R. 1988. CPC-18 Measurement of hardened concrete carbonation depth.
- ROSTAMI, V., SHAO, Y. & BOYD, A. J. 2011a. Carbonation curing versus steam curing for precast concrete production. *Journal of Materials in Civil Engineering*, 24, 1221-1229.
- ROSTAMI, V., SHAO, Y. & BOYD, A. J. 2011b. Durability of concrete pipes subjected to combined steam and carbonation curing. *Construction and Building Materials*, 25, 3345-3355.
- RUPNOW, T. & ICENOGLE, P. 2012. Surface Resistivity Measurements Evaluated as Alternative to Rapid Chloride Permeability Test for Quality Assurance and Acceptance. *Transportation Research Record: Journal of the Transportation Research Board*, 30-37.
- SHAO, Y. & MORSHED, A. Z. 2015. Early carbonation for hollow-core concrete slab curing and carbon dioxide recycling. *Materials and Structures*, 48, 307-319.
- SULAPHA, P., WONG, S., WEE, T. & SWADDIWUDHIPONG, S. 2003. Carbonation of concrete containing mineral admixtures. *Journal of materials in civil engineering*, 15, 134-143.
- TANESI, J. & ARDANI, A. 2012. Surface Resistivity Test Evaluation as an Indicator of the Chloride Permeability of Concrete. US Department of Transportation.
- TUUTTI, K. 1982. Corrosion of steel in concrete. Swedish Cement and Concrete Institute.
- UNO, P. J. 1998. Plastic shrinkage cracking and evaporation formulae. *ACI Materials Journal*, 95, 365-375.
- YOUNG, J., BERGER, R. & BREESE, J. 1974. Accelerated curing of compacted calcium silicate mortars on exposure to CO<sub>2</sub>. *Journal of the american ceramic society*, 57, 394-397.

### **CHAPTER 4**

\_

#### CARBONATION CURING OF PRECAST FLY ASH CONCRETE

#### **PREFACE**

Previous chapter developed process of carbonation curing on precast reinforced concrete. Improved early strength and recovered pH were observed. For implementation of the curing process, however, the chemical reaction of cementitious materials was necessary to be quantified. It was mentioned that the reaction of Ordinary Portland Cement (OPC) was at considerably high rate via carbonation curing which accounted for the accelerated strength gain. Nevertheless, the long term performance after carbonation was not clear. In addition to reaction of cement, mineral admixtures such as fly ash, silica fume were commonly added in concrete as partial replacement of ordinary Portland cement. Their reactions in concrete, also known as pozzolanic reaction might be impacted by carbonation curing.

In this chapter, cement reaction degree and the relation between carbonation reaction and pozzolanic reaction were examined. Fly ash was chosen to represent the mineral admixture. After carbonation curing with various duration and fly ash content, cement reaction degree was estimated through the equivalent non-evaporable water

content and fly ash reaction degree was analyzed through selective acid dissolution test. Both reactions were quantified from 1 day to 360 days with the assistance of Thermogravimetric analysis (TGA) and chemistry characterization.

It was found that pozzolanic reaction in the fly ash-OPC system was hindered by carbonation curing. Higher degree of early carbonation resulted in lower pozzolanic reaction of fly ash. In addition, carbon dioxide was more reactive with fly ash-OPC paste than plain cement paste. Therefore controlled carbonation at early age was necessary to trade off carbon emission reduction with performance improvement. The study in this chapter showed that with fly ash content limited to 20% of cementitious material and carbonation duration below 12 hours fly ash concrete could be produced by carbonation curing to gain higher early strength, comparable long term strength, enhanced durability performance and 36% reduction in carbon emission. After subsequent hydration, carbonated fly ash concrete was able to maintain pH comparable to hydration reference and could be used in precast concretes with steel reinforcement.

### 4.1. Introduction

The production of Portland cement accounted for over 5% of anthropogenic CO<sub>2</sub> emission worldwide (Chen et al., 2010). To reduce the emission supplementary cementitious materials (SCMs), such as fly ash, silica fume, slag and metakaolin, were used as partial replacement of Ordinary Portland Cement (OPC). The use of blended cement were proven effective in emission reduction and performance improvement (Lothenbach et al., 2011). The pozzolanic reaction between calcium hydroxide (CH) and reactive silica in SCMs generated calcium silicate hydrate (C-S-H). Concrete with SCMs was found less permeable leading to enhanced durability performance (Khan and Lynsdale, 2002; Alexander and Magee, 1999).

Carbonation curing was an accelerated curing process which was carried out within 24 hours after casting. If performed immediately after mixing of cement and water the reaction happened between high purity CO<sub>2</sub> gas and calcium silicate phases in anhydrous cement. The reaction was governed by Eqs. 4.1-4.2 (Young et al., 1974; Berger et al., 1972). The reaction products were hybrid of C-S-H and calcium carbonate (CaCO<sub>3</sub>). The variables 'x' and 'y' in Eqs. 4.1-4.2 were dependent on reaction degree (Young et al., 1974). If following a short period of hydration both calcium silicate phases and part of hydration products would be carbonated (Eqs. 4.1-4.4).

$$C_3S + (3-x)CO_2 + yH_2O \rightarrow C_xSH_y + (3-x)CaCO_3$$
 (4.1)

$$C_2S + (2-x)CO_2 + yH_2O \rightarrow C_xSH_y + (2-x)CaCO_3$$
 (4.2)

$$Ca(OH)_2 + CO_2 \rightarrow CaCO_3 + H_2O \tag{4.3}$$

$$C-S-H + 2CO_2 \rightarrow SiO_2 + 2CaCO_3 + H_2O$$
 (4.4)

Early carbonation of concrete was carbon dioxide sequestration process. Gaseous CO<sub>2</sub> was permanently stored in concrete in form of crystalline calcium carbonate (Bertos et al., 2004). Rather high early strength was obtained (Berger et al., 1972). Carbonation curing was also found to enhance durability performance of concrete due to precipitation of carbonates on surface (Rostami et al., 2011).

Implementation of carbonation curing on concrete incorporated with SCMs seemingly gained technical advantages in three aspects: (1) the low early strength of concrete with SCMs could be improved by carbonation reaction; (2) durability could be further enhanced by precipitation of carbonates; (3) carbon emission reduction would be doubled through the reduction in cement usage and the carbon dioxide uptake owing to carbonation. However, issue needed to be addressed if carbonation was compatible with pozzolanic reaction as both reactions competing for calcium hydroxide. The long term pozzolanic reaction could be hindered. Therefore trade-off between the benefits gained from the early age carbonation and pozzolanic reaction was necessary.

The purpose of this chapter was to examine the interaction between carbonation curing and pozzolanic reaction in fly ash-OPC system. Both paste and concrete samples were prepared through hydration and carbonation curing. Thermogravimetric analysis (TGA) and selective acid dissolution tests were conducted on fly ash-OPC paste with subsequent hydration up to 1 year to estimate reaction degree of cement and fly ash. Parameters of carbonation curing were chosen from testing results of pastes to be performed on fly ash concrete. Concrete subjected to carbonation curing was

characterized by carbonation depth, CO<sub>2</sub> uptake, compressive strength, pH distribution and electrical resistivity.

#### 4.2. EXPERIMENTAL PROGRAM

# 4.2.1. Materials and mix proportion

CSA (Canadian Standard Association) Type GU Ordinary Portland Cement (OPC) and fly ash were chosen to represent cementitious materials. The chemical compositions of cement and fly ash are given in Table 4.1. Fly ash was added in place of cement by 20% and 50% based on mass. Both pastes and concretes were studied, the former being used to quantify the reaction degree of cementitious binder and the latter to examine the effect of carbonation on concrete performance. The mixture proportions are summarized in Table 4.2. Water to cementitious binder (cement + fly ash) ratio in paste and concrete was maintained constant of 0.4.

### 4.2.2. Samples preparation

Fig. 4.1 shows the procedure of carbonation curing of paste and concrete samples following four-step process: (1) in-mold curing, (2) de-mold conditioning, (3) carbonation curing and (4) subsequent hydration.

To assure that the final water content in the cement pastes was representative for that in concrete after in-mold curing and demold conditioning, 6 mm thickness was

selected through trial tests for paste samples. After the 6 mm thick sheet was cast 6 mm cubes were cut from the thin sheets as samples of cementitious paste. Concrete samples were cast into 100 mm cubes. Crushed granite stone and granite sand were used as aggregates. Water absorption of fine and coarse aggregate was 4.3% and 1.6%, respectively. Fineness modulus of granite sand was 3.0 and the maximum aggregate size was 12 mm for coarse aggregate. Superplasticizer was added to obtain the slump of approximately 160 mm. Aggregates were used in saturated surface dry condition.

Table 4.1. Chemical composition of as-received materials (%)

	Cement	Fly ash
CaO	63.10	11.30
$SiO_2$	19.80	54.39
$Al_2O_3$	4.90	23.65
$Fe_2O_3$	2.00	3.90
MgO	2.00	1.17
$K_2O$	-	0.75
$Na_2O_{(eq)}$	0.85	2.91
$SO_3$	3.80	-
LOI	2.03	2.51

Due to the high slump of fresh mixture it is not possible to demold right after casting. The initial hydration curing in mold was necessary. The time required for this step was dependent on the mixture proportion. For the concrete used in this study it took approximately 5 hours to reach initial set at ambient condition (25 °C and 60% relative humidity) in the open air. It was also intended to remove part of the mixing water for carbonation. After in-mold curing the cube samples were demolded and left on bottom plates for fan drying conditioning of 5.5 hours at wind speed of 1 m/s in laboratory

condition of 25 °C and  $50 \pm 5$  % relative humidity. Step 2 was critical to implement the afterwards carbonation reaction. The de-mold conditioning further removed part of the free water and evacuate more space for penetration of carbon dioxide gas and thus carbonates to precipitate. In step 3 the conditioned samples were carbonated in pressure chamber with  $CO_2$  gas of 99.8% purity under constant pressure of 5 bar for 2, 12 or 24 hours. Samples after carbonation were placed in moisture room (25 °C, 95% RH) for subsequent hydration up to 360 days (Step 4). The hydration references were prepared as parallel test. The samples were cured in sealed mold within the first 24 hours followed by demolding and further curing in the same moisture room.

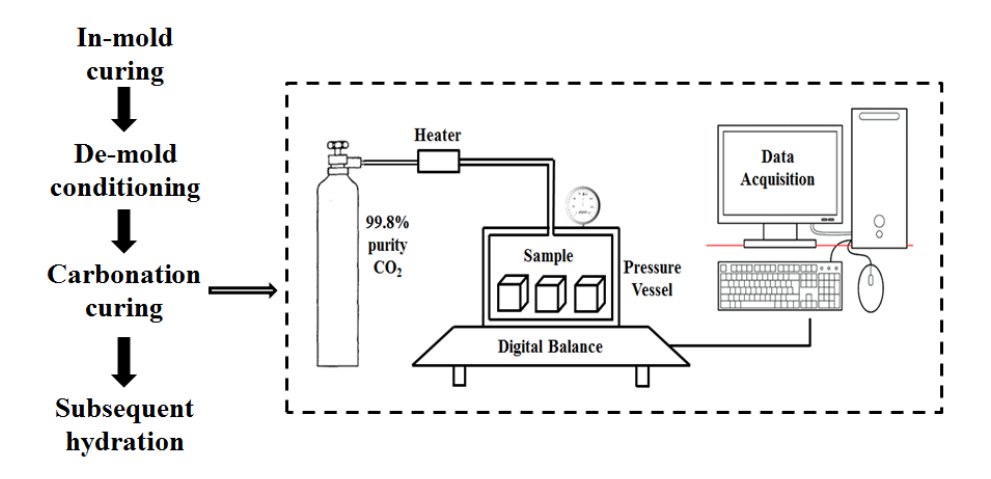


Fig. 4.1. Procedure of carbonation curing

The carbonation procedure applied to both paste and concrete samples. For paste samples, fly ash content was varied at 0%, 20% and 50% and the carbonation duration was at 2, 12 and 24 hours. The subsequent hydration was carried out in moist condition (25°C, 95% RH) and tested at 1.4, 28, 90, 180 and 360 days. The age of first strength test was determined from 24 hours carbonation batch and set at 1.4 days (=34.5 hours). In 24

hours carbonation process samples underwent 5 hours in-mold curing, 5.5 hours de-mold conditioning and 24 hours carbonation, totally 34.5 hours (1.4 days). To make the early strength test comparable all other batches were tested at 1.4 days as well. This was accomplished by adding short period of sealed hydration after carbonation curing. Based on testing results of cementitious paste concretes with 20% fly ash were selected for carbonation treatment with the reaction duration of 12 hours. Tests on concrete performance were conducted at the age of 1, 28 and 90 days. Early strength tests were conducted at 24 hours (5 hours in-mold curing, 5.5 hours de-mold conditioning, 12 hours carbonation and 1.5 hours hydration). Hydration controls were tested at the same age as reference.

Table 4.2. Mixture proportions (kg/m³)

Mixture	Paste			Concrete	
	OPC	FA200PC	FA500PC	OPC	FAOPC
Cement, kg/m <sup>3</sup>	1391	1113	696	452	362
Fly ash, kg/m³	0	278	696	0	90
Fly ash to binder ratio,%	0	20	50	0	20
Water, kg/m <sup>3</sup>	557	557	557	181	181
Water to binder ratio	0.4	0.4	0.4	0.4	0.4
Water to cement ratio	0.4	0.5	0.8	0.4	0.5
Coarse aggregate, kg/m <sup>3</sup>	0	0	0	1060	1060
Fine aggregate, kg/m <sup>3</sup>	0	0	0	680	680
Sp/c, %	N/A	N/A	N/A	0.5	0.5
Slump, mm	N/A	N/A	N/A	158	166

Note: sp/c denotes mass ratio of superplasticizer and cement

To examine carbonation reactivity of the as-received fly ash carbonation test was conducted by mixing fly ash with water following the water to fly ash ratio of 0.4. Fly ash paste was spread uniformly on steel plate and carbonated in pressure chamber with 5 bar

CO<sub>2</sub> gas (99.8% purity) at duration of 24 hours. Testing results showed that there was no mass increase in plain fly ash paste indicating that fly ash used in this work was unreactive with CO<sub>2</sub> and thus the CO<sub>2</sub> uptake measured in fly ash-OPC system was solely attributed to carbonation of cement.

## 4.2.3. Measurement of carbonation degree

Carbonation degree was quantified by  $CO_2$  uptake which was measured through mass gain and mass curve methods. Mass gain method calculated  $CO_2$  uptake through mass change of samples during the process of carbonation as shown in Eq. 4.5, in which  $m_1$  and  $m_2$  represent sample mass before and after carbonation reaction. Carbonation-induced water loss ( $m_{\text{water}}$ ) was collected by absorbent paper and added to final mass ( $m_2$ ). By treating the reaction chamber as closed system, it was imperative to include the evaporated water which was initially inside the samples prior to carbonation. Percent  $CO_2$  uptake was expressed with reference to the anhydrous cement mass ( $m_{\text{cement}}$ ).

$$CO_2 \text{ uptake}(\%) = \frac{m_2 + m_{water} - m_1}{m_{cement}} \times 100\%$$
 (4.5)

Mass curve method estimated the CO<sub>2</sub> uptake through digitally recorded mass. After samples (20 samples for paste or 3 samples for concrete) placed in the chamber the balance was zeroed and gas was injected to 5 bar. The mass increase was recorded as function of time. Since the pressure was maintained constant the increase in mass of the system was due to the carbon dioxide uptake by cement. At the end of reaction at which

time  $CO_2$  was released the residual mass M was measured. The system was calibrated by repeating the tests using  $CO_2$ -insensitive styrofoam samples of the same volume to obtain second residual mass, m. The difference between M and m represented the  $CO_2$  uptake by concrete (Eq. 4.6). Data collected by mass gain and mass curve methods were two simultaneous measurements from the same process and thus were comparable. They were also independent from any possible existence of carbon content before carbonation.

$$CO_2 \text{ uptake}(\%) = \frac{M - m}{m_{cement}} \times 100\%$$
 (4.6)

# 4.2.4. Compression test

Compression strength was tested on both pastes and concrete samples. For paste samples twenty of 6-mm cubes were tested for average. The trimmed mean value was used by discarding the highest and lowest 25% (5 samples for each) of 20 compression tests. For concrete three 100-mm cubes were tested and averaged.

The fractured pieces were collected after compression for further characterization. The samples were immersed in acetone to prevent further hydration. After 7 days in acetone, samples were oven dried at  $105^{\circ}$ C for 24 hours. The samples were pulverized and sieved passing 75  $\mu$ m for Thermogravimetric analysis (TGA) and selective acid dissolution test.

# 4.2.5. Determination of fly ash reaction degree

To determine reaction degree of fly ash in pastes subjected to carbonation curing selective acid dissolution test was conducted with picric acid - methanol solution and water system (<u>Li et al., 1985</u>). Theoretical basis of the method was in that when mixed with acid solution the only non-soluble phase in fly ash-OPC paste was the unreacted fly ash (<u>Ohsawa et al., 1985</u>; <u>Li et al., 1985</u>). Therefore it was assumed that the unreacted fly ash was the only residue in acid solution and able to be decoupled from the blended matrix (<u>Poon et al., 2000</u>; <u>Zeng et al., 2012</u>).

To make the results comparable all calculations were based on sample ignited mass. The percent loss on ignition (LOI) was calculated using Eq. 4.7.

LOI (%) = 
$$\frac{M_0 - M_1}{M_1} \times 100\%$$
 (4.7)

Where  $M_0$  and  $M_1$  represent the initial and ignited sample weight, respectively. The test was conducted at ignition temperature of 950 °C for 1 hour.

For selective acid dissolution test approximately 1 gram sample  $(m_0)$  was added with 15 grams of picric acid and 60 mL of methanol (AR Grade). After magnetic stirring for 15 min 40 mL distilled water was added. The mixture was stirred for another 60 min and then filtered through Whatman No.41 filter paper (ashless after burning). The filter paper was washed by methanol to remove the color of picric acid and further washed with 300 mL distilled water at  $60 \pm 5$  °C. The filter paper and residue were transferred into

porcelain crucible. The crucible was then ignited in an electric furnace at 950 °C for 3 hours and weighed after cooling to room temperature to obtain the residue mass  $m_{residue}$ .

$$W_{residue} = \frac{m_{residue}}{m_0 / (1 + \text{LOI})} \tag{4.8}$$

The percent residue weight  $W_{residue}$ , was calculated using Eq. 4.8, in which  $m_0$  represents the mass of initial powder sample,  $m_{residue}$  the mass of residue and  $m_0/(1+\text{LOI}) = M_1$  the ignited mass representing original cement and fly ash without reaction products.

In reality cement may not be fully dissolved and fly ash may contain soluble component. Hence calibration was necessary to count the actual amount of unreacted fly ash from the measured residue. It was accomplished by performing the same acid dissolution test on as-received fly ash and as-received cement (Zeng et al., 2012). The residue  $W_{residue,c}$  of as-received cement was subtracted from the gross residue weight obtained from fly ash-OPC paste,  $W_{residue,fac}$ . The residue  $W_{residue,fa}$  in as-received fly ash was used as initial fly ash reference. The fly ash reaction degree was thus calculated using Eq. 4.9.

$$\alpha \,(\%) = \frac{W_{residue,fac} - W_{residue,c} \times p_c}{W_{residue,fa} \times p_{fa}} \times 100\% \tag{4.9}$$

Where  $p_c$  and  $p_{fa}$  represent portion of cement and fly ash in binder material respectively,  $p_c + p_{fa} = 1$ . In 20% fly ash-OPC paste,  $p_c = 80\%$  and  $p_{fa} = 20\%$ , while in 50% fly ash-OPC paste,  $p_c = p_{fa} = 50\%$ .

# 4.2.6. Determination of cement reaction degree

Reaction degree of cement was assessed by the content of non-evaporable water ( $W_n$ ). It was assumed that when fully hydrated one gram of cement contained 0.23 gram of non-evaporable water (Neville, 1995) and one gram of fly ash contained 0.19 gram of non-evaporable water in reaction products (Zeng et al., 2012). To examine the reaction degree of cement subjected to carbonation curing the equivalent non-evaporable water was introduced (Berger et al., 1972). Calcium carbonate in carbonated sample was converted to calcium hydroxide. The conversion from  $CO_2$  to  $H_2O$  was based on carbonation reaction of calcium hydroxide in which one mole of water in CH was replaced by one mole of  $CO_2$  (Berger et al 1972). Thus the total equivalent non-evaporable water  $W_{n,eq}$  was calculated following Eq. 4.10.

$$W_{n,eq} = W_{n,csh} + W_{n,ch} + W_{n,cc} (4.10)$$

Where  $W_{n,csh}$ ,  $W_{n,ch}$  and  $W_{n,cc}$  are the non-evaporable water decomposed from C-S-H, the non-evaporable water from calcium hydroxide and the equivalent water converted from calcium carbonate, respectively.

For fly ash-OPC paste, the reaction degree of fly ash should be considered. The non-evaporable water in fly ash reaction products was calculated based on stoichiometry and chemical composition (Zeng et al., 2012) and subtracted from the total equivalent  $W_{n,eq}$  in Eq. 4.11. The cement reaction degree,  $\beta$ , was obtained.

$$\beta = \frac{W_{n,eq} - \alpha \times 0.19 \times p_{fa}}{0.23 p_c} \times 100\%$$
 (4.11)

Where 0.23 and 0.19 denote non-evaporable water in cement and fly ash reaction products after full reaction, respectively.  $\alpha$  is the fly ash reaction degree calculated from Eq. 4.9.  $p_c$  and  $p_{fa}$  represent portion of cement and fly ash in binder. For OPC paste without fly ash,  $p_c = 1$  and  $p_{fa} = 0$ .

The content of non-evaporable water and carbon dioxide was acquired from Thermogravimetric analysis (TA instrument Model Q500 with helium). Test started from 30 °C till 950 °C at the increasing rate of 5 °C/min.

### 4.2.7. Concrete test

Based on test results of paste samples carbonation curing was performed on concrete with 20% fly ash replacement of cement. The same carbonation procedure was followed (Fig. 4.1). Carbonation duration was fixed at 12 hours and 5 bar gas pressure. Compression tests of 100-mm cubes were conducted after 1, 28, and 90 days. Concrete samples were split to expose the cross section for phenolphthalein solution spray to measure carbonation depth. PH was measured through flat head pH probe using ion

extraction method (Heng and Murata, 2004). The measuring site was covered by absorptive paper with dimension of  $10 \times 10$  mm. The absorptive paper was then soaked with  $100~\mu L$  deionized water and set for 15 min to reach ions equilibrium. The extracted pore solution by the absorptive paper was measured using the pH probe. The pH value measured on hydrated OPC concrete was in range of 12.7 to 13.0. This method was non-destructive and applicable at both early and late ages.

Concrete permeability was evaluated through surface resistivity measurement as prescribed by AASHTO TP95. Samples were immersed in water for 48 hours before test (25 °C). The surface resistivity of saturated surface dry concretes was measured with Proceq Resipod Resistivity Meter with four-point probes. Electric current was induced between outer two probes and detected by inner ones for calculation of resistivity. Three measurements were averaged.

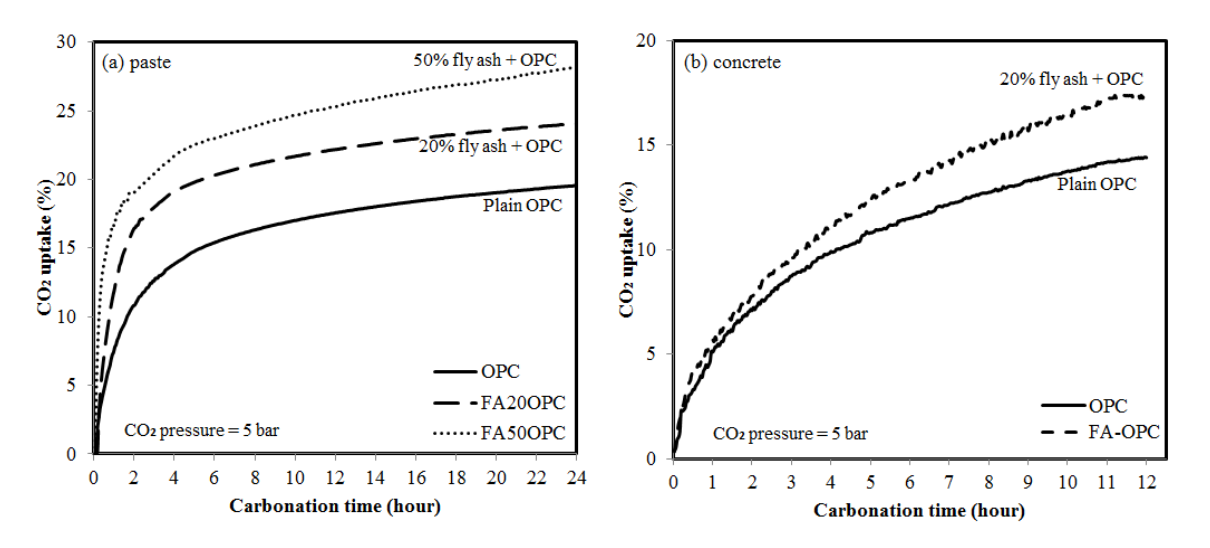


Fig. 4.2. CO<sub>2</sub> uptake mass curves of paste and concrete samples

#### 4.3. RESULTS AND DISCUSSIONS

### 4.3.1. Degree of carbonation reaction

Carbonation degree of fly ash-OPC pastes was quantified by CO<sub>2</sub> uptake according to OPC mass. Fig. 4.2(a) shows the mass curve of paste samples during 24-hour carbonation process. The reaction rate was high at beginning and significantly slowed down after 4 hours. It was clear that pastes with higher fly ash content absorbed more CO<sub>2</sub> with reference to mass of cement. CO<sub>2</sub> uptake after 24-hour carbonation increased from 19.57% in plain OPC to 24.10% and 28.20% in 20% and 50% blended cement, respectively. CO<sub>2</sub> uptake measured from mass gain method was 19.08% in OPC, 23.36% in FA20OPC and 26.98% in FA50OPC. Results of mass gain and mass curve methods were consistent with deviation less than 5%. Fig. 4.2(b) shows the mass curve of concrete samples during 12-hour carbonation. The mass curve recorded CO<sub>2</sub> uptake of 14.41% in OPC concrete and 17.38% in fly ash-OPC concrete while mass gain method showed 14.30% and 17.06% in OPC and fly ash-OPC concrete, respectively.

Fly ash concrete seemed more reactive with CO<sub>2</sub>. With the same water to binder ratio effective water to cement ratio increased as fly ash added because of the reduction in OPC content. Higher water to cement ratio prompted more porous structure and cement grains became easier to be separated by free water and fly ash grains. Hence the enlarged distance between cement grains provided higher possibilities for the reaction with CO<sub>2</sub>. On the other hand, carbonation reaction only took place in aqueous condition and thus more free water resulted in larger amount of CO<sub>2</sub> dissolution enabling higher degree of carbonation.

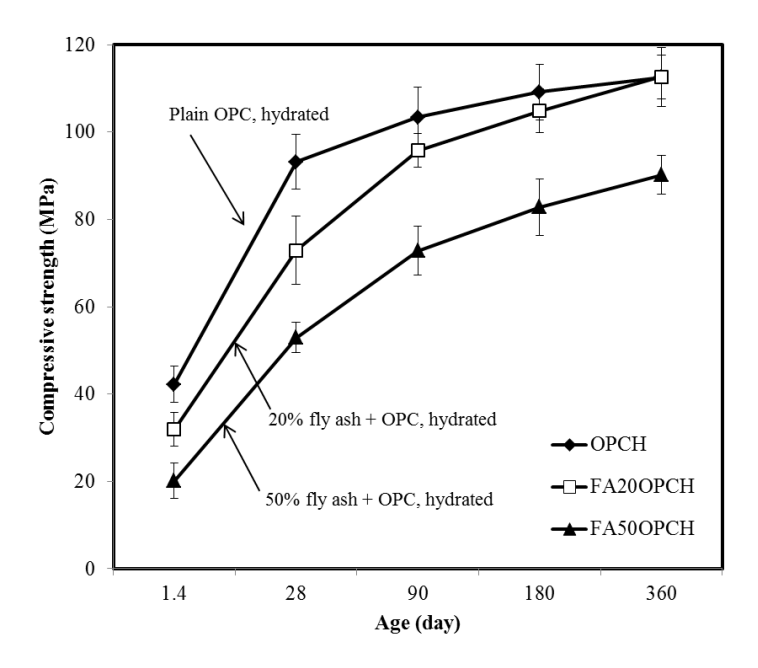


Fig. 4.3. Compressive strength of hydrated OPC and fly ash-OPC pastes

## 4.3.2. Compressive strength of fly ash-OPC pastes

Fig. 4.3 shows the hydration strength of OPC and FAOPC pastes from 1.4 days to 360 days (~ 1 year) as reference. OPC paste displayed highest early strength at 1.4 days comparing to samples with 20% (FA20OPCH) and 50% (FA50OPCH) fly ash replacement. This was due to the high cement content in OPC samples. At 28 days OPC paste gained strength of 93.22 MPa reaching about 83% of its 1-year strength. In contrast, FA20OPCH and FA50OPCH reached only 65% and 59% of the 1-year strength, respectively. This result was consistent with previous work (Lam et al., 2000; Neville, 1995) and indicated that reaction of fly ash was rather slow and took longer than 28 days. Strength gain after 90 days in OPC paste was less notable. However, strength of FA20OPCH and FA50OPCH still remained higher increasing rate. After 1 year curing, the strength of 20% fly ash-OPC cement appeared close to that of OPC paste.

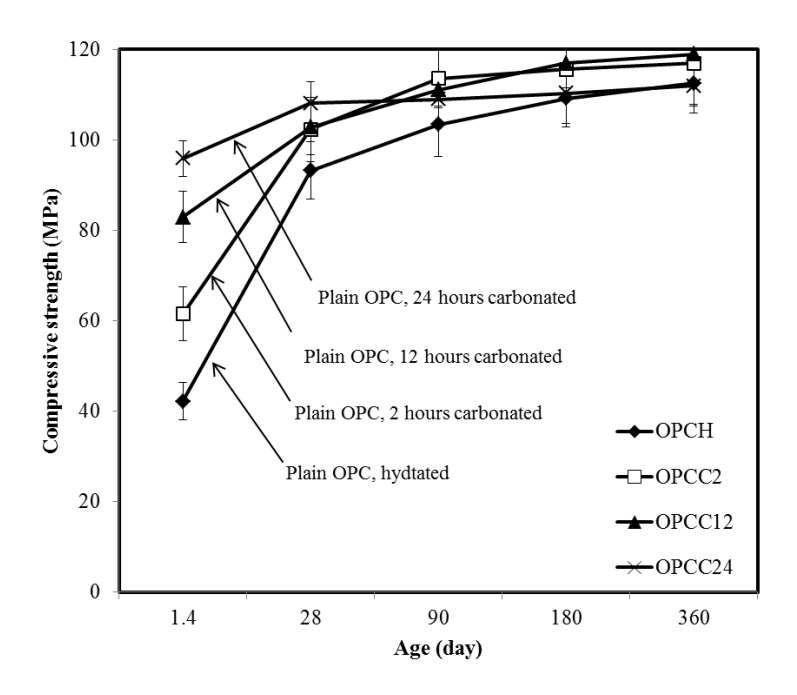


Fig. 4.4. Compressive strength of carbonated OPC pastes

Carbonation effect on strength of OPC paste is compared in Fig. 4.4. In the early age (within 1.4 days) carbonation curing produced higher strength (OPCC) than hydration reference (OPCH). The early strength seemed proportional to carbonation duration. 24-hour carbonation increased the 1.4-day strength from 42.22 MPa (OPCH) to 95.90 MPa (OPCC24) by more than 50%. After 1-year subsequent hydration carbonation cured sample still demonstrated slightly higher strength than hydrated control. The difference of 1-year strength was mainly due to microstructure change created by early carbonation (Rostami et al., 2012). Strength measured on OPC paste suggested that carbonation accelerates strength gain in early age while maintaining high strength in the long term.

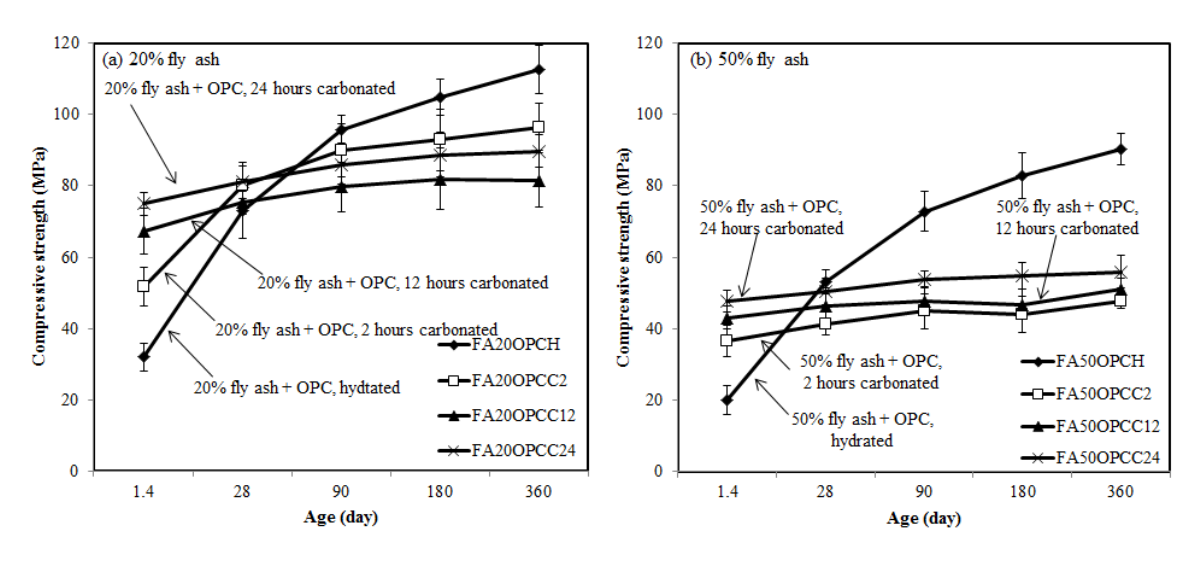


Fig. 4.5. Compressive strength of carbonated OPC pastes

The effect of carbonation on fly ash-OPC paste is compared in Fig. 4.5. It was seen that 1.4-day strength was increased from 31.95 MPa (FA20OPCH) to 74.93 MPa (FA20OPCC24) in 20% fly ash-OPC paste and from 20.15 MPa (FA50OPCH) to 47.69 MPa (FA50OPCC24) in 50% fly ash-OPC paste. Carbonation curing of 24 hours increased early strength by 134% and 136% in FA20OPC and FA50OPC, respectively which appeared more significant than that in OPC paste (127%). It was also consistent with the results of CO<sub>2</sub> uptake.

Despite of the enhanced early strength by carbonation curing strength gain after 28 days seemed slower in carbonated pastes. In Fig. 4.5(a) for 20% fly ash-OPC pastes, with reference to the strength at 24 hours strength increase in 1 year was 252% in hydrated reference (FA20OPCH), 86% in 2-hour carbonation, 21% in 12-hour carbonation and 20% in 24-hour carbonation. Carbonation degree played a role as well. Carbonation of 2-hour duration produced lower early strength but higher 1-year strength in comparison with 12-hour and 24-hour carbonation. It was likely that less carbonation

left more space for subsequent hydration. The same trend was observed in 50% fly ash-OPC samples shown in Fig. 4.5(b). With reference to 1.4-day strength the increase of 1-year subsequent hydration was 347% in hydrated reference (FA50OPCH), 30% in 2-hour carbonation, 19% in 12-hour carbonation and only 17% in 24-hour carbonation.

It was indicative that pozzolanic reaction in fly ash-OPC system was hindered by early carbonation. It seemed more severe in high volume fly ash concrete. In concrete with 20% fly ash replacement, however, the difference was not significant. The 1-year strength after 2-hour carbonation curing (96.52 MPa) was still comparable to hydration reference (112.69 MPa). To balance between the early age carbonation and pozzolanic reaction degree of carbonation curing should be controlled.

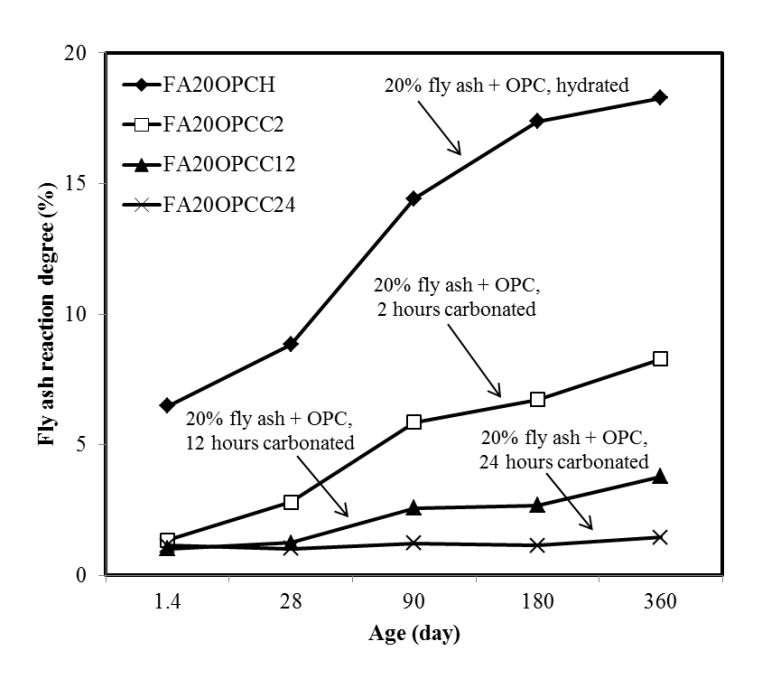


Fig. 4.6. Fly ash reaction degree of 20% fly ash-OPC pastes

# 4.3.3. Reaction degree of fly ash

Selective acid dissolution test was conducted on fly ash-OPC pastes from 1.4 days to 360 days to evaluate the impact of carbonation curing on pozzolanic reaction. The calculation was based on original mass of cement and fly ash without reaction products, i.e. the ignited mass for comparison. Results of fly ash reaction degree are shown in Fig. 4.6 and Fig. 4.7 for 20% and 50% fly ash-OPC pastes, respectively.

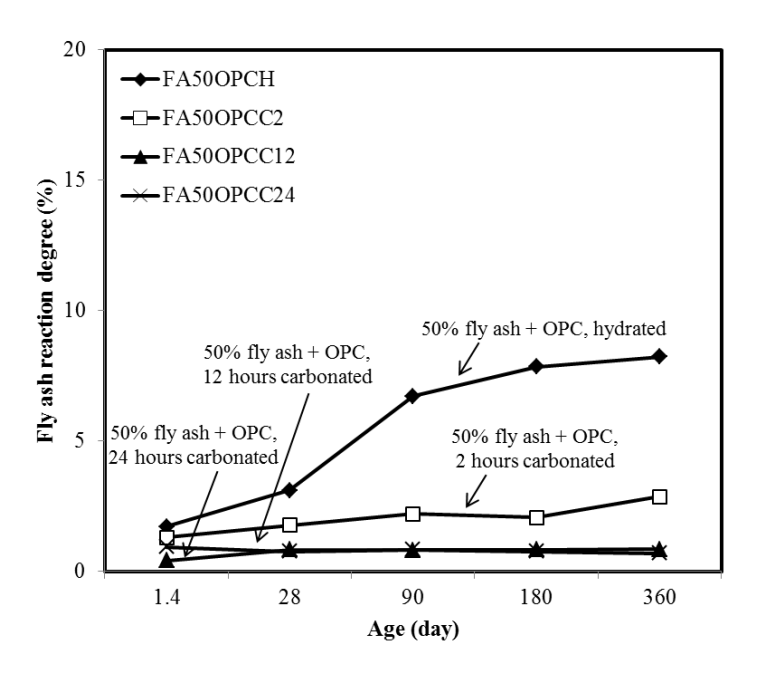


Fig. 4.7. Fly ash reaction degree of 50% fly ash-OPC pastes

For paste with 20% fly ash (Fig. 4.6) approximately 6.5% of fly ash was consumed before 28 days in hydrated sample (FA20OPCH). This was possibly caused by fly ash participation of ettringite formation (<u>Lam et al., 2000</u>). In contrast, fly ash reaction was measured rather low in carbonated samples since carbonation reduced the alkalinity which was essential condition for pozzolanic reaction. It was found in Fig. 4.6 that

carbonation curing slowed down fly ash reaction immediately at the age of 1.4 days. Reaction of fly ash in carbonated pastes took place only after 27 days subsequent hydration. Nevertheless, as curing proceeded samples with higher carbonation degree displayed lower degree of fly ash reaction. After 1-year subsequent hydration the highest result in carbonated samples was measured on 2-hour carbonation curing (FA20OPCC2) in which case reacted portion of fly ash reached 8.27% corresponding to about half of that in the hydration reference of 18.27% (FA20OPCH). Comparatively carbonation of 24 hours only reached the reaction degree of 1.44% after 1 year indicating less opportunity for pozzolanic reaction. The reaction degree of fly ash seemed highly sensitive to carbonation extent. It was clear that controlled carbonation was necessary to gain pozzolanic reaction through subsequent hydration in the long term.

Fig. 4.7 shows fly ash reaction degree in 50% fly ash-OPC paste. After 1-year hydration fly ash reaction degree was 8.23% while 2-hour carbonation curing sample reached only 2.85%. Curves of 12-hour and 24-hour carbonation seemed close to each other and both measured the 1-year reaction degree less than 1%. Consequently most of the fly ash acted as filler in cement paste. This observation was consistent with the compressive strength results as well.

# 4.3.4. Reaction degree of cement

The content of equivalent non-evaporable water acquired from TGA was used to determine the reaction degree of cement. Fig. 4.8 shows typical TG/DTG curves for hydrated and carbonated samples after 360 days. Based on DTG curve the mass loss from

105 °C to 420 °C was attributed to the non-evaporable water detached from C-S-H and calcium hydroxide.  $CO_2$  accounted for mass loss from 450 °C till 900 °C in which range calcium carbonate was decomposed.

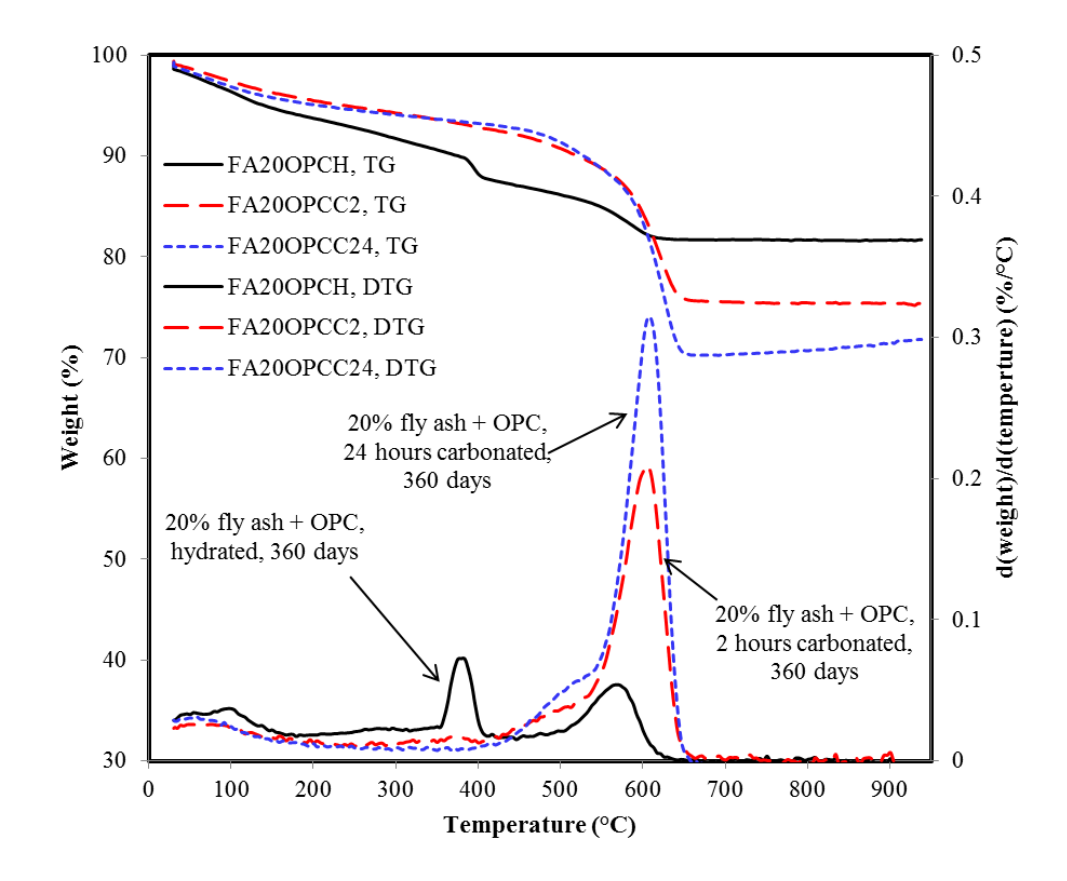


Fig. 4.8. Typical TG/DTG curve of fly ash-OPC pastes at 360 days

Equivalent non-evaporable water was calculated considering water bound in C-S-H and calcium hydroxide and the converted equivalent water from calcium carbonate. Fig. 4.9 compares the reaction degree of cement in OPC paste with respect to curing ages. It was evident that the cement reaction was accelerated by carbonation curing. Prolonged carbonation promoted higher degree of cement reaction. Carbonation of 24 hours consumed 76.90% of cement compared to 53.08% in hydration reference. The

accelerated strength gain was the primary contribution to the improved early age properties. Cement reaction remained increasing after the early carbonation. Nevertheless, this increase was seen at slower rate comparing to the hydration reference. After 1 year, cement reaction degrees between the carbonated and the hydrated were of close despite that carbonation was slightly higher.

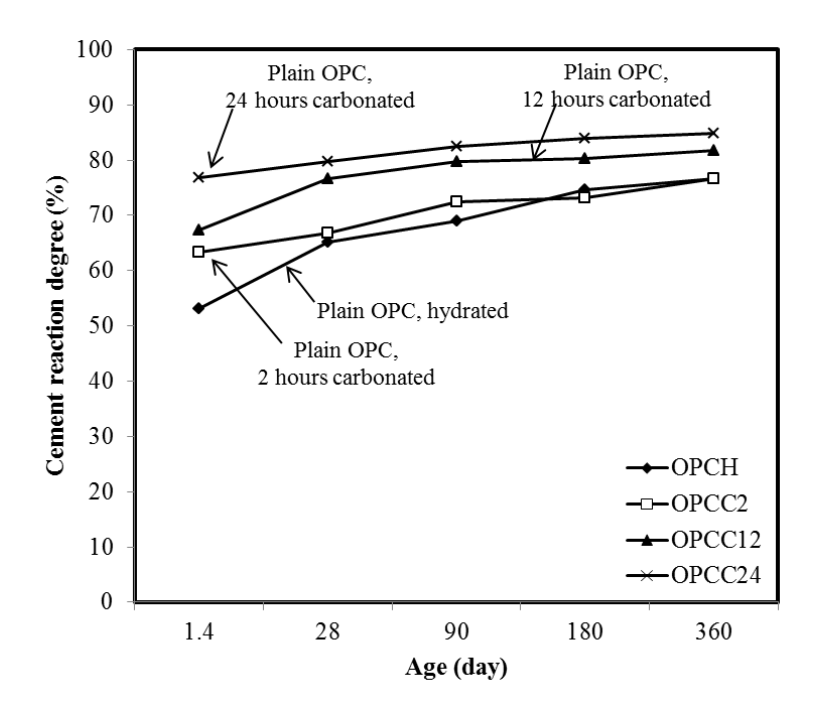


Fig. 4.9. Cement reaction degree in OPC paste

Cement reaction degrees in fly ash-OPC paste are compared in Fig. 4.10 and 4.11 for 20% and 50% fly ash-OPC systems. As observed in OPC paste carbonation curing accelerated cement reaction at early age. Cement reaction degree was slowed down after early carbonation but still maintained higher than hydration reference in total. It was suggestive for low volume of fly ash replacement such as 20%, carbonation curing could achieve relatively higher cement reaction degree in both short and long terms. Fig. 4.11

shows the case of high volume fly ash (HVFA) with 50% cement replacement. The acceleration effect of carbonation curing on cement reaction was still noticeable at 1.4 days. However, the four curves appeared of close after 90 days. Reaction degrees were over 90%. It was noted that cement reaction degree was assessed in terms of hydration and carbonation. The high degree of cement reaction in high volume fly ash cement was attributed to the significant carbonation. It would lead to less subsequent hydration as well as less calcium hydroxide produced in the late age.

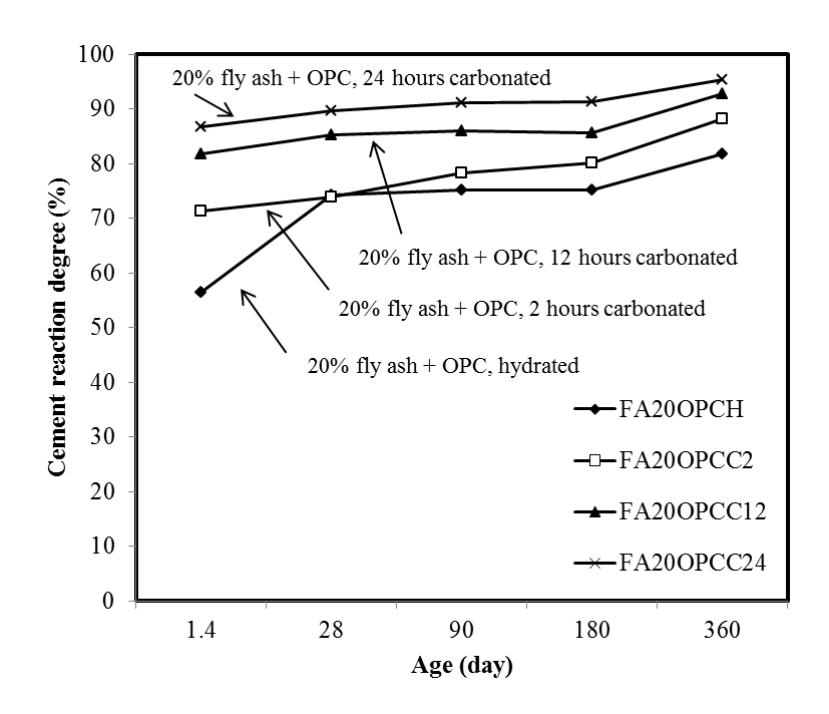


Fig. 4.10. Cement reaction degree in 20% fly ash-OPC paste

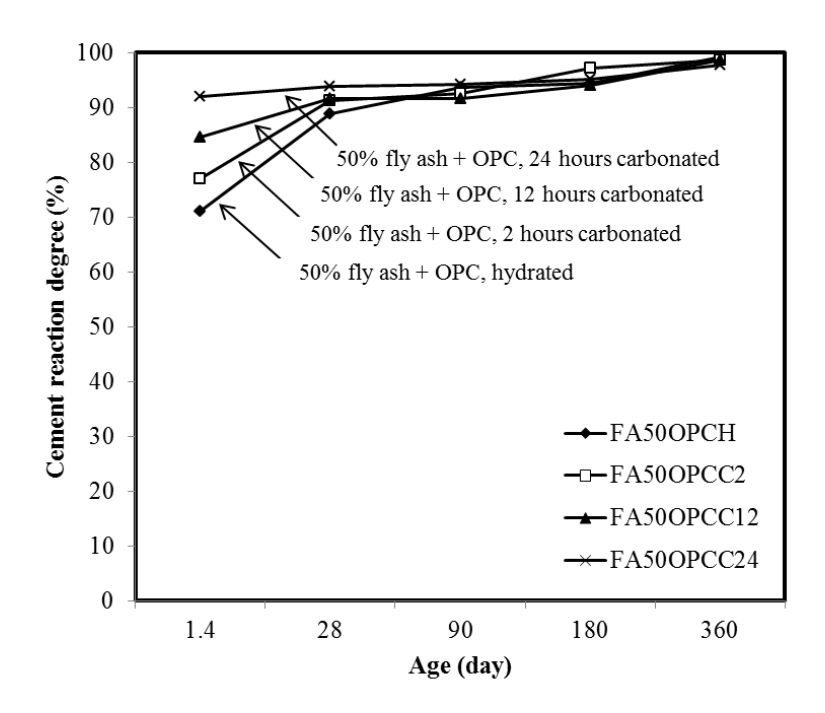


Fig. 4.11. Cement reaction degree in 50% fly ash-OPC paste

Table 4.3. Calcium hydroxide content in hydrated and carbonated cement pastes

Fly ash	Curing ragima	Calcium hydroxide content, wt %				
addition Curing regime		1.4 days	90 days	360 days		
OPC	Hydration	14.40	16.77	17.82		
	Carbonation, 2 hours	2.77	4.23	4.77		
	Carbonation, 12 hours	2.34	3.97	4.34		
	Carbonation, 24 hours	2.29	3.37	3.42		
FA=20%	Hydration	10.61	11.90	11.44		
	Carbonation, 2 hours	2.68	4.10	2.02		
	Carbonation, 12 hours	2.04	3.96	2.65		
	Carbonation, 24 hours	1.53	2.97	1.49		
FA=50%	Hydration	7.61	6.72	5.74		
	Carbonation, 2 hours	1.51	2.36	2.07		
	Carbonation, 12 hours	1.35	2.30	1.90		
	Carbonation, 24 hours	1.23	2.23	1.67		

Table 4.3 summarizes the calcium hydroxide (CH) content in fly ash-OPC paste batches as indication of hydration degree. In OPC pastes hydration produced CH in range

from 14.40% at 1.4 d to 17.82% at 1 year. Carbonated OPC pastes had shown CH content below 5%. For fly ash batches CH content was decreased with the increase of fly ash or the decrease of cement. It seemed that formation of CH mostly took place in the first 24 hours in all batches. The subsequent hydration did not considerably promote CH growth, although the strength gain was obvious (Fig 4.4 and 4.5). The reduction of CH in carbonated fly ash-OPC system was attributed to both carbonation and pozzolanic reactions.

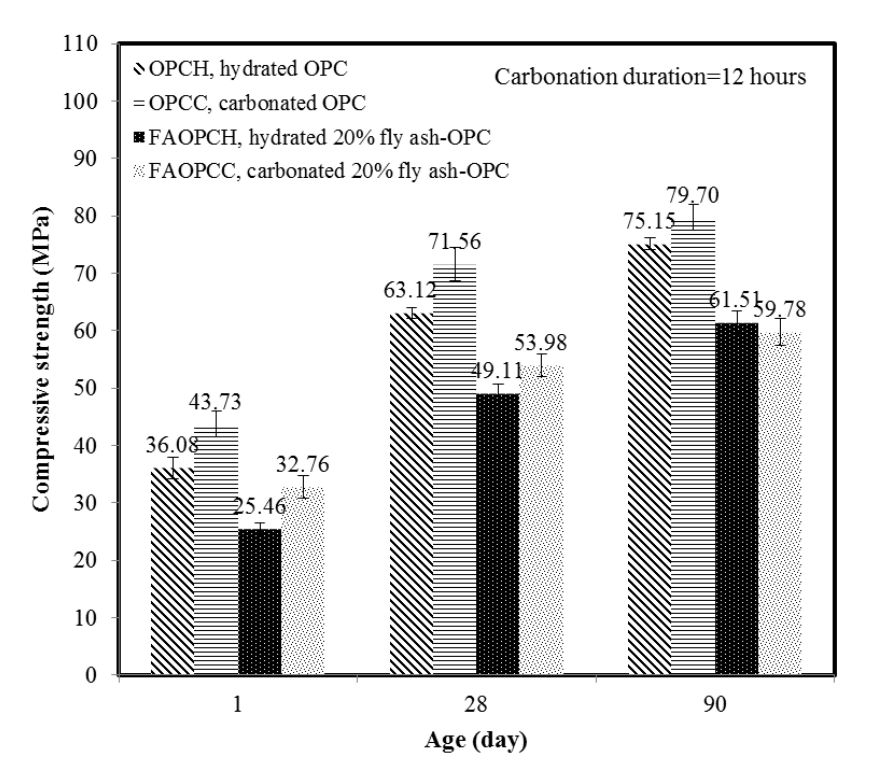


Fig. 4.12. Compressive strength of hydrated and carbonated concrete

## 4.3.5. Properties of carbonated fly ash concrete

Based on the above studies on pastes, concrete with 20% fly ash was selected for carbonation curing of 12 hours at 5 bar to examine its feasibility on fly ash concrete. Fig.

4.12 compares compressive strength at 1, 28 and 90 days. Compressive strength of OPC concrete was enhanced through carbonation curing (OPCC) and the advantage maintained up to 90 days. Nevertheless, compressive strength increase was marginal after 28 days. This trend was in agreement with strength development in the paste samples showing that carbonation accelerated early strength without sacrificing the long term strength with absence of fly ash.

For fly ash-OPC concrete the strength was improved by carbonation curing at 1 and 28 days. It was more significant on 1-day strength which increased from 25.46 MPa to 32.76 MPa by approximately 29%. However, after 90 days hydrated concrete showed compressive strength of 61.51 MPa which was slightly higher than that of carbonated sample of 59.78 MPa. Since 90-day strength was attributed to the summed up effect of both early carbonation and pozzolanic reaction of fly ash it was indicative that pozzolanic reaction was weakened in concretes cured by carbonation. Nevertheless, unlike pastes the difference in strength was not as significant since carbonation occurred mostly on the surface of 100-mm concrete. Both hydrated and carbonated fly ash-OPC concretes had shown lower strength than the OPC concretes.

Table 4.4. Carbonation profile and pH distribution in concrete

Sample	CO <sub>2</sub> uptake	Carbonation depth, mm		pH - 1 day		pH - 28 days	
	%	1 day	28 days	Core	Surface	Core	Surface
ОРС-Н	N/A	N/A	N/A	12.8	13.0	12.7	12.8
OPC-C	14.3	15.5	0	12.7	9.3	12.8	12.7
FAOPC-H	N/A	N/A	N/A	12.5	12.8	12.9	12.6
FAOPC-C	17.06	18.5	0	12.8	9.4	12.7	12.5

Table 4.4 summarizes CO<sub>2</sub> uptake, carbonation depth and pH values of concrete subjected to carbonation curing. Carbonation degree was higher as fly ash added. CO<sub>2</sub> uptake was 17.1% in fly ash concrete versus 14.3% in OPC concrete based on cement mass. The carbonation depth was also increased from 15.5 mm in OPC concrete to 18.5 mm in fly ash-OPC concrete. However, the carbonation depth was reduced to 0 mm after 27-day subsequent hydration. The pH value was measured on both surface and core of the 100-mm cube. For OPC concrete pH was measured 9.3 on surface right after carbonation. However, core region pH remained 13.0 indicating that the region was free from carbonation. Similar pH profile was found in fly ash-OPC concrete. It was suggested that carbonation was limited on concrete surface. After 27-day subsequent hydration surface pH increased to normal level (higher than 12.5). In OPC concrete, surface pH was recovered to 12.7 which was close to that of hydration sample (12.8). In fly ash concrete, the surface pH was increased to 12.5 as well. Despite consumption of calcium hydroxide due to carbonation and pozzolanic reaction, the alkalinity in pore solution was able to maintain pH above 12.5. The protection for passivation of steel rebar was not affected by carbonated fly ash-OPC concrete.

Table 4.5. Surface resistivity of concrete

Λαο	Curing regime		Resistivity,
Age	Curing regime		kΩ.cm
		OPC	FA-OPC
1 day	Hydration	4.9	8.9
	Carbonation curing	40.9	38.4
28 days	Hydration	8.9	22.5
	Carbonation curing	47.3	52.0
90 days	Hydration	12.0	31.2
	Carbonation curing	51.6	66.9

Surface resistivity is shown in Table 4.5. It was noted that the addition of fly ash resulted in higher resistivity thus improved resistance to permeation in comparison to OPC concrete. This was attributed to less permeable microstructure created by pozzolanic reaction. In addition, carbonation effect seemed more profound. At 1 day carbonated concretes showed dramatically higher surface resistivity in contrast to hydration reference. The impact on OPC concrete appeared more effective than on fly ash-OPC concrete. Surface resistivity increased with subsequent hydration due to more hydrates deposited in the pore structure. Nevertheless, carbonated concretes maintained higher resistivity value with prolonged curing ages. The result of surface resistivity indicated that carbonation densified pore structure on surface by precipitating more carbonates in the early age. Accordingly less permeable structure was formed at least on the concrete surface.

#### 4.4. CONCLUSIONS

- 1. The relation between carbonation reaction and pozzolanic reaction in fly ash concrete was studied through quantitative analysis of fly ash reaction degree and cement reaction degree. It was found that pozzolanic reaction of fly ash in fly ash-OPC system was hindered by early carbonation reaction. Higher early carbonation degree led to lower degree of pozzolanic reaction.
- 2. To maximize benefits gained from both reactions it was necessary to conduct controlled carbonation on concrete with proper content of fly ash. It was found that concrete with 20% fly ash was able to achieve improved early strength by carbonation

reaction, comparable late strength by pozzolanic reaction and enhanced durability performance as duration of carbonation limited below 12 hours.

- 3. Fly ash-OPC concrete was more reactive with carbon dioxide in comparison to OPC concrete. With 12 hours carbonation concrete with 20% fly ash was able to uptake 17% carbon dioxide based on cement mass, in comparison to 14% in OPC concrete. In fly ash-OPC system, cement grains gained higher chance to react with carbon dioxide since fly ash was inert to carbonation.
- 4. Carbonation curing was carbon sequestration process. Gaseous carbon dioxide was stored in concrete as calcium carbonates for emission reduction. With 20% less cement and 17% carbon uptake by cement, carbon emission reduction by using carbonated fly ash concrete was able to reach 36% with reference to hydrated OPC concrete. The concrete gained high early strength, comparable late strength and significantly improved resistance to permeation. With reduced calcium hydroxide and reduced surface permeability, durability performance was expected to be enhanced.
- 5. Carbonation occurred on concrete surface within 20 mm thick layer. Although the pH value in this layer was reduced to 9.3 immediately after carbonation, it could be increased to above 12.5 after 27 days subsequent hydration. The ultimate pH value of carbonated fly ash concrete was comparable to hydration reference. Therefore the carbonated fly ash concrete is able to be used in reinforced concrete applications.

# ACKNOWLEDGEMENT

The financial supports by Natural Sciences and Engineering Research Council (NSERC) of Canada and by Climate Change and Emissions Management Corporation (CCEMC) of Alberta are gratefully acknowledged.

#### REFERENCES

- ALEXANDER, M. & MAGEE, B. 1999. Durability performance of concrete containing condensed silica fume. *Cement and concrete research*, 29, 917-922.
- BERGER, R., YOUNG, J. & LEUNG, K. 1972. Acceleration of hydration of calcium silicates by carbon dioxide treatment. *Nature*, 240, 16-18.
- BERTOS, M. F., SIMONS, S., HILLS, C. & CAREY, P. 2004. A review of accelerated carbonation technology in the treatment of cement-based materials and sequestration of CO<sub>2</sub>. *Journal of hazardous materials*, 112, 193-205.
- CHEN, C., HABERT, G., BOUZIDI, Y. & JULLIEN, A. 2010. Environmental impact of cement production: detail of the different processes and cement plant variability evaluation. *Journal of Cleaner Production*, 18, 478-485.
- HENG, M. & MURATA, K. 2004. Aging of concrete buildings and determining the pH value on the surface of concrete by using a handy semi-conductive pH meter. *Analytical sciences*, 20, 1087-1090.
- KHAN, M. & LYNSDALE, C. 2002. Strength, permeability, and carbonation of high-performance concrete. *Cement and Concrete Research*, 32, 123-131.
- LAM, L., WONG, Y. & POON, C. 2000. Degree of hydration and gel/space ratio of high-volume fly ash/cement systems. *Cement and Concrete Research*, 30, 747-756.
- LI, D., CHEN, Y., SHEN, J., SU, J. & WU, X. 2000. The influence of alkalinity on activation and microstructure of fly ash. *Cement and Concrete Research*, 30, 881-886.
- LI, S., ROY, D. M. & KUMAR, A. 1985. Quantatative determination of pozzolanas in hydrated systems of cement or Ca(OH)<sub>2</sub> with fly ash or silica fume. *Cement and Concrete Research*, 15, 1079-1086.
- LOTHENBACH, B., SCRIVENER, K. & HOOTON, R. 2011. Supplementary cementitious materials. *Cement and Concrete Research*, 41, 1244-1256.
- NEVILLE, A. M. 1995. *Properties of concrete*, Longman Group UK Limited.

- OHSAWA, S., ASAGA, K., GOTO, S. & DAIMON, M. 1985. Quantitative determination of fly ash in the hydrated fly ash-CaSO<sub>4</sub>· 2H<sub>2</sub>O· Ca(OH)<sub>2</sub> system. *Cement and Concrete Research*, 15, 357-366.
- POON, C., LAM, L. & WONG, Y. 2000. A study on high strength concrete prepared with large volumes of low calcium fly ash. *Cement and Concrete Research*, 30, 447-455.
- ROSTAMI, V., SHAO, Y. & BOYD, A. J. 2011. Durability of concrete pipes subjected to combined steam and carbonation curing. *Construction and Building Materials*, 25, 3345-3355.
- ROSTAMI, V., SHAO, Y., BOYD, A. J. & HE, Z. 2012. Microstructure of cement paste subject to early carbonation curing. *Cement and Concrete Research*, 42, 186-193.
- YOUNG, J., BERGER, R. & BREESE, J. 1974. Accelerated curing of compacted calcium silicate mortars on exposure to CO<sub>2</sub>. *Journal of the american ceramic society*, 57, 394-397.
- ZENG, Q., LI, K., FEN-CHONG, T. & DANGLA, P. 2012. Determination of cement hydration and pozzolanic reaction extents for fly-ash cement pastes. *Construction and Building Materials*, 27, 560-569.

#### CHAPTER 5

\_

# PORE STRUCTURE OF CEMENTITIOUS PASTES SUBJECT TO CARBONATION CURING AND ITS EFFECT ON CONCRETE PERFORMANCE

#### **PREFACE**

Hydration and carbonation reactions of cement and fly ash were quantitatively studied in previous chapter. Carbonation curing displayed different reaction products as well as accelerated reaction rate. Concrete strength was improved and surface resistivity increased as a consequence. Durability properties, however, needed to be fully evaluated. In addition to the chemical reaction, physical pore structure in cementitious pastes played critical role in concrete durability performance. Pore structure of binder phase dominated the transport behavior of concrete which was generally considered primary factor of corrosion resistance in reinforced concrete. Another durability issue on concrete in cold regions was frost damage due to freeze and thawing cyclic exposure. Both pore size and volume had impact on the frost deterioration by physically affecting ice formation inside the porous media.

This chapter aimed to investigate the pore structure in cementitious pastes by early carbonation curing and its effect on concrete performance. The pore structure of Ordinary Portland Cement (OPC) and fly ash-OPC pastes was characterized by Mercury Intrusion Porosimetry (MIP) and Nitrogen Adsorption / Desorption (NAD) techniques to cover pore size till 3 nm. Pore structure was tested from 1 day to 1 year to evaluate both short and long term effects of carbonation curing. The performance of corresponding concretes was assessed by permeable porosity, surface resistivity and freeze-thaw scaling resistance. It was found that early carbonation could significantly reduce porosity and pore size at both early (1 day) and late ages (1 year). The process had the capacity to reduce large capillary pores and create more gel pores and ink-bottle pores. As a consequence, concrete porosity was reduced, surface electrical resistivity was enhanced and freeze-thaw resistance was improved.

#### **5.1. Introduction**

Carbonation curing of concrete received an increasing interest in recent years. The process accelerated early strength (Young et al., 1974), enhanced durability (Rostami et al., 2011) and facilitated carbon dioxide utilization (Shao et al., 2006). Performed immediately after casting the reaction took place between calcium silicate phases and carbon dioxide (Eqs. 5.1-5.2) (Young et al., 1974). Reaction products were typically hybrid of calcium silicate hydrates (C-S-H) and calcium carbonates. The ratio of x and y in Eqs. 5.1-5.2 depended on the degree of carbonation at early age (Young et al., 1974). If carbonation carried out after short period of hydration, both calcium silicates and early hydration products were involved in the reaction (Eqs. 5.1-5.4).

$$C_3S + (3-x)CO_2 + yH_2O \rightarrow C_xSH_v + (3-x)CaCO_3$$
 (5.1)

$$C_2S + (2-x)CO_2 + yH_2O \rightarrow C_xSH_y + (2-x)CaCO_3$$
 (5.2)

$$Ca(OH)_2 + CO_2 \rightarrow CaCO_3 + H_2O \tag{5.3}$$

$$C-S-H + 2CO_2 \rightarrow SiO_2 + 2CaCO_3 + H_2O$$
 (5.4)

Unlike weathering carbonation which happened to matured concrete leading to decomposition of calcium hydroxide and calcium silicate hydrates, the early age carbonation occurred on fresh concrete through curing process and was followed by subsequent hydration (El-Hassan et al., 2013). Weathering carbonation reduced pH of concrete and was responsible for steel corrosion (Ahmad, 2003). Nevertheless, research showed weathering carbonation might be beneficial for pore structure of hydrated cement pastes. It was reported on cement pastes that weathering carbonation reduced total

porosity, lowered the water vapour sorption isotherms, and reduced pore size particularly those of radius smaller than 0.1 μm (Houst, 1997). The same phenomenon was observed in lime and lime-cement systems. Carbonation of hydrated products decreased porosity by 10%. The pore size distribution shifted towards smaller pores (Arandigoyen et al., 2006). It was found in blend cements that the total porosity for OPC, OPC-fly ash and OPC-slag pastes was reduced as result of carbonation. However, there was redistribution in pore sizes. The proportion of large pores (diameter > 30 nm) was increased slightly for OPC pastes but much more significantly for the fly ash and slag pastes (Ngala and Page, 1997). The other study found that permeability of concrete subjected to weathering carbonation was increased due to weathering carbonation (Song and Kwon, 2007). It was the coarsening of the pore structure by weathering carbonation that led to the increased permeability (Ngala and Page, 1997).

It remained unclear if early carbonation curing was beneficial to the pore structure refinement. The major difference was the reaction time and duration. Hydration products were enhanced through short but intense carbonation in the early age. In contrast, prolonged carbonation attacked hydration products as the case of weathering carbonation. The purpose of this chapter was to examine the pore structure created in cementitious pastes subjected to carbonation curing and subsequent hydration. Both Ordinary Portland Cement (OPC) and fly ash-OPC systems were studied. Mercury intrusion porosimetry (MIP) and Nitrogen adsorption / desorption (NAD) methods were utilized for pore structure analysis at early (1 day) and late age (1 year). The effect of pore structure change on concrete performance was assessed through permeable porosity, surface electrical resistivity and freeze-thaw resistance tests.

## **5.2. EXPERIMENTAL PROGRAM**

## 5.2.1. Materials and mix proportion

The chemical compositions of CSA (Canadian Standard Association) GU Ordinary Portland Cement (OPC) and fly ash used are shown in Table 5.1. Both cementitious pastes and concretes were investigated. The former was used for pore structure analysis and the latter for assessing effect of pore structure change on concrete performance. The mixture proportions of cementitious paste and concrete are given in Table 5.2. Water to cementitious binder ratio was 0.4 for both paste and concrete. Fly ash was added as 20% replacement of cement by mass. Crushed granite stones and sand were chosen as aggregate in concrete mixture. Fineness modulus of fine aggregate was 3.01 and maximum size of coarse aggregate was 12 mm. The water absorption of fine and coarse aggregate was about 4.3% and 1.6%, respectively. Superplasticizer was added to achieve slump of approximately 160 mm for both OPC and fly ash-OPC concretes.

Table 5.1. Chemical compositions of cement and fly ash (%)

	Ca0	SiO <sub>2</sub>	$Al_2O_3$	$Fe_2O_3$	MgO	$Na_2O_{(eq)}$	SO <sub>3</sub>
Cement	63.10	19.80	4.90	2.00	2.00	0.85	3.80
Fly ash	11.30	54.39	23.65	3.90	1.17	2.91	-

# 5.2.2. Sample preparation and carbonation curing process

Carbonation curing of pastes and concretes followed the process composed of four steps: (1) 5-hour in-mold curing, (2) 5.5-hour de-mold conditioning, (3) 12-hour

carbonation curing and (4) 27-day subsequent hydration. The first two steps were critical to remove portion of free water and facilitate carbonation.

Table 5.2. Mixture proportions of pastes and concretes

	Paste		Сс	oncrete
	OPC	FAOPC	OPC	FAOPC
Cement, kg/m <sup>3</sup>	1391	1113	452	362
Fly ash, kg/m <sup>3</sup>	0	278	0	90
Fly ash to binder ratio, %	0	20	0	20
Water, kg/m <sup>3</sup>	557	557	181	181
Water to binder ratio	0.4	0.4	0.4	0.4
Water to cement ratio	0.4	0.5	0.4	0.5
Coarse aggregate, kg/m <sup>3</sup>	0	0	1060	1060
Fine aggregate, kg/m <sup>3</sup>	0	0	680	680
Superplasticizer to cement ratio, %	N/A	N/A	0.5	0.5
Slump, mm	N/A	N/A	158	166

Pore structure was characterized on paste samples. To simulate the paste in concrete thin sheet of 6 mm thick was chosen based on trial tests to assure the water content in paste remained the same as in concrete after the first two steps. After in-mold curing, thin sheet was cut into 6-mm cubes as paste samples for further conditioning and carbonation curing. Concretes were cast into 100 mm cubes and compacted on vibration table.

Because of the high slump mixture used in both pastes and concretes, in-mold curing for initial set was necessary before demolding. The setting time depended on mix proportion. For the paste and concrete used in this work it took approximately 5 hours in open air (25 °C and 60% relative humidity). Paste and concrete samples were demolded afterwards and left on bottom plate for conditioning by fan drying at wind speed of 1 m/s

in laboratory condition ( $50 \pm 5\%$  RH, 25 °C). It took 5.5 hours to remove 40% of free water. Removal of the free water was necessary to create sufficient space for carbon dioxide to penetrate and for carbonates to precipitate. Carbonation curing was then conducted in pressure chamber with continuous  $CO_2$  supply at gas pressure of 5 bar and purity of 99.8%. The apparatus of carbonation curing is shown in Fig. 5.1. After 12-hour carbonation, the water inside chamber was collected and the final mass was measured. Water was generated during the reaction and should be added to final mass in  $CO_2$  uptake calculation (El-Hassan et al., 2013). The  $CO_2$  uptake was determined based on Eq. 5.5.

CO<sub>2</sub> uptake (%) = 
$$\frac{m_2 + m_{water} - m_1}{m_{cement}} \times 100\%$$
 (5.5)

Where  $m_1$  and  $m_2$  represent sample mass before and after carbonation, and  $m_{\text{water}}$  is the collected water due to evaporation. After carbonation curing samples were transited in moist room (95% RH, 25 °C) for subsequent hydration until the designated testing age. Pore structure was analyzed on paste samples at 1 day and 1 year. Concrete performance was tested at 1, 28 and 90 days. As reference hydration samples were cured in-mold for 24 hours followed by demolding and further curing in the same moisture room.

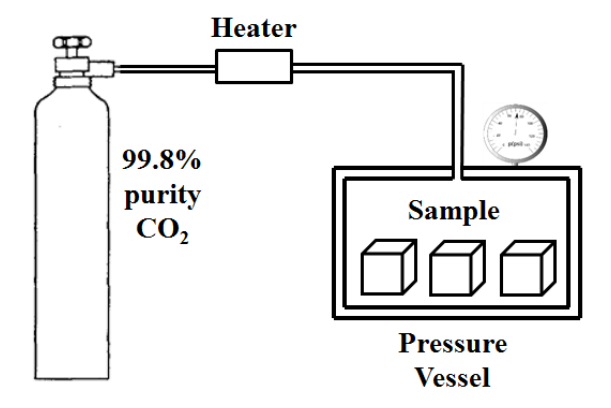


Fig. 5.1. Carbonation curing apparatus

At the designated test age of 1 day and 1 year paste samples were immersed in methanol for 7 days to remove the remaining pore water and then oven dried at 105°C for 2 hours before being crushed into pieces smaller than 0.5 cm. Crushed samples were analyzed by Mercury intrusion porosimetry (MIP) and Nitrogen adsorption / desorption (NAD) methods.

At the age of 1, 28 and 90 days concrete samples were measured compressive strength and surface pH value. Three tests were averaged for compressive strength at designated age. The 1 day test was accomplished by 5 hours in-mold hydration, 5.5 hours de-mold conditioning, 12 hours carbonation and 1.5 hours further hydration. The pH measurement was conducted on sample surface with flat head pH probe (Extech PH110). The testing area was covered by absorptive paper (10 mm  $\times$  10 mm) soaked with 100  $\mu$ L deionized water. The readings were recorded approximately 15 mins at which time the equilibrium was assumed. At least three readings were averaged. The test was non-destructive and suited to both early and late ages. Permeable porosity and surface electrical resistivity tests were also conducted on concrete at the same time. Freeze-thaw scaling tests started at the age of 28 days.

# **5.2.3.** Determination of pore structure

Hydrated cementitious material was typically porous media with pore size ranging broadly from nanometers to millimeters (<u>Taylor</u>, <u>1997</u>). Various techniques were developed to characterize the pore structure. Mercury intrusion porosimetry (MIP) and Nitrogen adsorption / desorption (NAD) were the most widely used methods regarding

pore structure analysis. MIP measured pore size and volume by intruding mercury from low to high pressure corresponding to the various diameters percolated based on Washburn equation (Washburn, 1921). MIP remained widely used due to the comparatively large range in spite of its reduced accuracy on ink-bottle pores in which mercury was not able to be intruded until the pressure increases high enough to percolate the narrow entrance (Diamond, 2000). NAD was based on the phenomenon of gas adsorption on solid surface. The quantity of the adsorbed gas molecules was measured and used to calculate the surface area and pore size. The applied relative pressure  $P/P_0$ was corresponding to pore diameter through Kelvin equation on basis of capillary condensation. Theories were developed on data interpretation including Brunauer-Emmett-Teller (BET) and Barrett-Joyner-Halenda (BJH) based on assumption of multilayer condensation (Barrett et al., 1951; Brunauer et al., 1938). NAD failed to measure pores larger than 60 nm which were too large for molecule condensation to occur. To acquire a full scope of pore size, MIP and NAD were combined to compensate the pore size range (Kaufmann et al., 2009). Comparison between the two methods provided information of pore shape as well (Aligizaki, 2005).

Mercury intrusion porosimetry (MIP) provided information of pore size ranging from a few nanometers to hundreds of micrometers. Calculation of pore diameter from applied mercury pressure was based on Washburn equation shown in Eq. 5.6.

$$d = -\frac{4\gamma\cos\theta}{P} \tag{5.6}$$

Where d represents pore diameter based on assumption of cylindrical geometry shape.  $\gamma$  is surface tension of mercury (0.485 N/m) and  $\theta$  represents the contact angle

between mercury and cementitious material (130°). Volume of mercury intruded at the applied pressure P is corresponding to volume of pores with diameter of d. The testing facility used in this study was Quantachrome Poremaster 33 with maximum applied pressure of 227 MPa which corresponded to the pore diameter of 5.5 nm. To calculate total porosity from total pore volume, a separated test was performed based on the principle of gravimetry by mercury to determine density as shown in Eq. 5.7. Total porosity was acquired by multiplying sample density and total volume measured by MIP.

$$\rho_s = \frac{m_s}{[m_{c1} - (m_{c2} - m_s)]/\rho_{Ho}}$$
 (5.7)

Where  $m_s$  and  $\rho_s$  represent mass and density of sample.  $m_{c1}$  is mass of cell full of mercury at atmospheric pressure and  $m_{c2}$  is mass of cell filled with sample and mercury at atmospheric pressure.  $\rho_{Hg}$  is density of mercury (13.6 g/mL).

Nitrogen adsorption / desorption (NAD) experiment was based on the physical phenomenon of gas adsorption on solid surface. Certain quantity of gas molecules were adsorbed on internal pore wall as pressure increased and recorded with corresponding gas pressure. Desorption followed the same principle with decreasing applied pressure. The adsorption isotherm between adsorption quantity and gas pressure provided basic information of micropores and mesopores. Further assumptions were necessary to acquire interpretations from isotherm. Kelvin equation was used to calculate pore size from gas pressure assuming capillary condensation in small cylindrical pores. The pore size distribution was estimated by Barrett-Joyner-Halenda (BJH) method and specific surface

area was determined by Brunauer-Emmett-Teller (BET) theory. Facility used for NAD experiment was of type TriStar II Micromeritics with nitrogen gas.

#### **5.2.4.** Evaluation of concrete performance

Effect of pore structure change on concrete performance was evaluated by permeable porosity, surface resistivity and freeze-thaw scaling resistance.

Permeable porosity of concrete samples at the age of 1, 28 and 90 days were measured through water absorption experiment prescribed by ASTM C642-06. Concrete mass  $m_A$  was measured after 24 hours drying in 105°C and subsequently cooling in desiccator. Samples were then fully immersed in water for 48 hours at 21°C, boiled in tap water for 5 hours and cooled for 24 hours to temperature of 21°C. They were surface-dried and weighed to gain saturated surface dry mass  $m_B$ . The mass of boiled samples suspended in water was also measured as  $m_C$  to compute the volume of samples. The permeable porosity was calculated by Eq. 5.8. Three samples were tested for average.

Porosity = 
$$(m_B - m_A)/(m_B - m_C) \times 100\%$$
 (5.8)

Surface resistivity was an electrical-based non-destructive test to estimate permeability of hardened concrete (McCarter et al., 2000; Kessler et al., 2008). Studies showed strong correlation between surface resistivity and transport behaviour of concrete. Higher value of surface resistivity indicated more resistance to permeation (Tanesi and Ardani, 2012). Surface resistivity test was conducted on carbonated and hydrated samples at the age of 1, 28 and 90 days as prescribed by AASHTO TP95. Concrete samples were

immersed in water for 48 hours as saturation before test (25 °C). Saturated surface dried samples were measured surface resistivity with Proceq Resipod Resistivity Meter with four-point probe. Electric current was induced between outer two probes and detected by inner ones for calculation of resistivity. Three measurements were taken and the average was used.

Freeze-thaw scaling tests were also conducted to estimate the effect of pore structure on concrete resistance to frost damage. Capillary pores were commonly believed to dominate concrete freeze-thaw behaviour. Due to the low w/c ratio used in this work the test was conducted based on the RILEM TC-154 recommendation to examine the surface scaling. Concrete samples at the age of 28 days were surface dried for 21 days at  $20 \pm 2$  °C and 65% RH. Dried samples were measured mass and half immersed in 3% sodium chloride solution at  $20 \pm 2$  °C for another 7 days. The freeze-thaw cycle followed daily base with 18 hours freezing and 6 hours thawing with temperature range between -20 °C and 20 °C. Mass loss was measured every 25 cycles up to 150 cycles. The results were the average of three sample tests.

#### 5.3. RESULTS AND DISCUSSIONS

### 5.3.1. Carbonation and hydration performance of paste and concrete

Table 5.3 summarizes CO<sub>2</sub> uptake, pH value and strength gain for both pastes and concretes after carbonation and hydration. CO<sub>2</sub> uptake was 17.6% for OPC paste, 14.3% for OPC concrete, 22.2% for fly ash-OPC paste and 17.1% for fly ash concrete. In

comparison to plain OPC samples, both fly ash-OPC paste and concrete appeared more reactive to carbon dioxide showing 26% and 19% increase in CO<sub>2</sub> uptake, respectively. Since carbonation occurred between Portland cement and carbon dioxide, the addition of fly ash enabled each cement particle to react more efficiently with carbon dioxide. Although water to cementitious ratio was kept constant in all batches, the water to cement ratio was higher in fly ash-OPC system because of the reduced cement content, leading to greater contribution to carbon dioxide dissolution and carbonate precipitation.

Table 5.3. Carbonation and hydration performance of pastes and concretes

	Age, day	Carbonation curing		Hydration curing	
		OPC	FAOPC	OPC	FAOPC
Paste CO <sub>2</sub> uptake, %	1	17.6	22.2	-	-
Concrete CO <sub>2</sub> uptake, %	1	14.3	17.1	-	-
Paste surface pH	1	9.1	9.0	12.7	12.6
	360	12.7	12.5	12.6	12.5
Concrete surface pH	1	9.2	9.5	13.0	12.8
	28	12.8	12.7	12.9	12.7
	90	12.6	12.5	12.7	12.5
Concrete strength, MPa	1	$44 \pm 2$	$33 \pm 1$	$37 \pm 2$	$25 \pm 1$
	28	$72 \pm 3$	$54 \pm 2$	$63 \pm 1$	$49 \pm 3$
	90	$80 \pm 2$	$60 \pm 3$	75 ± 2	62 ± 2

Note: CO<sub>2</sub> uptake is based on cement mass.

Surface pH was measured on pastes and concretes. It seemed that the surface was more carbonated than the core area. Carbonation reduced pH on surface to below 10.0 for all carbonation batches. However, with subsequent hydration in moisture room the pH at 28 days, 90 days and 1 year could reach values of above 12.5, which was comparable to hydration references. The pH value of carbonated concrete after 28 days was in the same order of magnitude as that of hydrated concrete.

The effect of carbonation curing on concrete compressive strength was obvious. There was notable increase in 1 day strength by carbonation curing. In comparison to hydration reference at 1 day carbonated concretes showed strength 18% higher in OPC concrete and 29% higher in fly ash-OPC concrete. This strength advantage was retained until 90 days subsequent hydration. Strengths at 90 days appeared comparable. It was 80 MPa in carbonated OPC concrete and 60 MPa in carbonated fly ash-OPC concrete. Correspondingly, their counterpart hydration strength was 75 MPa in OPC concrete and 62 MPa in fly ash-OPC concrete. It seemed that early carbonation reaction did not significantly hinder pozzolanic reaction.

## 5.3.2. Pore structure analysis by MIP

The total pore volume was measured by MIP on cementitious pastes based on cumulative pore volume curves. The measured pore size was in the range from 5.5 nm to 10 µm. Table 5.4 summarizes the pore volume and the corresponding bulk porosity. The comparison between carbonation and hydration suggested that carbonation curing significantly reduced the total pore volume in both OPC and fly ash-OPC pastes. Immediately after carbonation (1 day), the pore volume reduction reached 22% in OPC paste and 19% in fly ash-OPC. After 1 year subsequent hydration the reduction rate was 40% in OPC and 26% in fly ash-OPC paste. The pore volume reduction appeared more obvious in OPC than in fly ash-OPC. This was because in fly ash-OPC paste 20% of cement was replaced by fly ash which was inert to carbonation reaction. The reduction in pore volume at 1 day was exclusively due to carbonation. Carbon dioxide was converted

to calcium carbonate precipitated in pores. After 1 year subsequent hydration and pozzolanic reaction the effect of early carbonation was still able to be observed. The carbonated pastes showed less pore volume than the hydrated, indicating that carbonation was of more dominant role than pozzolanic reaction. The similar trend was observed in porosity change.

Table 5.4. Total pore volume and porosity by MIP

Sample	Total volu	ıme, ml/g	Bulk po	rosity, %
	1 day	1 day 1 year		1 year
OPC - H	0.1110	0.0964	23.61	21.80
OPC - C	0.0865	0.0574	18.84	13.06
FAOPC - H	0.1310	0.1107	26.54	23.88
FAOPC - C	0.1058	0.0822	22.17	18.60

The cumulative and differential pore size distributions are displayed in Figs. 5.2 and 5.3 for OPC pastes and fly ash-OPC paste, respectively. Based on Mehta (Mehta, 1986) pore size in cement paste were classified into five types: C-S-H inter-layer space (1  $\sim$  3 nm), gel and small capillary pores (3  $\sim$  10 nm), medium capillary pores (10  $\sim$  50 nm), large capillary pores (50  $\sim$  100 nm) and macropores (> 100 nm).

For OPC system, the pore size was mostly measured in range of 50-100 nm for hydrated paste and 10-50 nm for carbonated paste (Fig. 5.2b). It seemed that immediately after carbonation (1 day) the dominant pore size shifted to gel pores and small capillary pores as result of carbonation curing. After 1 year subsequent hydration the pore size was further refined from medium capillary pores in hydration reference to gel and small capillary pores in carbonation cured paste (Fig. 5.2d).

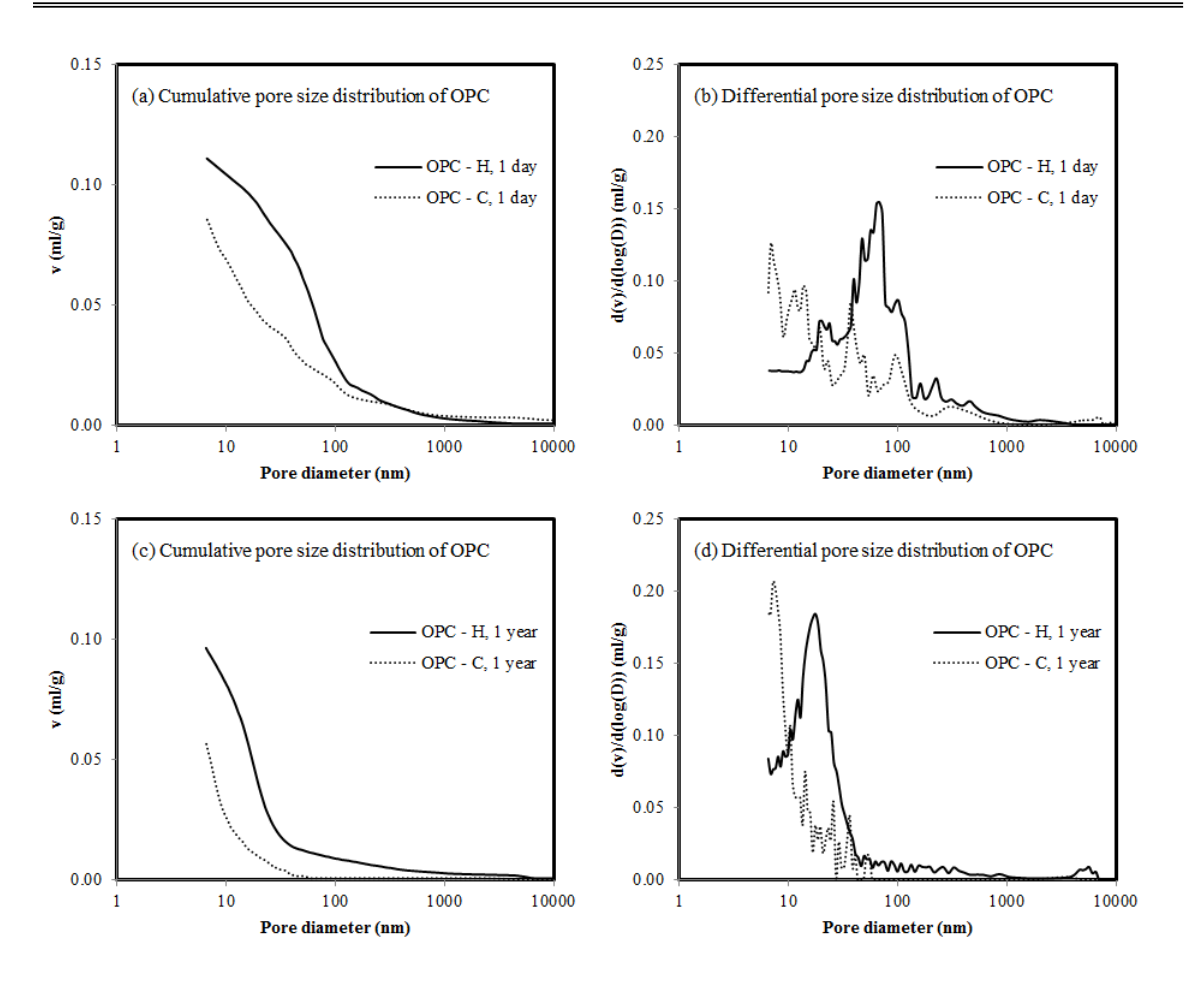


Fig. 5.2. Pore size distribution of OPC pastes by MIP

For fly ash-OPC system, Figs. 5.3(b) and 5.3(d) compare the differential pore size distribution at 1 day and 1 year. Unlike OPC paste, carbonated fly ash-OPC paste showed two peaks in differential pore size distribution curve, both of which shifted to smaller diameter in comparison to hydration reference. With 1 year subsequent hydration and pozzolanic reaction, the pore size was of close value for the two curing processes.

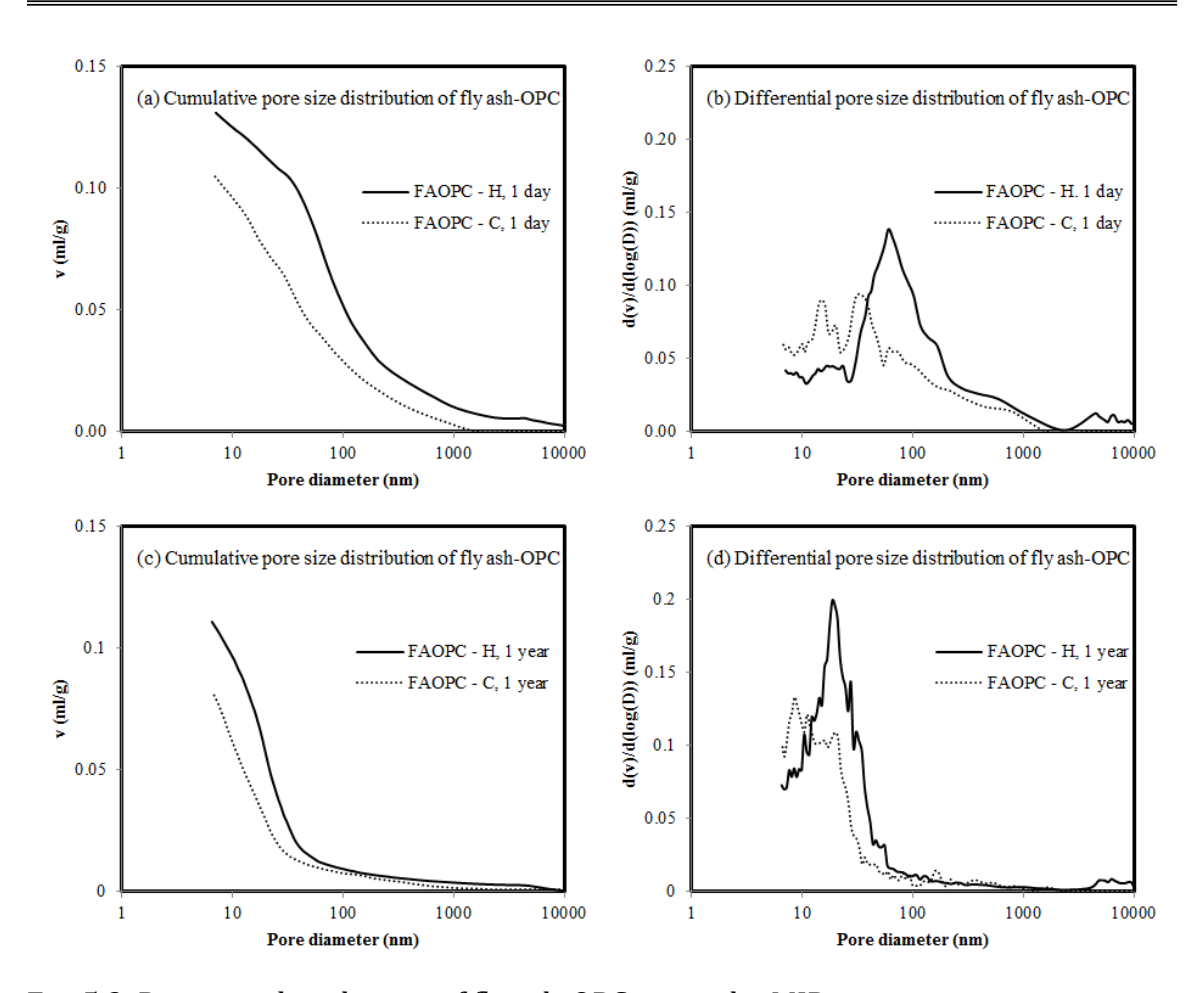


Fig. 5.3. Pore size distribution of fly ash-OPC pastes by MIP

To understand the effect of carbonation on the pore size refinement Fig. 5.4 presents the pore volume in terms of pore size. At 1 day, the dominant pore size shifted from large capillary pores and macropores (larger than 50 nm) in hydrated OPC paste to medium capillary and gel pores in the carbonation cured one. This evolution was quantified as percentage in Fig. 5.4(b). The fraction of large capillary pores and macropores was 55% in hydrated OPC paste but reduced to 31% by carbonation curing (OPC-C, 1 day). It was noted that 1 year subsequent hydration increased difference between the two curing methods. In carbonated OPC paste (OPC-C, 1 year), more than 55% of total pore volume was occupied by pores smaller than 10 nm. Large pores with

diameter more than 100 nm were decreased to only 1% in total porosity. Similarly in fly ash-OPC paste shown in Figs. 5.4(c) and 5.4(d), small pores with diameter less than 50 nm counted for 32% and 58% of total porosity in hydrated (FAOPC-H, 1 day) and carbonated samples (FAOPC-C, 1 day), respectively. The pore structure was further refined after 1 year subsequent hydration and pozzolanic reaction. The small capillary and gel pores (less than 10 nm) were 13% in hydrated pastes (FAOPC-H, 1 year) and 25% in carbonated samples (FAOPC-C, 1 year). Macropores (larger than 100 nm) were reduced to less than 10% by both curing methods.

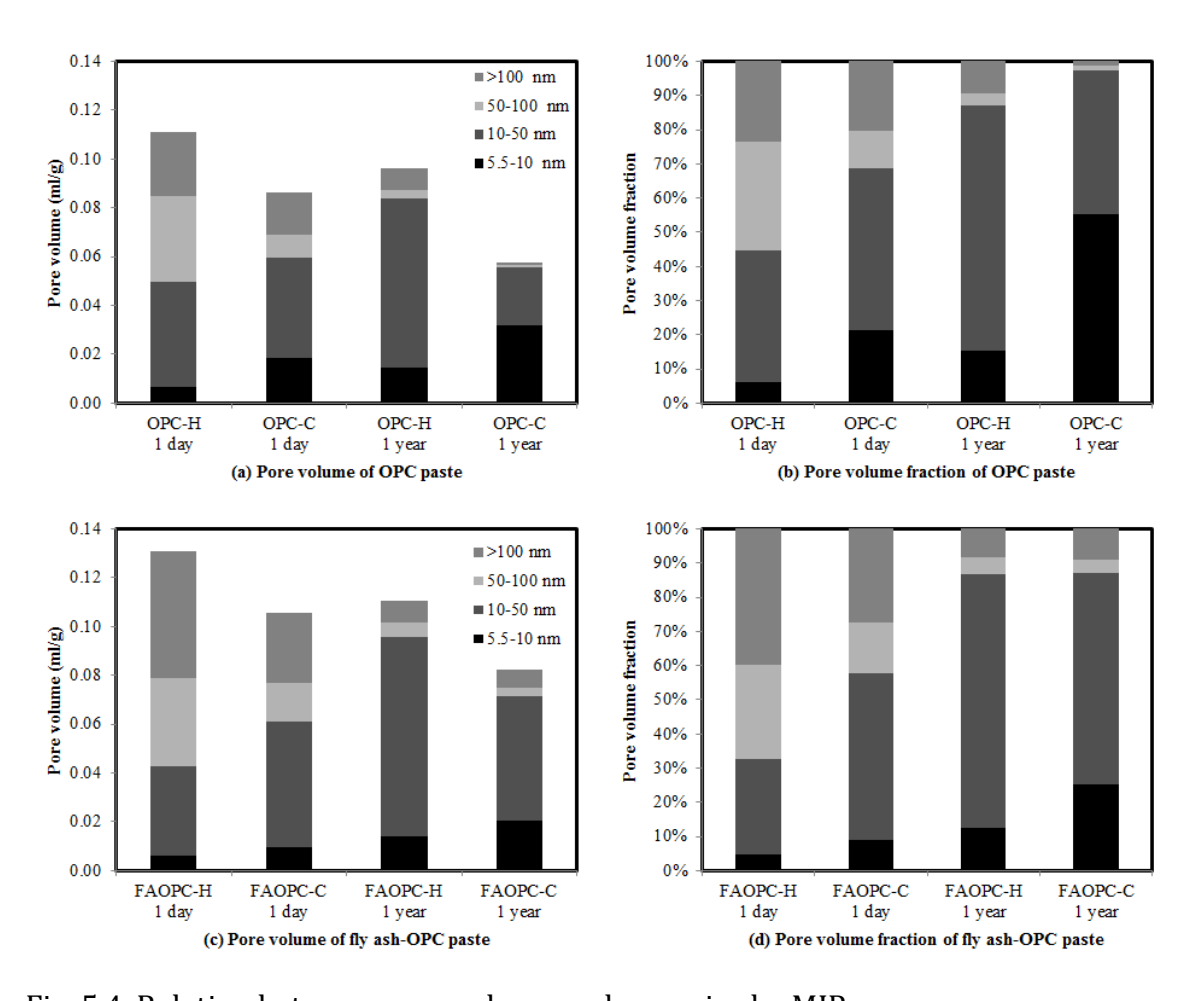


Fig. 5.4. Relation between pore volume and pore size by MIP

Table 5.5. Critical and threshold diameter of pastes measured by MIP

Sample	Critical diameter, nm		Threshold diameter, nn	
	1 day	1 year	1 day	1 year
OPC - H	68.2	17.8	251.7	38.8
OPC - C	6.9	7.2	133.0	15.9
FAOPC - H	60.4	18.8	274.7	46.5
FAOPC - C	33.0	8.5	168.0	33.1

Table 5.5 compares two commonly used parameters in pore structure analysis by MIP. Critical diameter was defined as the pore size corresponding to the steepest slope of the cumulative pore size distribution curve. It generally represented the largest interconnected pores which controlled the transport behaviour (Winslow and Diamond, 1970; Berodier and Scrivener, 2015). It was observed that critical pore diameter was considerably reduced in carbonation cured paste. At 1 day critical pore diameter in carbonated cement paste was 6.9 nm which was 10 times smaller in comparison to hydration reference (68.2 nm). It was implicative that carbonation curing produced interconnected pores with the size smaller than 10 nm. Another parameter calculated from MIP was the threshold diameter. It was defined as the largest pore size below which significant mercury intrusion started. Carbonation curing was able to considerably reduce threshold diameter as well. The reduction at 1 year was measured about 59% and 28% in OPC and fly ash-OPC paste, respectively. It was suggested that threshold diameter played critical role on permeability of pastes since the volume of pores larger than threshold diameter was only composed of interconnected large capillary pores and thus smaller threshold diameter usually meant less volume of large pores (Young, 1974; Winslow et al., 1994). It was likely that permeability could be decreased after carbonation curing being applied.

Table 5.6. Pore volume by NAD

Sample	1 day, ml/g	1 year, ml/g
OPC - H	0.0873	0.0723
OPC - C	0.0516	0.0862
FAOPC - H	0.0855	0.1051
FAOPC - C	0.0436	0.0634

#### 5.3.3. Pore structure analysis by NAD

As the small pore size measured by MIP was limited by 5.5 nm, the actual fraction of small capillary and gel pores was underestimated. Therefore NAD analysis was performed to estimate the pore structure with pore size ranging from 3 nm to 100 nm. Table 5.6 summarizes pore volume calculated based on desorption branch of NAD isotherm using BJH method. Note that the result of NAD was trustworthy in a relatively narrowed range of pore diameter and thus represented primarily small capillary and gel pores which were close to the measurement low limit of MIP. Thus the two methods could compensate each other to examine full range of pore size. Similar to MIP, the pore volume measured by NAD at 1 day was reduced by carbonation curing in both pastes. However, after subsequent hydration and pozzolanic reaction of one year, the change in pore volume did not exhibit the same pattern. Except hydrated OPC paste in which the pore volume was seen a decrease, all other batches showed increased pore volume including the two carbonated pastes. With reference to the pore volume by MIP shown in Table 5.4 in which decrease was observed in total pore volume after one-year subsequent hydration, the increase in NAD measurement was indicative that subsequent hydration and pozzolanic reaction decreased the volume of large capillary pores and increased gel pores. It was also suggestive that more C-S-H was produced in subsequent hydration. For

carbonated OPC, hydration was likely promoted by the process-induced calcium carbonate crystals which served as precipitation sites for more hydration products (<u>Péra et al., 1999</u>; <u>Lothenbach et al., 2008</u>). In fly ash-OPC system, it was the pozzolanic reaction that further generated reaction products thus higher fraction of gel pores.

Figs. 5.5 and 5.6 exhibit the pore size distribution from NAD. Obviously carbonation curing showed significantly reduced pore volume in the pore size range between 3 nm to 100 nm in OPC at 1 day (Fig. 5.5a). However, after 1 year subsequent hydration in carbonation cured sample (Fig. 5.5c) the cumulative pore volume by carbonation had exceeded that by hydration reference. It was also observed that the two peaks appeared on the differential pore size distribution curve. As shown in Fig 5.5(b), the first peak (Peak I) located at about 3.5 nm representing C-S-H gel (interlayer) pore. The second one (Peak II), corresponding to the diameter of about 20 nm in hydration reference, was considered as the smallest pore size for pore condensation percolated. It is shown in Fig. 5.5(d) that Peak II was shifted to smaller diameter after carbonation curing while Peak I remained barely changed. This indicated that carbonation curing was more effective in refining the capillary pores than the gel pores in C-S-H.

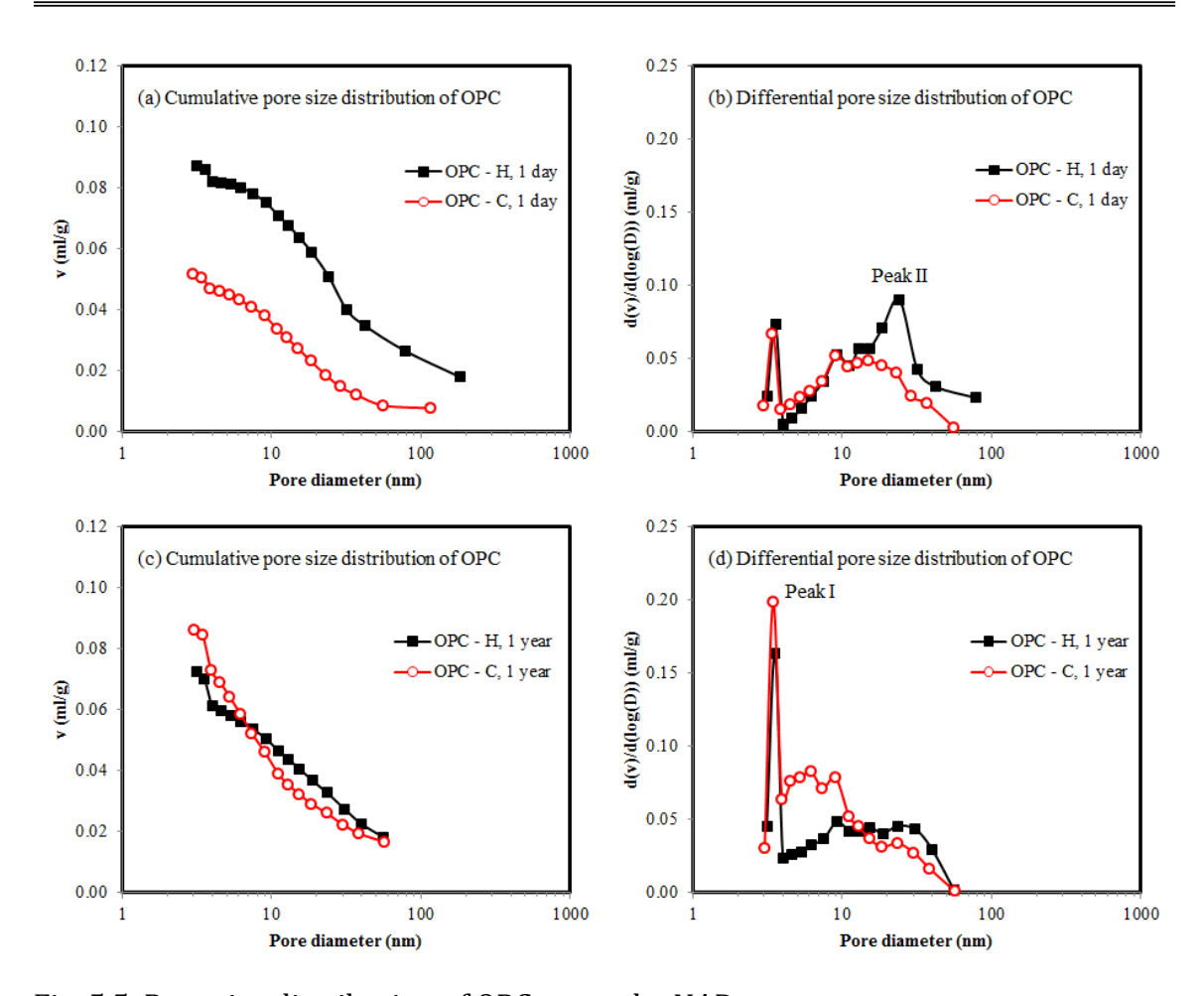


Fig. 5.5. Pore size distribution of OPC pastes by NAD

Fig. 5.6 compares the size distribution of small pores (from 3 nm to 100 nm) for fly ash-OPC system. Similar trend was observed between carbonation curing and hydration reference. At 1 day shown in Fig. 5.6(a) carbonated paste displayed much smaller pore volume in the range of 3 nm to 100 nm. Unlike OPC paste, this advantage was remained till 1 year as shown in Fig. 5.6(c). The differential curve of fly ash-OPC paste displayed similar trend as in OPC. Peak II was shifted to smaller range below 10 nm after carbonation curing as shown in Figs. 5.6(c) and 5.6(d). Differential curves showed slightly higher pore diameter corresponding to the peak I after carbonation

curing. Nevertheless, little difference was observed after 1 year between the two curing methods.

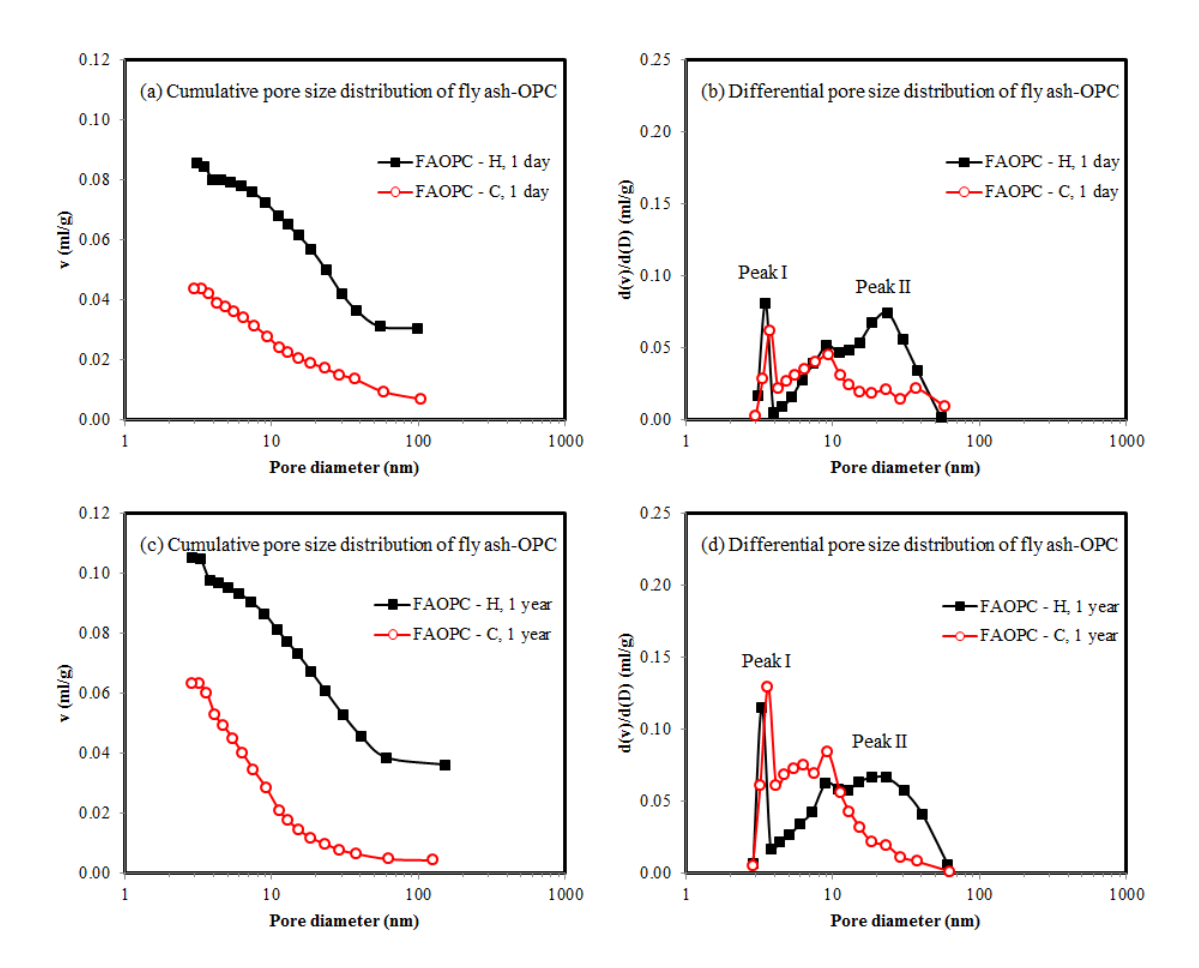


Fig. 5.6. Pore size distribution of fly ash-OPC pastes by NAD

The specific surface area was calculated from NAD adsorption isotherm using BET method and is shown in Fig. 5.7. The specific surface area was highly correlated to the solid phase of pore structure. Pastes with smaller pore size usually exhibited larger specific surface area (Mikhail, 1963). Carbonation curing showed slightly lower surface area in OPC but higher in fly ash-OPC paste at 1 day. The specific surface area was

observed higher in both carbonated batches after 1 year. It was suggestive that pore structure formed by carbonation became finer than its hydrated counterpart.

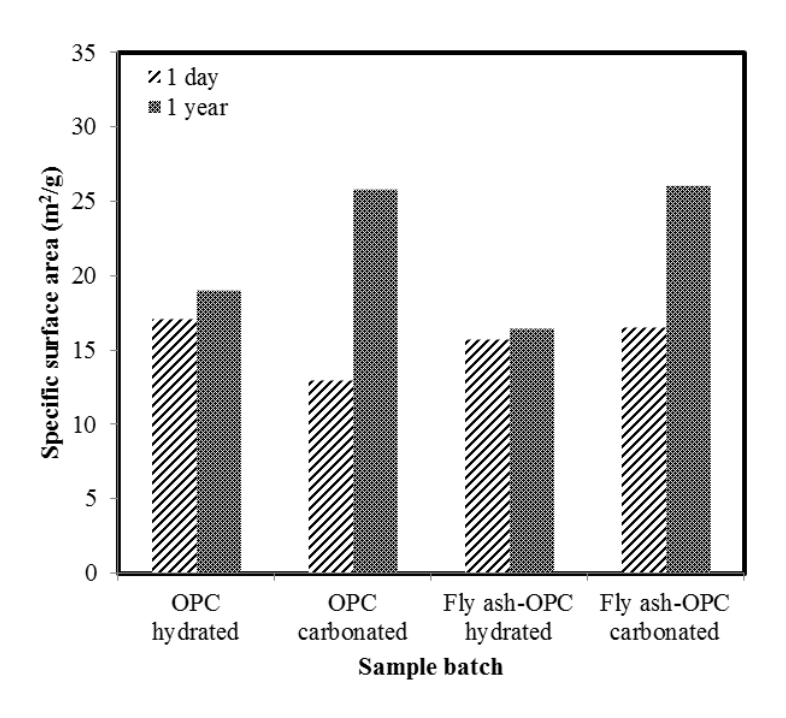


Fig. 5.7. Specific surface area calculated by BET

#### 5.3.4. Comparison of MIP and NAD on ink-bottle pores

In cementitious pastes pores with large diameter but connected by relatively smaller channel (Bossa et al.) were defined as ink-bottle pores. During mercury intrusion test, mercury had to pass the 'neck' to get to the 'bottle' space. Therefore the pressure of mercury required to intrude ink-bottle pores was dependent on neck diameter than on the actual pore size. The ink-bottle pores required relatively higher intrusion pressure based on which its volume was counted as smaller pores ('neck'). In contrast, NAD was based on capillary condensation of nitrogen gas. The condensation phenomenon was not affected by ink-bottle effect as long as the size of the narrowest pore was larger than the

gas molecule diameter. Therefore NAD was more realistic in characterization of small nanometer pores (<10 nm). Comparison of pore size distribution between NAD and MIP in range of small pores could indirectly reflect the 'ink-bottle' effect. Figs. 5.8 and 5.9 compare the pore size of NAD and MIP. Basically the two curves showed consistent within the overlapped range. However, for pores smaller than 10 nm, pastes subjected to carbonation curing exhibited large difference between MIP and NAD especially in OPC paste. As shown in Fig. 5.8(b) and 5.8(d), MIP showed strong peak approximately at 7 nm where NAD curve appeared flat. The phenomenon was also obvious in carbonated fly ash-OPC sample at the age of 1 year as shown in Fig. 5.9(d). There was notable peak measured on MIP corresponding to pore size of smaller than 10 nm but not observed on NAD curve. It was indicative that MIP measured considerable volume of small nanometer pores which were not detected by NAD. The overestimated porosity of pores below 10 nm by MIP was likely the effect of ink-bottle pores since the presence of latter counted volume of larger pores into smaller one. It was thus inferred that carbonation curing formed more distinguished ink-bottle pores in comparison to hydration reference. The increased 'ink-bottle' effect required further investigation by visual characterization techniques.

Table 5.7. Permeable porosity of concrete

Sample	Curing regime	1 day	28 days	90 days
OPC	Hydration, %	11.0	8.6	8.5
	Carbonation, %	9.0	7.4	7.3
FAOPC	Hydration, %	12.2	9.1	7.9
	Carbonation, %	9.4	7.7	7.6

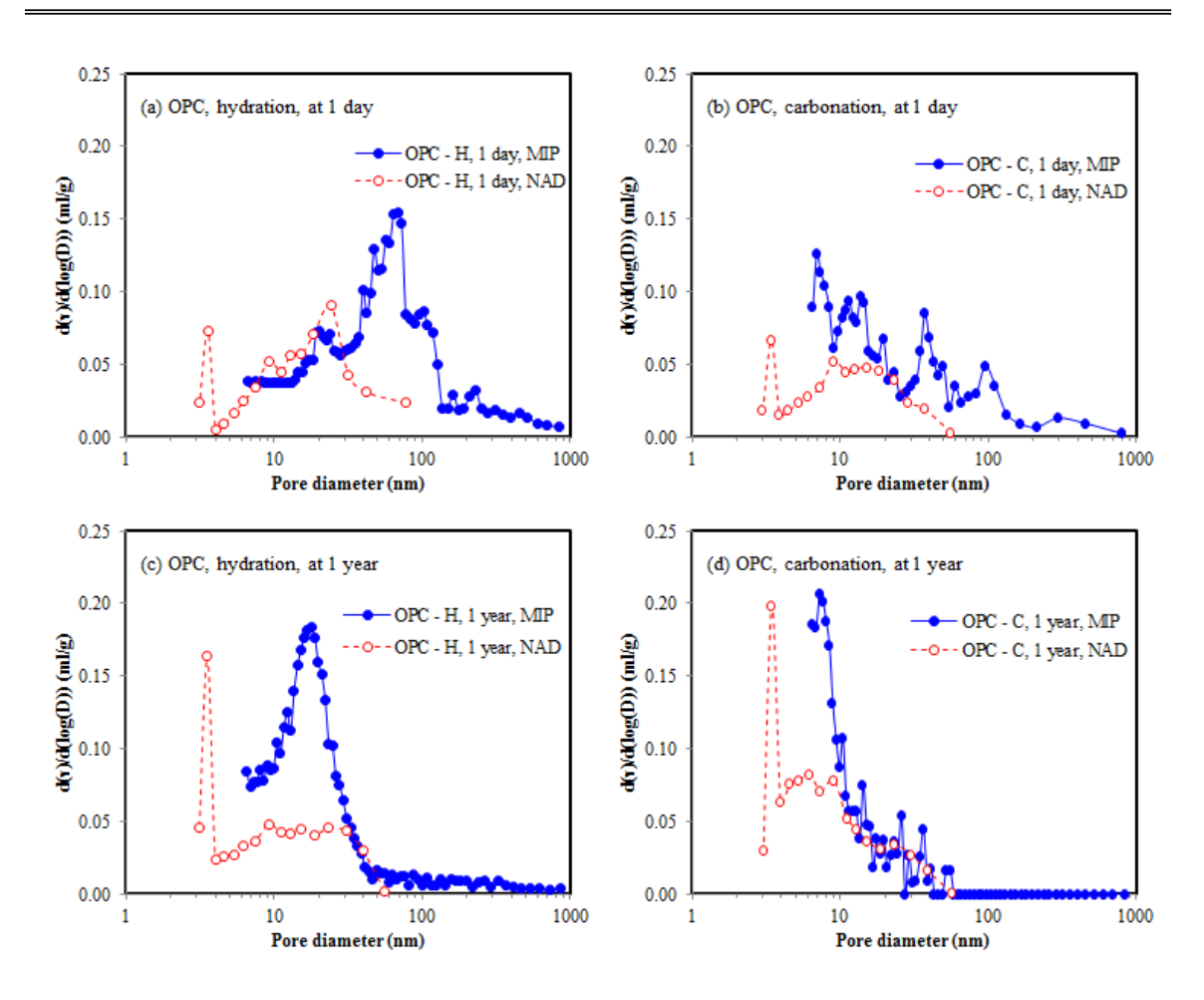


Fig. 5.8. Comparison of MIP with NAD for OPC pastes

#### 5.3.5. Effect of pore structure change on concrete performance

Effect of pore structure change in paste on durability of concrete was evaluated by permeable porosity, surface resistivity and freeze-thaw scaling resistance of concrete. Concrete porosity was measured through water absorption test as permeable porosity. Table 5.7 compares the permeable porosity of concrete subjected to carbonation and hydration. Concrete porosity at 1 day was decreased by 18% in OPC concrete and 23% in fly ash-OPC concrete due to the carbonation curing. Fly ash concrete showed higher reduction in porosity at early age because of the more severed carbonation reaction

(Table 5.3). Subsequent hydration further reduced concrete porosity. Up to 90 days, the reduction was 23% in hydrated OPC, 20% in carbonated OPC, 35% in hydrated fly ash-OPC, and 19% in carbonated fly ash-OPC. It seemed that carbonation could reduce the early porosity and this advantage was maintained up to 90 days. It was consistent with observation in pore structure analysis of paste by MIP and NAD. It should be noted that the permeable porosity measured from concrete was different from porosity measured from pastes by MIP and NAD. The former was determined by water absorption based on concrete mass and represented much larger pore size including interfacial transition zones.

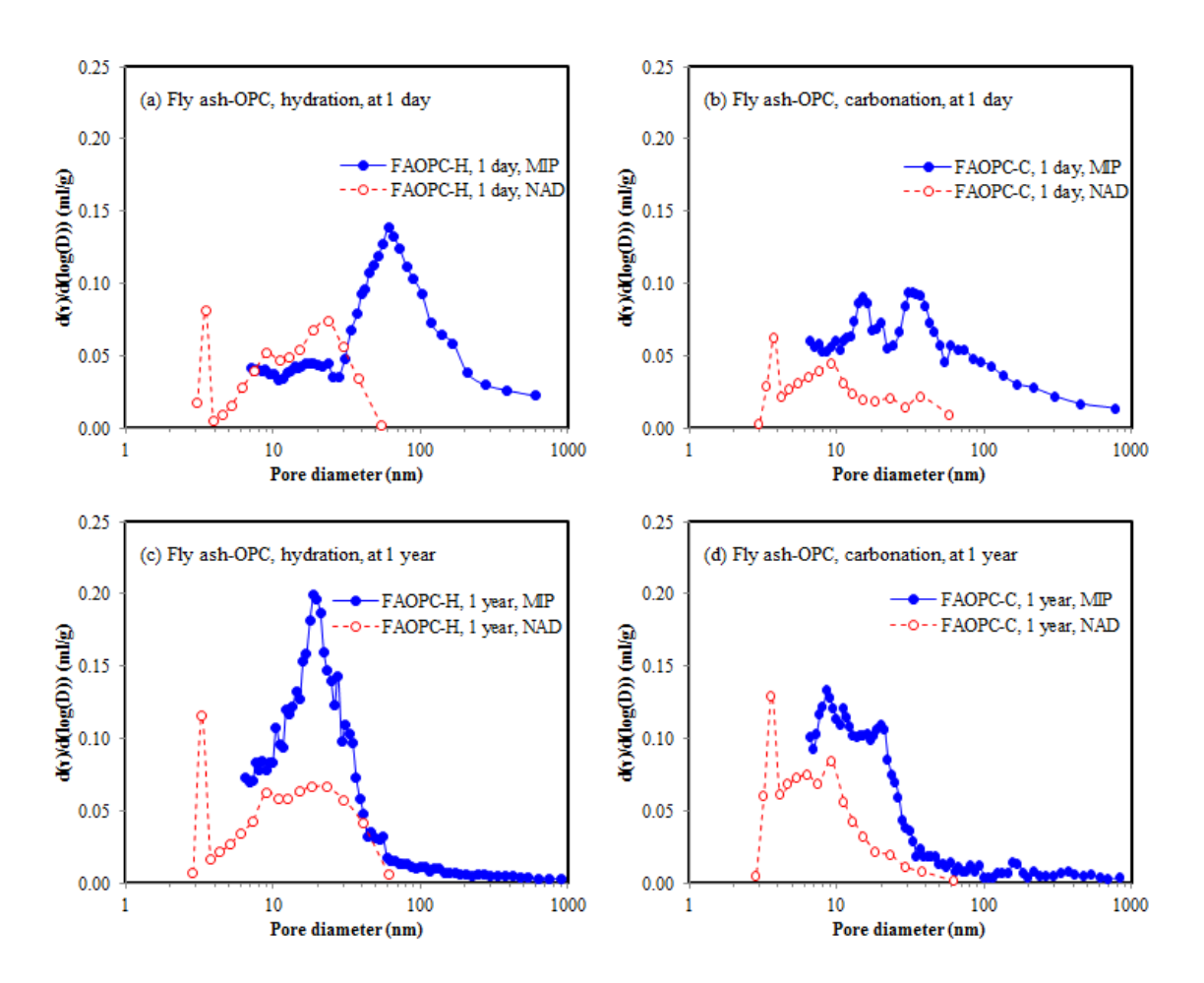


Fig. 5.9. Comparison of MIP with NAD for fly ash-OPC pastes

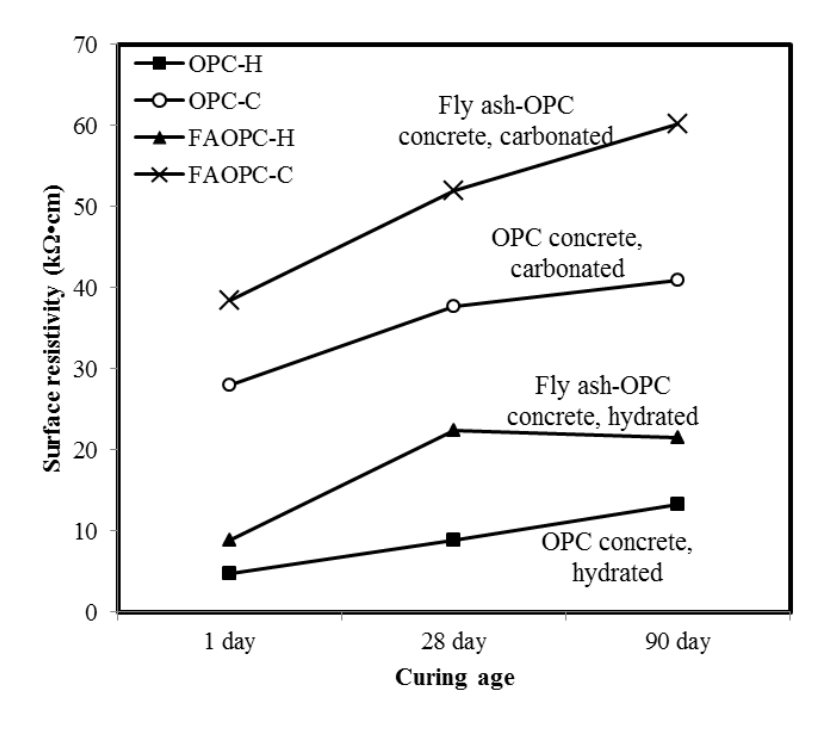


Fig. 5.10. Concrete surface resistivity

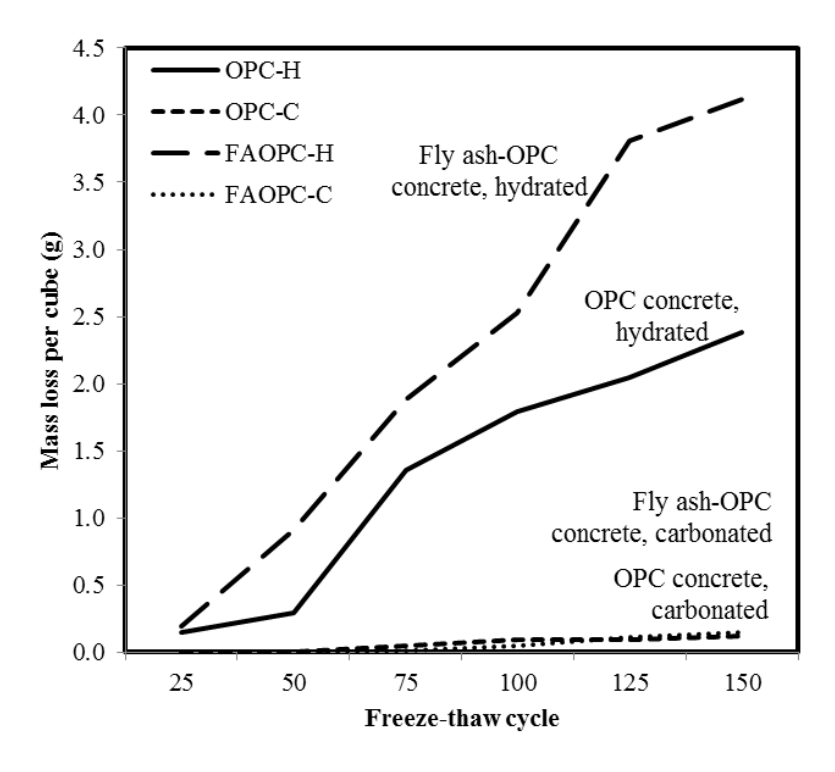


Fig. 5.11. Concrete mass loss due to freeze-thaw cycles

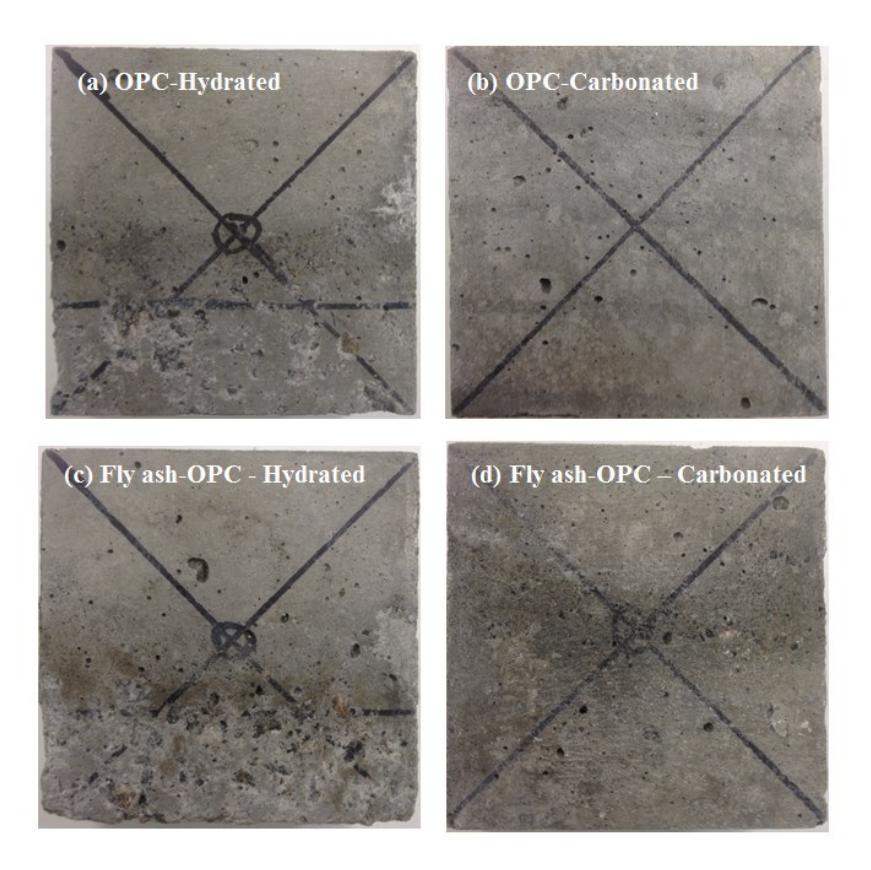


Fig. 5.12. Concrete scaling damage after 150 freeze-thaw cycles

The effect of pore structure change in paste on permeability of concrete was also evaluated. Permeability of concrete was assessed by surface electrical resistivity measurement. Surface resistivity was non-destructive method using electrical resistivity based on the assumption that electrical circuit was formed only if pores were connected (Polder, 2001; Vivas et al., 2007). Therefore higher resistivity indicated less pore connectivity and lower permeability. Fig. 5.10 compares surface resistivity measured on concrete at 1 day, 28 days and 90 days. After carbonation curing, both OPC and fly ash concretes showed more than doubled resistivity comparing to the hydration reference. It was rather apparent for both 1 day and 1 year after subsequent hydration. It was indicative that the carbonated concrete formed densified surface layer owing to the

calcium carbonate precipitation. As suggested by pore structure analysis using MIP and NAD, this surface layer had refined pore size distribution with more gel pores. The critical and threshold diameter were also smaller. Permeability was reported strongly correlated to capillary pores (Powers, 1958). Moreover the existence of ink-bottle pore reduced permeability as well due to its low connectivity (Moro and Böhni, 2002). Thus the resistivity increase was attributed to the refined pore structure by carbonation.

Freeze-thaw scaling resistance of the concrete was also influenced by pore structure change. Freeze-thaw tests were conducted in sodium chloride solution. Fig. 5.11 compares mass loss due to freeze thaw cycles. Surface scaling was clearly observed. For 100 mm concrete cubes, the mass loss after 150 cycles was 2.38 g in hydrated OPC, 0.12 g in carbonated OPC, 4.12 g in hydrated fly ash-OPC and 0.15 g in carbonated fly ash-OPC. With reference to carbonation, the mass loss in hydrated concrete was significantly higher. The scaling damage of concrete surface after 150 cycles is shown in Fig. 5.12. Hydrated concretes were seen considerable mass loss on surface especially in fly ash concrete. However, after carbonation curing, both concretes seemed not affected by the freeze-thaw exposure. This was mainly due to the refined pore structure from large capillary pores to small capillary or gel pores (< 10 nm) as well as the reduced water permeability and total porosity of concrete. Early carbonation technology seemed an effective method to significantly improve freeze-thaw durability without air entraining.

#### **5.4. CONCLUSIONS**

In the present study, effect of carbonation curing on pore structure of OPC and fly ash-OPC pastes was examined through Mercury Intrusion Porosimetry and Nitrogen Adsorption / Desorption methods. The corresponding concrete durability performance was also evaluated by permeable porosity, electrical resistivity and freeze-thaw resistance. The following conclusions could be drawn.

- 1. Total pore volume was significantly reduced by carbonation curing in comparison to hydration references. Immediately after carbonation the pore volume reduction was 22% in OPC and 19% in fly ash-OPC pastes. After 1 year subsequent hydration the reduction rate became 40% in OPC and 26% in fly ash-OPC. The precipitated calcium carbonate due to carbonation enhanced the early strength and was responsible for pore structure refinement in late hydration.
- 2. The pore size was significantly reduced by carbonation curing as well. Critical pore diameter was decreased by approximately 10 times in OPC paste and twice in fly ash-OPC at the age of 1 day. After 1 year subsequent hydration, carbonation curing reduced critical pore diameter to about 50% of that in hydration reference in both OPC and fly ash-OPC systems. Pore shape was also changed by carbonation curing. More ink-bottle pores smaller than 10 nm were seemingly formed during carbonation. The pore structure was considerably refined in carbonated pastes.
- 3. Although carbonation curing occurred at early age with short period, it exhibited impact on subsequent hydration as well. The carbonated OPC concrete showed higher strength and much refined pore structure at late age in comparison to hydration-

only reference. It was evident that the precipitated calcium carbonates not only accelerated early strength but also served as precipitation sites for late hydration. This effect was more obvious in OPC than in fly ash-OPC.

- 4. Fly ash-OPC system are able to be treated by carbonation. The system was more environment-friendly in that it reduced carbon footprint by using less cement and consuming more carbon dioxide. Fly ash-OPC concrete was of higher reactivity to carbon dioxide and developed comparable strength with OPC reference.
- 5. The refinement of pore structure in paste due to carbonation played critical role in improving concrete strength and durability. The carbonated concrete was stronger and more durable because of the reduced porosity, permeability and enhanced freeze-thaw resistance. The pH value of carbonated concrete was comparable to hydration reference after subsequent hydration, prompting the early carbonation curing process suitable for reinforced concrete production.

## ACKNOWLEDGEMENT

The financial supports by Natural Sciences and Engineering Research Council (NSERC) of Canada and by Climate Change and Emissions Management Corporation (CCEMC) of Alberta are gratefully acknowledged.

#### REFERENCES

- AHMAD, S. 2003. Reinforcement corrosion in concrete structures, its monitoring and service life prediction—a review. *Cement and Concrete Composites*, 25, 459-471.
- ALIGIZAKI, K. K. 2005. Pore structure of cement-based materials: testing, interpretation and requirements, CRC Press.
- ARANDIGOYEN, M., BICER-SIMSIR, B., ALVAREZ, J. I. & LANGE, D. A. 2006. Variation of microstructure with carbonation in lime and blended pastes. *Applied surface science*, 252, 7562-7571.
- BARRETT, E. P., JOYNER, L. G. & HALENDA, P. P. 1951. The determination of pore volume and area distributions in porous substances. I. Computations from nitrogen isotherms. *Journal of the American Chemical society*, 73, 373-380.
- BERODIER, E. & SCRIVENER, K. 2015. Evolution of pore structure in blended systems. *Cement and Concrete Research*, 73, 25-35.
- BOSSA, N., CHAURAND, P., VICENTE, J., BORSCHNECK, D., LEVARD, C., AGUERRE-CHARIOL, O. & ROSE, J. 2015. Micro-and nano-X-ray computed-tomography: A step forward in the characterization of the pore network of a leached cement paste. *Cement and Concrete Research*, 67, 138-147.
- BRUNAUER, S., EMMETT, P. H. & TELLER, E. 1938. Adsorption of gases in multimolecular layers. *Journal of the American chemical society*, 60, 309-319.
- DIAMOND, S. 2000. Mercury porosimetry: an inappropriate method for the measurement of pore size distributions in cement-based materials. *Cement and concrete research*, 30, 1517-1525.
- EL-HASSAN, H., SHAO, Y. & GHOULEH, Z. 2013. Effect of initial curing on carbonation of lightweight concrete masonry units. *ACI Materials Journal*, 110, 441-450.
- HOUST, Y. 1997. Microstructural changes of hydrated cement paste due to carbonation.

  Mechanisms of Chemical Degradation of Cement-Based Systems (KL Scrivener and JF Young Eds), Spon, London.

- KAUFMANN, J., LOSER, R. & LEEMANN, A. 2009. Analysis of cement-bonded materials by multi-cycle mercury intrusion and nitrogen sorption. *Journal of colloid and interface science*, 336, 730-737.
- KESSLER, R. J., POWERS, R. G., VIVAS, E., PAREDES, M. A. & VIRMANI, Y. P. Surface resistivity as an indicator of concrete chloride penetration resistance. Concrete Bridge Conference, St. Louis, Missouri, 2008.
- LI, D., CHEN, Y., SHEN, J., SU, J. & WU, X. 2000. The influence of alkalinity on activation and microstructure of fly ash. *Cement and Concrete Research*, 30, 881-886.
- LOTHENBACH, B., LE SAOUT, G., GALLUCCI, E. & SCRIVENER, K. 2008. Influence of limestone on the hydration of Portland cements. *Cement and Concrete Research*, 38, 848-860.
- MCCARTER, W., STARRS, G. & CHRISP, T. 2000. Electrical conductivity, diffusion, and permeability of Portland cement-based mortars. *Cement and Concrete Research*, 30, 1395-1400.
- MEHTA, P. K. 1986. Concrete. Structure, properties and materials, Prentice-Hall.
- MORO, F. & BÖHNI, H. 2002. Ink-bottle effect in mercury intrusion porosimetry of cement-based materials. *Journal of Colloid and Interface Science*, 246, 135-149.
- NGALA, V. & PAGE, C. 1997. Effects of carbonation on pore structure and diffusional properties of hydrated cement pastes. *Cement and Concrete Research*, 27, 995-1007.
- PÉRA, J., HUSSON, S. & GUILHOT, B. 1999. Influence of finely ground limestone on cement hydration. *Cement and Concrete Composites*, 21, 99-105.
- POLDER, R. B. 2001. Test methods for on site measurement of resistivity of concrete—a RILEM TC-154 technical recommendation. *Construction and building materials*, 15, 125-131.
- POWERS, T. C. 1958. Structure and physical properties of hardened Portland cement paste. *Journal of the American Ceramic Society*, 41, 1-6.
- ROSTAMI, V., SHAO, Y. & BOYD, A. J. 2011. Durability of concrete pipes subjected to combined steam and carbonation curing. *Construction and Building Materials*, 25, 3345-3355.

- SHAO, Y., MIRZA, M. S. & WU, X. 2006. CO<sub>2</sub> sequestration using calcium-silicate concrete. *Canadian Journal of Civil Engineering*, 33, 776-784.
- SONG, H.-W. & KWON, S.-J. 2007. Permeability characteristics of carbonated concrete considering capillary pore structure. *Cement and Concrete Research*, 37, 909-915.
- TANESI, J. & ARDANI, A. 2012. Surface Resistivity Test Evaluation as an Indicator of the Chloride Permeability of Concrete. US Department of Transportation.
- TAYLOR, H. F. 1997. Cement chemistry, Thomas Telford.
- VIVAS, E., BOYD, A. J., HAMILTON III, H. & BERGIN, M. 2007. Permeability of Concrete—Comparison of Conductivity and Diffusion Methods. University of Florida, Gainesville.
- WASHBURN, E. W. 1921. Note on a method of determining the distribution of pore sizes in a porous material. *Proceedings of the National Academy of Sciences of the United States of America*, 115-116.
- WINSLOW, D. N., COHEN, M. D., BENTZ, D. P., SNYDER, K. A. & GARBOCZI, E. J. 1994. Percolation and pore structure in mortars and concrete. *Cement and concrete research*, 24, 25-37.
- WINSLOW, D. N. & DIAMOND, S. 1970. A MERCURY POROSIMETRY STUDY OF THE POROSITY IN PORTLAND CEMENT. *Journal of Materials*, 5, 564-585.
- YOUNG, J. 1974. Capillary porosity in hydrated tricalcium silicate pastes. *Powder Technology*, 9, 173-179.
- YOUNG, J., BERGER, R. & BREESE, J. 1974. Accelerated curing of compacted calcium silicate mortars on exposure to CO<sub>2</sub>. *Journal of the american ceramic society*, 57, 394-397.

#### CHAPTER 6

\_

# EFFECT OF EARLY CARBONATION CURING ON CHLORIDE PENETRATION AND WEATHERING CARBONATION IN CONCRETE

#### **PREFACE**

Previous chapters investigated the effect of carbonation curing in aspects of mechanical properties, chemical reactions and physical pore structure. Carbonation curing was considered to form a densified layer on concrete surface via deposit of carbonates. Less pore volume as well as smaller pore size accounted for the reduced permeability, improved early strength and higher resistance to freeze-thaw deterioration. However, the issue of early carbonation effect on steel corrosion needed to be addressed before the technology applied on reinforced concrete.

Generally two factors contributed to corrosion in reinforced concrete: chloride ions and reduced alkalinity due to weathering carbonation. It was also reported in past studies that the weathering carbonation possibly increased the penetration of chloride in concrete. Therefore it was necessary to clarify the effect of carbonation curing considering the contributions from both factors.

In this chapter carbonation cured and hydration cured concretes with and without fly ash were exposed to two severe cyclic conditions: (1) chloride immersion / air drying cycles and (2) chloride immersion / accelerated weathering carbonation cycles. It was purposed to study the corrosion potential of reinforced concrete subjected to carbonation curing.

It was found through one-year cyclic tests that total chloride content was actually reduced by more than 50% in concrete subjected to carbonation curing comparing to hydration reference. Reduction in free chloride (water-soluble) in carbonation cured concrete reached more than 60%. It was also found that carbonation cured concrete was not more vulnerable to weathering carbonation. This was attributed to the carbonate-rich surface protective layer which was less permeable, less absorptive, and with comparable pH value, prompting the carbonation cured concretes higher resistance to chloride penetration.

#### **6.1. Introduction**

Corrosion of steel in concrete was one of major durability issues for reinforced concrete. Deterioration appeared more severe in harsh marine environment (Thomas, 1996). It was believed that corrosion of steel in concrete was induced by chloride penetration and weathering carbonation (Taylor, 1997). The cyclic exposure of air drying and seawater wetting increased the ingress of chloride salts (Hong and Hooton, 1999). Corrosion occurred once free chloride content reached the threshold value which varied with pH of pore solution (Ann and Song, 2007). Another mechanism, known as weathering carbonation corrosion, happened in both coastal and on-land structures. Calcium hydroxide in concrete was reacted with atmospheric carbon dioxide during service life leading to reduction of pH value (Richardson, 1988; Ahmad, 2003). When pH dropped below 9.5, passivation film on steel surface started to decompose and corrosion initiated (Berkeley and Pathmanaban, 1990). Reinforced concrete simultaneously subjected to both chloride penetration and weathering carbonation was reported even more vulnerable than to individual action (Neville, 1995). Extensive studies showed that reduced pH caused by weathering carbonation reduced threshold value of chloride content for corrosion initiation (Glass and Buenfeld, 1997). Accordingly, corrosion starts at lower chloride content as concrete was exposed to weathering carbonation at the same time (Hussain et al., 1995). Corrosion rate was also increased as pH reduced and chloride content increased (Alonso et al., 1988; Glass et al., 1991). Some other studies suggested that weathering carbonation accelerated penetration of chloride salt (Lee et al., 2013; Hilsdorf and Kropp, 2004). In the meantime, both total chloride content and its penetrating depth were increased. It was also mentioned that as result of global warming

and increased concentration of atmospheric carbon dioxide (<u>Yoon et al., 2007</u>; <u>Bastidas-Arteaga et al., 2010</u>; <u>Stewart et al., 2011</u>), carbonation of concrete structures would become more serious during their service life (<u>Bastidas-Arteaga et al., 2010</u>).

Unlike weathering carbonation, early carbonation was curing process intentionally introduced within 24 hours after concrete casting. High early strength was observed in a short period (Berger et al., 1972). In addition to the accelerated effect on strength gain, early carbonation curing showed improved performance of concrete in exposure to freeze-thaw cycle and sulfate attack (Rostami et al., 2011b). The technique also received increasing interests due to its capacity of carbon dioxide sequestration (Shao et al., 2006).

Previous work showed that early carbonation curing was able to be applied to reinforced concrete as well (Zhang and Shao, 2016). The pH value of early-age carbonated concrete was comparable to hydration reference owing to the subsequent hydration. However, the effect of early carbonation curing on chloride penetration in concrete remained unclear. The purpose of this work was to investigate if the early carbonation curing would promote the penetration of chloride ions in concrete as observed in weathering carbonation. The study also examined if the early carbonation curing increased the weathering carbonation depth in service. In this study, concrete cured by early carbonation was compared chloride penetration and weathering carbonation depth with hydrated concrete. Two exposure conditions were adopted including chloride immersion / air drying cycles and chloride immersion / accelerated weathering carbonation cycles. Both OPC and fly ash-OPC concretes with carbonation and hydration curing were compared.

#### **6.2.** EXPERIMENTAL PROGRAM

#### **6.2.1.** Materials and mix proportion

The chemical compositions of Type GU Ordinary Portland Cement (OPC) and fly ash are shown in Table 6.1. Crushed granite stone and granite sand were used as aggregates. Maximum aggregate size was 12 mm and the fineness modulus of fine aggregate was 3.0. The water adsorption was approximately 4.3% for fine aggregate and 1.6% for coarse aggregate. To avoid chloride contamination from other sources, aggregates had been washed three times and used in condition of saturated surface dry (SSD). De-ionized water was used instead of tap water to eliminate the possible chlorides from mixing water.

The ratio of water to cementitious materials was chosen as 0.4. Two mixture proportions were used in making OPC and fly ash-OPC concretes. Fly ash was added as 20% replacement of cement by mass in fly ash-OPC concrete. Superplasticizer was used to achieve the slump of about 160 mm for both concretes. The detailed mixture proportions are listed in Table 6.2.

## 6.2.2. Sample preparation and carbonation curing process

Concretes were cast into 100 mm cube steel mold and compacted on vibration table. The fresh concrete samples were treated two different curing methods: early carbonation curing (denoted as C) and conventional hydration curing (denoted as H). For hydration reference concretes were sealed for 24 hours in molds and then demolded

followed by further curing in moisture room at 25 °C and 95% relative humidity (RH). Early carbonation curing of concrete was involved with four steps as shown in Fig. 6.1: (1) 5 hours in-mold curing, (2) 5.5 hours de-mold conditioning, (3) 12 hours carbonation curing and (4) 27 days subsequent hydration.

Table 6.1. Chemical compositions of cement and fly ash (%)

Material	CaO	SiO <sub>2</sub>	$Al_2O_3$	$Fe_2O_3$	Mg0	$Na_2O_{(eq)}$	SO <sub>3</sub>
Cement	63.10	19.80	4.90	2.00	2.00	0.85	3.80
Fly Ash	11.30	54.39	23.65	3.90	1.17	2.91	-

Table 6.2. Mixture proportion of concrete

Mixture components	OPC	FAOPC
Cement, kg/m <sup>3</sup>	452	362
Fly ash, kg/m <sup>3</sup>	0	90
Fly ash to binder ratio, %	0	20
Water, kg/m <sup>3</sup>	181	181
Water to binder ratio	0.4	0.4
Water to cement ratio	0.4	0.5
Coarse aggregate, kg/m <sup>3</sup>	1060	1060
Fine aggregate, kg/m³	680	680
Superplasticizer to cement ratio, %	0.5	0.5
Slump, mm	158	166

As the fresh concrete showed high slump initial hydration before demolding was necessary. The demolding schedule was dependent on the mixture proportion. For the concrete shown in Table 6.2 it took approximately 5 hours in the open air (25 °C and 60% RH) to reach the initial set. In step 2 concretes were demolded and left on the bottom plates for fan drying conditioning at wind speed of 1 m/s in ambient condition (50  $\pm$  5% RH, 25 °C) to remove about 40% of mixing water. This procedure was necessary to

create sufficient paths for carbon dioxide to penetrate and carbonate to precipitate. The conditioned samples were then moved to enclosed carbonation chamber filled with pure  $CO_2$  gas (99.8% purity) at constant pressure of 5 bar for 12 hours. The early carbonation curing setup is shown in Fig. 6.2. Mass change in concrete samples was measured during the 12-hour carbonation reaction. Water generated in the chamber by the reaction was collected by absorbent paper and weighed. The  $CO_2$  uptake by mass gain method was calculated using Eq. 6.1.

$$CO_2 \text{ uptake}(\%) = \frac{m_2 + m_{water} - m_1}{m_{cement}} \times 100\%$$
 (6.1)

Where  $m_1$  and  $m_2$  are the concrete mass before and after the carbonation reaction, respectively.  $m_{water}$  is the mass of water collected in the reaction chamber.  $m_{cement}$  is the mass of anhydrous cement in carbonated concrete.

Carbonated concretes were surface sprayed by de-ionized water immediately after carbonation and were moved to moisture room (95% RH, 25 °C) for additional 27 days subsequent hydration. Concrete at the age of 1 day and 28 days were tested for compressive strength. Phenolphthalein solution was sprayed on the split cross section to determine the carbonation depth due to early carbonation curing. PH meter with flat head (Extech PH110) was used to measure pH at different depths (0-10 mm, 10-25 mm, 25-50 mm) at 1 day and 28 days. The testing area was covered by an absorptive paper (10 mm  $\times$  10 mm) soaked with 100  $\mu$ L deionized water for 15 minutes when the diffusion equilibrium was reached. The pH readings were then recorded (Rostami et al., 2011a; Heng and Murata, 2004). Concretes after pH measurement were chiseled off at the three

depths and crushed into 5-10 mm particle size to determine carbon content through thermal pyrolysis (Zhang and Shao, 2016). About 100 g of concrete samples were heated and measured mass up to 105, 550 and 950 °C. The mass loss between 550 and 950 °C was attributed to decomposition of calcium carbonate and calculated in reference to cement mass to obtain the carbon dioxide content in each depth. Carbon dioxide content was presented as mass percentage of anhydrous cement.

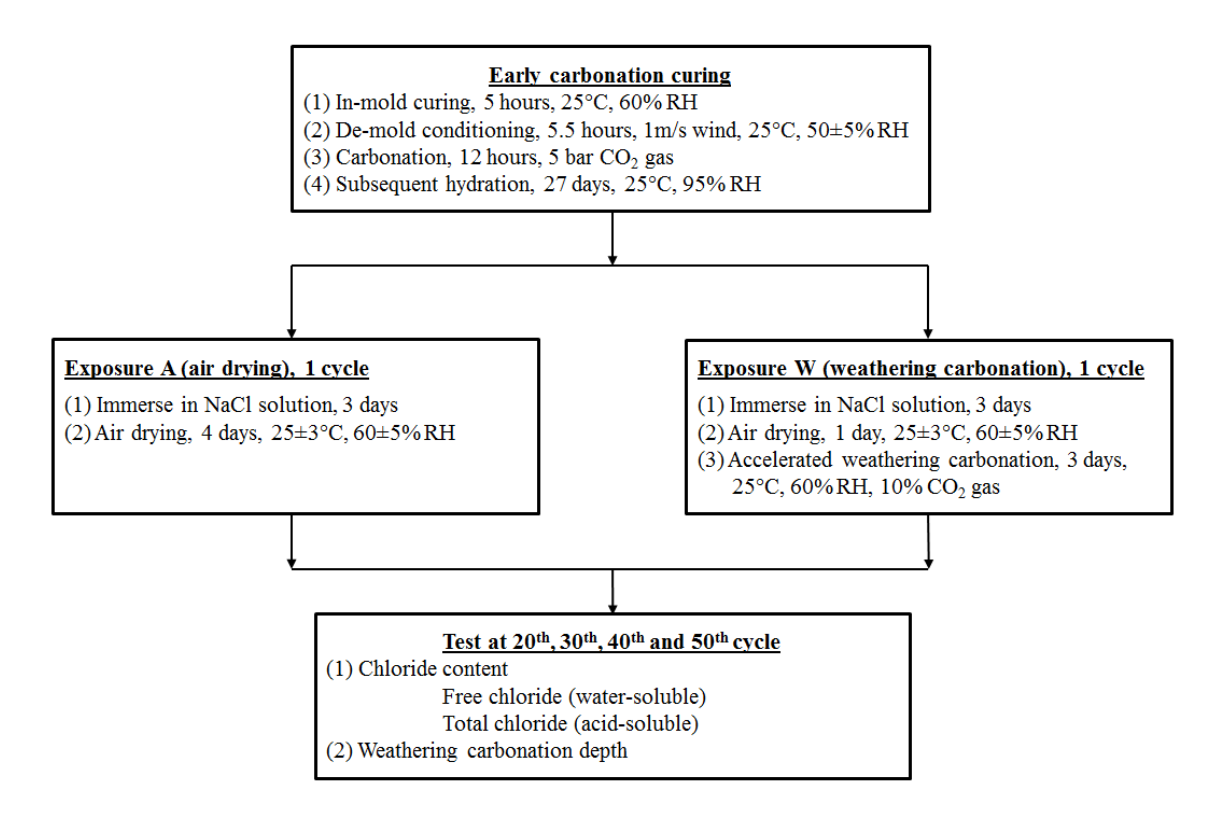


Fig. 6.1. Experimental flow chart

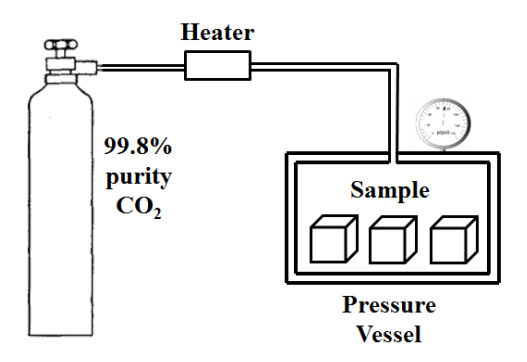


Fig. 6.2. Setup of early carbonation apparatus

#### **6.2.3.** Absorption and surface electrical resistivity

Permeable porosity of carbonated and hydrated concretes was measured at 1 day and 28 days following ASTM C642-06. Tested concrete was dried at 105 °C for 24 hours and the mass was measured as  $m_A$ . After fully immersed in water for another 48 hours at 21 °C, concrete was boiled for 5 hours and cooled for 24 hours in environmental chamber at 21 °C. The concrete was surface dried and recorded mass as  $m_B$ . The mass of concrete in suspended submersion was also measured as  $m_C$ . The permeable porosity due to absorption was calculated by Eq. 6.2.

Porosity = 
$$(m_B - m_A)/(m_B - m_C) \times 100\%$$
 (6.2)

Surface electrical resistivity was non-destructive test for estimation of permeability on concrete surface. Higher resistivity value indicates more resistance to permeation (McCarter et al., 2000). Surface electrical resistivity test was conducted on concrete at 1 day and 28 days following AASHTO TP95. Concrete was immersed in water for 48 hours at 25 °C. The surface dried concrete was measured resistivity on

surface by Proceq Resipod Resistivity Meter with four-point probe. Three measurements were acquired and averaged.

### 6.2.4. Chloride penetration and weathering carbonation tests

After 1 day early carbonation curing and 27 days subsequent moisture curing both hydration and carbonation cured concretes were placed in environmental chamber (60% RH, 25°C) for one week to reach the moisture equilibrium. The concrete cubes were then sealed four sides by impermeable epoxy to facilitate unidirectional chloride penetration.

Chloride penetration tests were performed in simulated seawater solution with 3.5 wt% sodium chloride (NaCl). After one week of drying in environmental chamber (60% RH, 25°C) concrete cubes were exposed to two alternations of environmental cycles. The experimental flow chart is also illustrated in Fig. 6.1. To investigate the effect of carbonation curing on chloride penetration concretes were alternatively immersed in chloride solution and dried in the open air. One cycle of the alternation test took one week including 3 days fully immersion in chloride solution and another 4 days dry in the air. This exposure condition was denoted as 'A' and repeated 50 cycles (50 weeks). Air drying condition was maintained  $60 \pm 5\%$  RH and  $25 \pm 3$ °C. To examine the effect of early carbonation on chloride penetration with presence of weathering carbonation, parallel study was carried out on concrete subjected to cyclic exposure. The period of each cycle was one week including 3 days full immersion in chloride solution, 1 day in open air drying and 3 days accelerated weathering carbonation. Weathering carbonation was conducted in enclosed chamber with 10% CO<sub>2</sub> gas at 60% RH and 25 °C for 3 days.

This cyclic exposure was denoted as 'W' and also repeated 50 cycles with the same schedule as exposure 'A'.

There were four combinations of curing methods (H and C) and cyclic exposures (A and W), HA, HW, CA and CW, respectively representing the hydration cured concrete subjected to chloride immersion / air drying cycle, the hydration cured concrete subjected to chloride immersion / weathering carbonation cycle, the carbonation cured concrete subjected to chloride immersion / air drying cycle and the carbonation cured concrete subjected to chloride immersion / weathering carbonation cycle. The same labeling method was used in both OPC and fly ash-OPC concretes.

## 6.2.5. Determination of chloride and weathering carbonation extent

Concretes were tested every 10 cycles starting from 20<sup>th</sup> till 50<sup>th</sup>. Tested concrete samples were split and sprayed phenolphthalein solution for measurement of carbonation depth. Acid- and water-soluble chloride content at different locations on the cross section were measured through titration analysis following ASTM C1152/C1152M - 04 (2012) and ASTM C1218/C1218M - 99 (2008) representing the total and free chloride content in concretes, respectively. A rotary impact drill was used to acquire concrete powders from various depths. To understand the effect of early carbonation on chloride transport behavior, powder samples were acquired from three different locations according to early carbonation depth: fully carbonated surface area, layer 1 (0~10 mm), lightly carbonated area, layer 2 (10~25 mm) and non-carbonated core region, layer 3 (25~50 mm).

## **6.3. RESULTS AND DISCUSSIONS**

## **6.3.1.** Early carbonation behavior of concrete

Table 6.3 summarizes early carbonation behavior of concrete in comparison to hydration references. Through 12 hours carbonation reaction, OPC and fly ash-OPC concrete achieved the CO<sub>2</sub> uptake of 14.30% and 17.06% by mass of cement, respectively. The carbonation depth due to early carbonation was 15.5 mm in OPC concrete and 18.5 mm in fly ash concrete as detected by phenolphthalein solution spray on cross section. Fly ash-OPC concrete was obviously more reactive with carbon dioxide than OPC concrete. However, after 27 days subsequent hydration the entire cross section turned to purple-red color and carbonation depth decreased to zero. It was indicative that pH value of heavily carbonated surface layer was increased as result of the subsequent hydration.

Table 6.3. Results of carbonation curing

Sample ID	ОРС-Н	OPC-C	FAOPC-H	FAOPC-C
CO <sub>2</sub> uptake, % by cement	-	14.30	-	17.06
Carbonation depth, 1 day, mm	-	15.5 ± 2.5	-	$18.5 \pm 2.0$
Carbonation depth, 28 days, mm	-	0	-	0
Strength, 1 day, MPa	36.08 ±1.83	43.73 ±2.25	25.46 ±1.03	32.76 ±1.91
Strength, 28 days, MPa	63.12 ±0.93	71.56 ±2.95	49.11 ±1.51	53.98 ±2.01

Compression test was conducted on the 100-mm cubes at age of 1 day and 28 days. Table 6.3 compares the strength for various series. In comparison with hydration, carbonation curing was able to increase 1-day strength by 21% (from 36.08 MPa to 43.73 MPa) in OPC concrete and 29 % (from 25.46 MPa to 32.76 MPa) in fly ash-OPC

concrete. Apparently the carbonation curing process accelerated strength gain in the early age. The compressive strength at 28 days in Table 6.3 suggested that carbonation cured concretes still exhibited higher strength despite that the difference was less significant as seen at the early age. The increase in both pH value and strength at 28 days was indicative that early carbonation seemed not to hinder the subsequent hydration.

Laver 1: 0-10 mm

Layer 2: 10-25 mm

Layer 3: 25-50 mm

Layer 3

Laver 2

Sample location

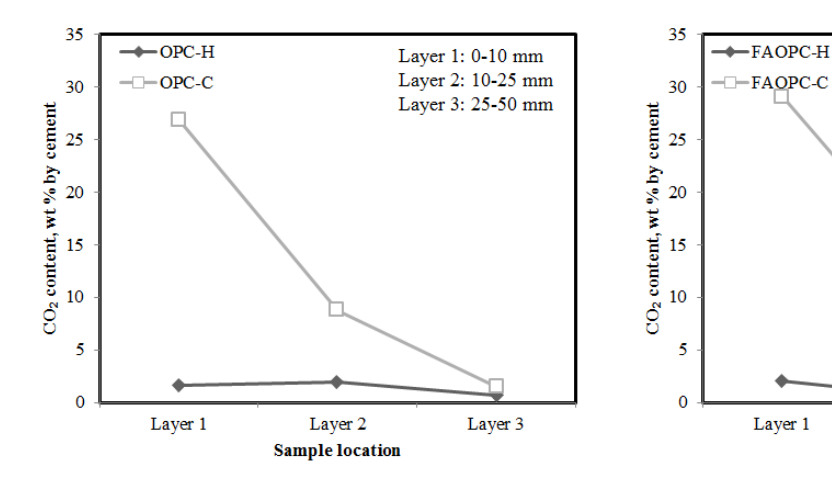


Fig. 6.3. CO<sub>2</sub> content along the thickness

To correlate the degree of carbonation with the pH value distribution, carbon content and pH values were measured along the thickness. Fig. 6.3 shows the CO<sub>2</sub> content in each layer as measured from thermal pyrolysis. It was obvious that the CO<sub>2</sub> content was decreased along the depth. Layer 1 (0-10 mm) was heavily carbonated and layer 2 (10-25 mm) showed much lower degree of reaction. CO<sub>2</sub> content measured in layer 3 (25-50 mm) was in close value of hydration reference which was attributed to the limestone admixture in cement. It was thus indicative that the core area was free of carbonation. The pH values measured at the same layer locations are shown in Fig 6.4. In comparison to hydration cured concrete which measured pH of 12.8~13.0 at 1 day and 28

days, early carbonation curing significantly reduced pH of concretes on surface (0-10 mm) immediately after early carbonation (1 day). The pH of layer 1 (0-10 mm) dropped to 9.2 and 9.4 for OPC and fly ash-OPC concrete, respectively. In layer 2 (10-25 mm) pH varied with large deviation suggesting the existence of a transition zone. In core area (layer 3 at 25-50 mm) concrete showed pH value close to that of reference hydration further confirming that the core was non-carbonated. It was interesting to notice that after 27 days subsequent hydration pH of both carbonated concretes, either on surface or at core was increased to the level comparable to that of hydration reference. It was consistent with the observation on the evolution of carbonation depth. Clearly early carbonation curing produced a sandwich structure that was rich in calcium carbonates on surface and maintained high pH at core. The pH on surface was reduced right after carbonation but able to be recovered through subsequent hydration.

Table 6.4. Surface electrical resistivity ( $k\Omega$ .cm)

Sample	Curing method	1 day	28 days
OPC	Hydration reference	4.9	8.9
	Early carbonation	40.9	47.3
FAOPC	Hydration reference	8.9	22.5
	Early carbonation	38.4	52.0

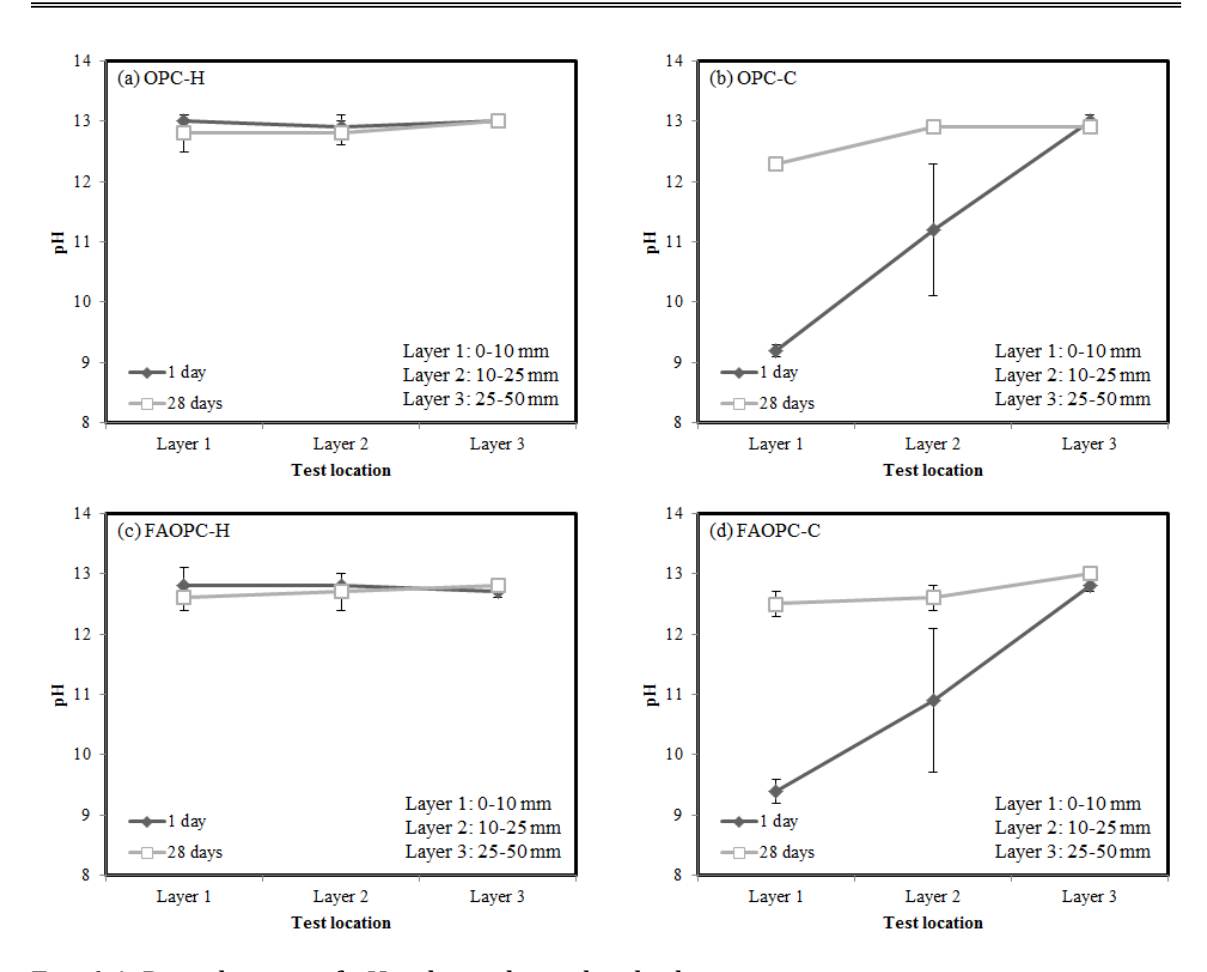


Fig. 6.4. Distribution of pH values along the thickness

Fig. 6.5 compares the permeable porosity measured via water absorption test. It was notable that early carbonation curing reduced concrete porosity at both 1 day and 28 days. The effect was more considerable at 1 day. In OPC concrete, 1-day porosity was reduced from 11.0% in hydration reference to 9.0% by early carbonation. Fly ash-OPC concrete seemed more affected by carbonation curing. The porosity was reduced from 12.2% to 9.4% at 1 day owing to the higher degree of carbonation. The advantage of early carbonation curing was observed even after 27 days subsequent hydration. This effect was also evident by surface resistivity measurement shown in Table 6.4. Early carbonation curing considerably improved surface resistivity at both 1 day and 28 days

despite that the increasing rate at 1 day appeared more significant. Surface electrical resistivity at 28 days was more than doubled by carbonation curing in both OPC and fly ash-OPC concrete. It was thus indicative that the carbonated concretes gained higher resistance to permeation of external ions.

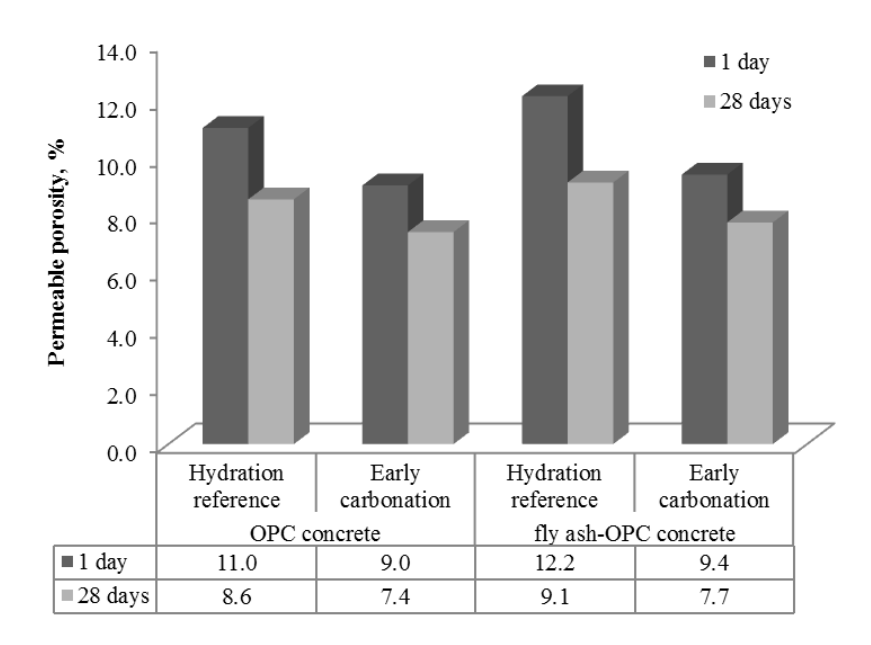


Fig. 6.5. Permeable porosity of hydrated and carbonated concrete

#### 6.3.2. Effect of weathering carbonation on chloride penetration

Effect of weathering carbonation on chloride penetration was firstly studied using hydrated concretes. Total chloride penetration was compared between the two exposure conditions shown in Fig. 6.6 for OPC concrete and Fig. 6.7 for fly ash-OPC. Typical results presented were collected after 20<sup>th</sup> cycle and 50<sup>th</sup> cycle. Generally chloride content was decreased along the depth. For OPC concrete the effect of two exposure conditions

was not apparent. After 50<sup>th</sup> cycles, chloride content was slightly higher in concrete exposed to weathering carbonation (Fig. 6.6b).

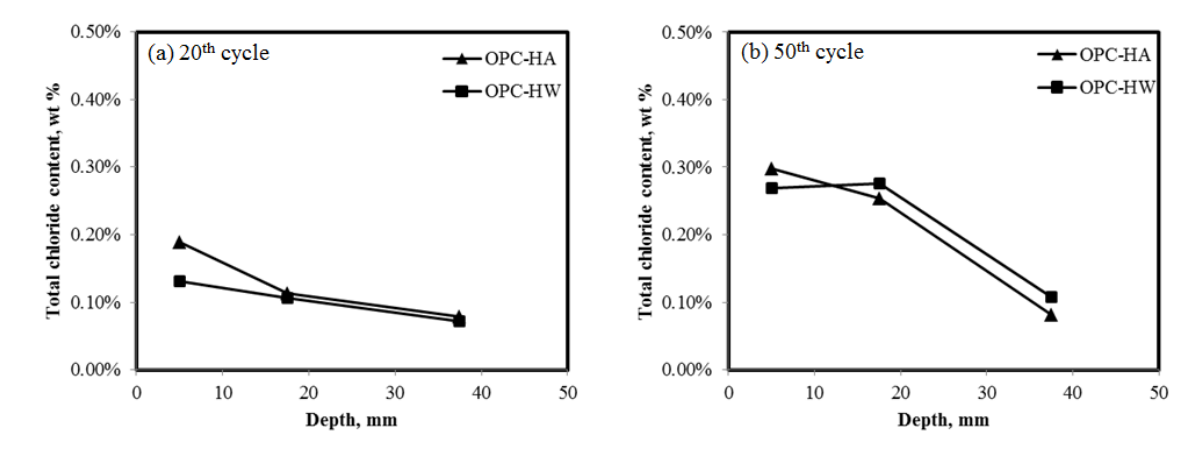


Fig. 6.6. Total chloride content in hydrated OPC concrete

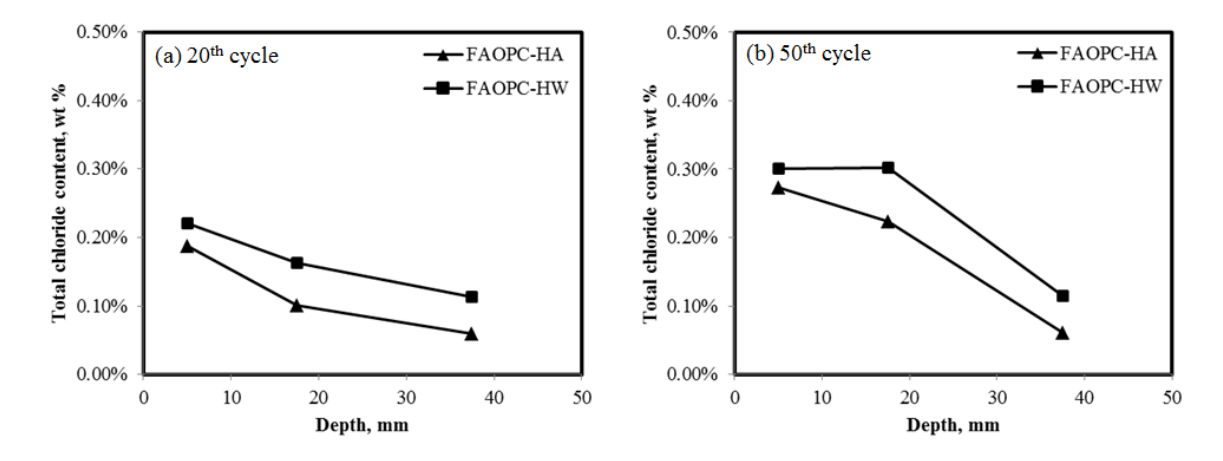


Fig. 6.7. Total chloride content in hydrated fly ash-OPC concrete

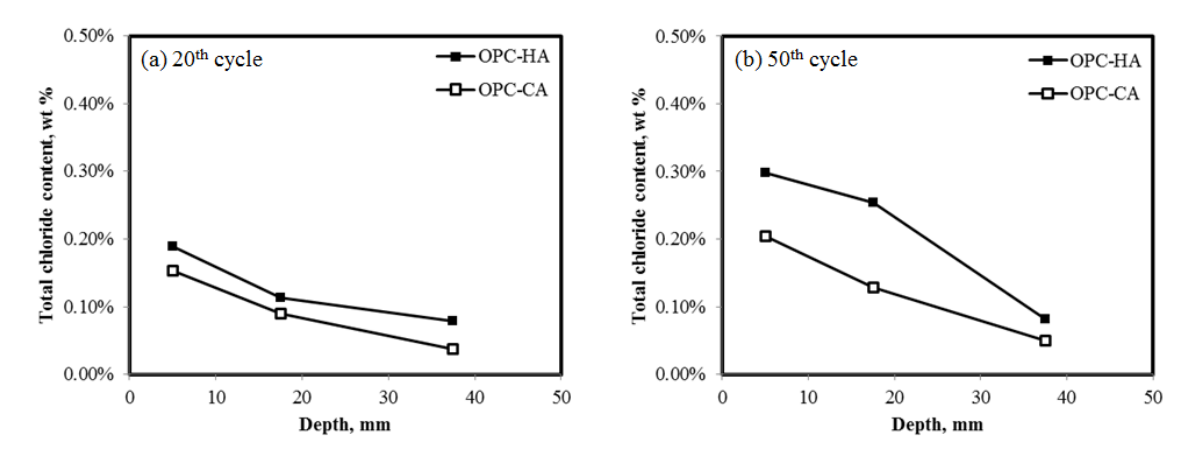


Fig. 6.8. Effect of early carbonation curing on chloride penetration in OPC concrete exposed to chloride immersion and air drying cycles

It was quite different in fly ash-OPC concrete shown in Fig. 6.7. The chloride distribution curve changed from concave shape at 20<sup>th</sup> cycle (Fig. 6.7a) to convex at 50<sup>th</sup> cycle (Fig. 6.7b). It seemed that more chloride tended to penetrate into deeper area with time. Fly ash-OPC concrete was observed more vulnerable to weathering carbonation. Therefore increased amount of chloride ions turned to be released and was able to penetrate deeper in concrete (FAOPC-HW). It was clear that in addition to the reduction of pore solution alkalinity, weathering carbonation possibly aggravated chloride penetration and increased the risk of chloride corrosion. The aggravation effect was more severe as fly ash was added.

## 6.3.3. Effect of early carbonation curing on chloride penetration (air drying)

Effect of early carbonation curing on chloride penetration was examined through the exposure of chloride immersion and air drying cycles. Fig. 6.8 compares the results at 20<sup>th</sup> and 50<sup>th</sup> cycle for OPC concrete. It was clearly shown in Fig. 6.8(a) that less chloride content was measured in all layers in early carbonation cured concrete than in hydration reference. The phenomenon was more considerable at 50<sup>th</sup> cycle presented in Fig. 6.8(b). At surface region (within 10 mm from surface), carbonation curing reduced the total chloride content from 0.30% (OPC-HA) to 0.20% (OPC-CA) based on concrete weight, leading to reduction by 33%. The reduction was even higher in layer 2 (10-25 mm) in which the total chloride content was reduced by about 48% in early carbonation cured concrete comparing to hydration. This phenomenon agreed with measurements of surface electrical resistivity in Table 6.4 which showed that more resistant layer was created on concrete surface by early carbonation curing. Carbonate deposit due to carbonation curing seemingly densified the physical structure of concrete. Consequently penetration of detrimental ions from outside was reduced.

Fig. 6.9 presents the case of fly ash-OPC concrete. At 20<sup>th</sup> cycle shown in Fig. 6.9(a) chloride distribution along the depth was quite similar between hydrated reference (FAOPC-HA) and carbonation cured (FAOPC-CA) samples. More pronounced difference was observed after 50<sup>th</sup> cycle. As presented in Fig. 6.9(b) the two concretes showed large difference at layer of 10-25 mm where early carbonation curing reduced chloride content to 0.13% from 0.22% in hydrated reference by reduction rate of 41%. Seemingly early carbonation curing slowed down the ingress of chloride ions and was able to limit the detrimental ions within the surface area. It was conclusive that early carbonation curing would not promote chloride penetration as observed by weathering carbonation.

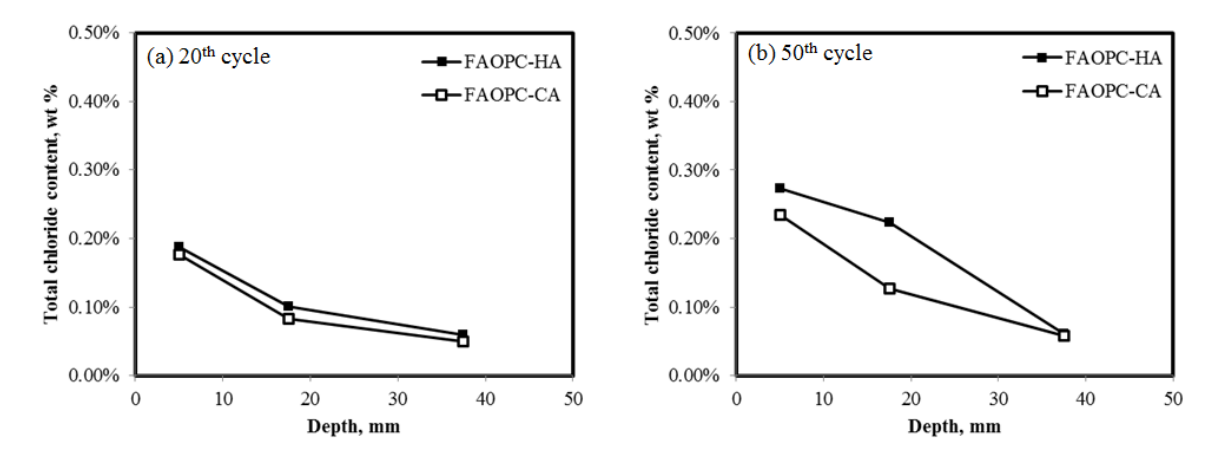


Fig. 6.9. Effect of early carbonation curing on chloride penetration in fly ash-OPC concrete exposed to chloride immersion and air drying cycles

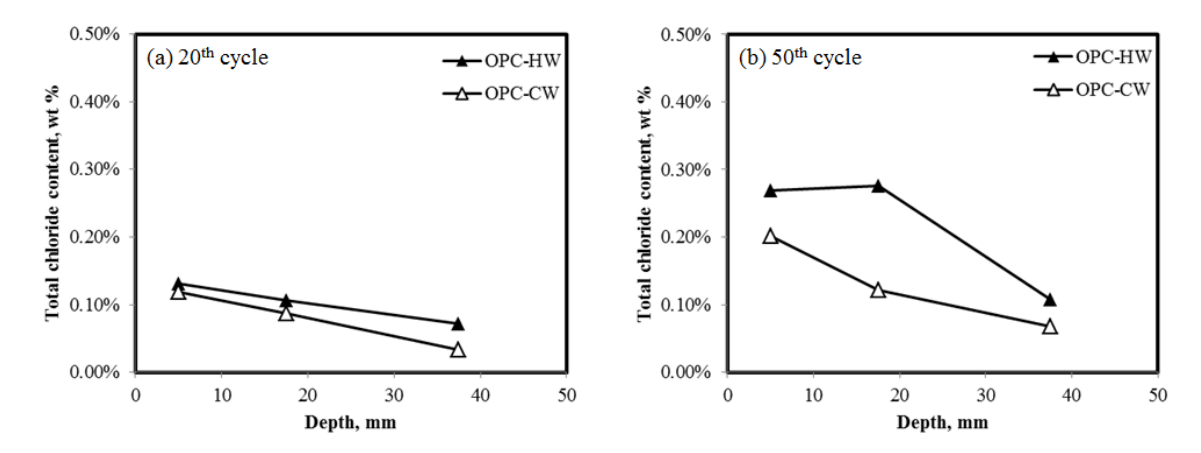


Fig. 6.10. Total chloride content in OPC concrete exposed to chloride immersion and accelerated weathering carbonation cycles

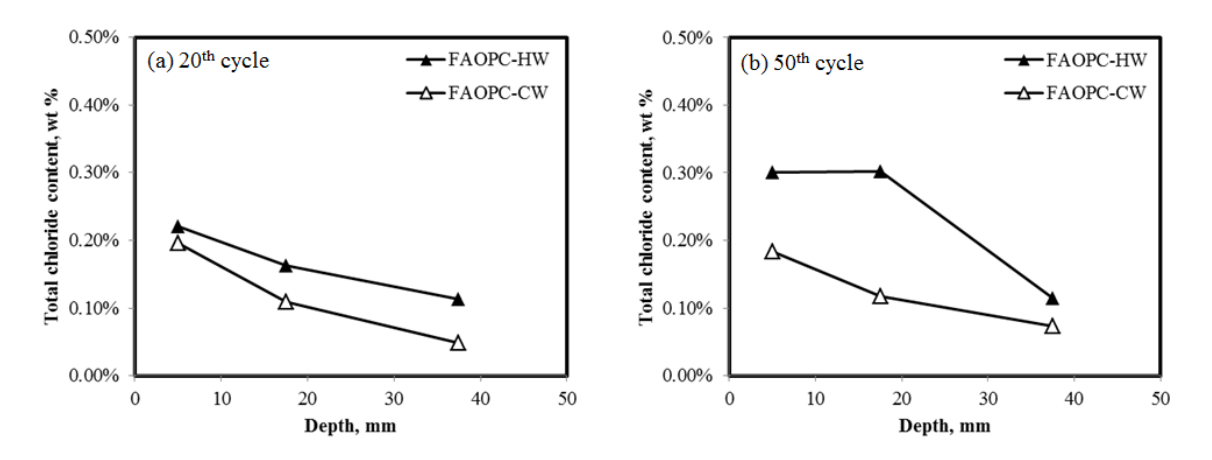


Fig. 6.11. Total chloride content in fly ash-OPC concrete exposed to chloride immersion and accelerated weathering carbonation cycles

# 6.3.4. Effect of early carbonation curing on chloride penetration at the presence of weathering carbonation

Marine and coastal structures are generally subjected to both carbonation-induced and chloride-induced corrosion. To examine the effect of early carbonation curing on concrete exposed to severe environment, chloride profiles were measured at the presence of weathering carbonation in both carbonation and hydration cured concretes. The results are shown in Figs. 6.10 and 6.11. At 20<sup>th</sup> cycle in Fig. 6.10(a), total chloride content was of close between hydration cured (OPC-HW) and early carbonation cured (OPC-CW) concretes while the latter slightly lower. Chloride profile after 50<sup>th</sup> cycle, however, behaved rather different in Fig. 6.10(b). Chloride distribution in hydrated concrete (OPC-HW) showed more chloride accumulated at layer of 10-25 mm. On contrary, early carbonation cured concrete was observed less chloride at the same depth. Total chloride content at layer 2 was reduced more than 57% by early carbonation curing (from 0.28% to 0.12%). Fly ash-OPC concrete displayed the similar phenomenon. Early carbonation

cured concrete (FAOPC-CW) contained much less chloride ions in all three layers especially in layer 2 where total chloride was reduced by more than 60%. It is likely that penetration of chloride was weakened by early carbonation curing and chloride ions were limited on the carbonate-rich surface.

# 6.3.5. Effect of early carbonation curing on weathering carbonation

Carbonation depth was the most used indicator in determining the degree of weathering carbonation since the reduced pore solution alkalinity could be compared quantitatively by colorless edge on the fractured cross section. Together with the chloride content measurement, carbonation depth was also recorded at 20<sup>th</sup>, 30<sup>th</sup>, 40<sup>th</sup> and 50<sup>th</sup> cycles. The results are shown in Table 6.5. It could be clearly seen that carbonation depth increased as testing cycles being increased. Carbonation front of hydrated concrete, for instance, moved from 2.2 mm at 20<sup>th</sup> cycle to 3.9 mm at 50<sup>th</sup> cycle. The increase rate was high at the beginning and gradually slowed down after 40<sup>th</sup> cycle. Carbonation cured concrete exhibited similar trend with respect to testing cycles. Comparison suggested that the two curing methods made little difference on concrete resistance to weathering carbonation.

Table 6.5. Weathering carbonation depth (mm)

Sample	20th	30th	40th	50th
ОРС-Н	2.2	3.0	3.6	3.9
OPC-C	2.4	2.9	3.4	4.0
FAOPC-H	3.5	4.5	5.6	6.1
FAOPC-C	3.4	4.5	5.7	6.1

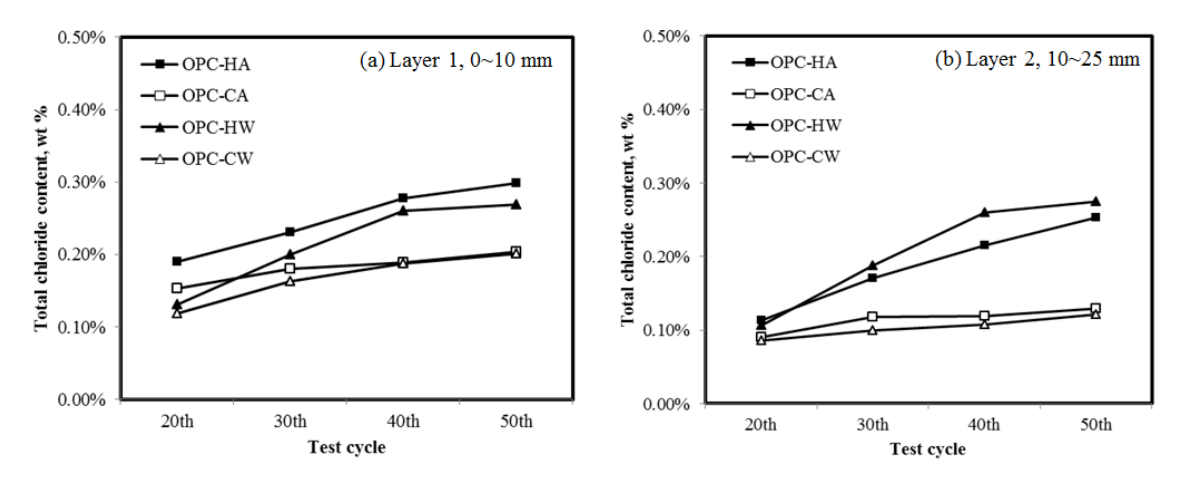


Fig. 6.12. Evolution of total chloride content in OPC concrete

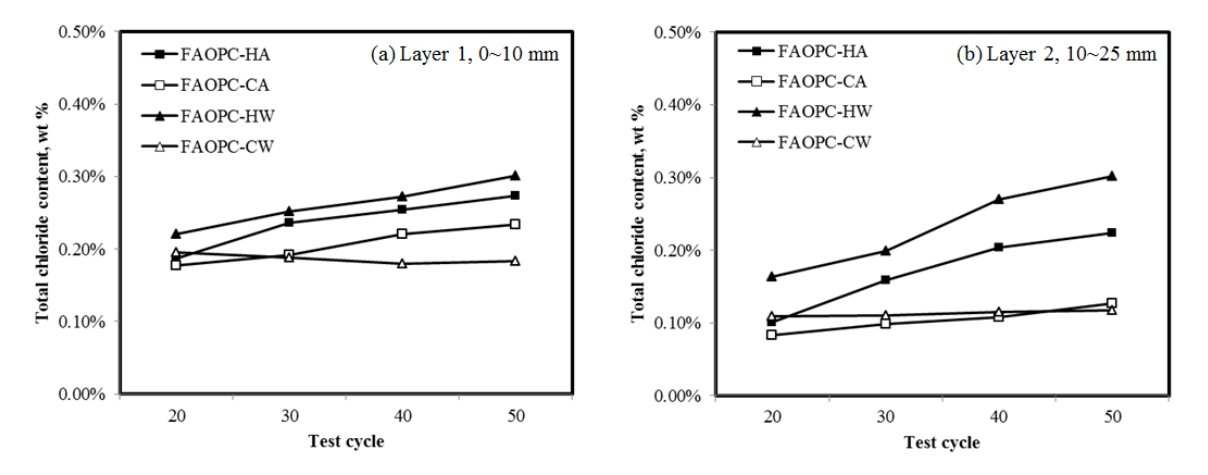


Fig. 6.13. Evolution of total chloride content in fly ash-OPC concrete

The presence of fly ash significantly increased carbonation depth as shown in Table 6.5. The same phenomenon was reported in other study (Atis, 2003). It was likely caused by the low calcium hydroxide due to pozzolanic reaction and the dispersed cement grains which were more reactive with CO<sub>2</sub> (Papadakis, 2000). Similar to OPC concrete, the curing methods showed no effect on the weathering carbonation depth in fly ash-OPC concrete. In both concretes, early carbonation curing did not create more weathering

carbonation depth although the calcium hydroxide content might be reduced by early carbonation (Rostami et al., 2011a).

# 6.3.6. Chloride profile evolution

Fig. 6.12 depicts the evolution of total chloride content versus testing cycles in different layers. In layer 1 (Fig. 6.12a), the chloride uptake rate was slower in early carbonation cured concrete (OPC-CA and OPC-CW) than in hydrated references. The effect of the curing methods was apparent after 30<sup>th</sup> cycle when early carbonation cured concrete was measured less increase in chloride content. The impact of early carbonation curing was more notable in layer 2 shown in Fig. 6.12(b). The hydrated reference showed much higher chloride content and chloride uptake rate after 20<sup>th</sup> cycle. Fly ash-OPC concrete exhibited the same evolution pattern in Fig. 6.13. It was noticed that as weathering carbonation involved, carbonated fly ash-OPC concrete (FAOPC-CW) showed slight decrease in chloride content in respect to testing cycles in Fig. 6.13(a). This was probably because more chloride ions were released from binding state and diffused out of the region. Fig. 6.13(b) compares chloride contents in layer 2 (10-25 mm) against testing cycles. The chloride uptake rate by carbonation cured fly ash-OPC concrete appeared quite constant while it was steep in hydration cured concrete. Comparison between OPC and fly ash-OPC concretes upon different environmental exposure was indicative that presence of fly ash or weathering carbonation did not change the chloride profile as significantly as early carbonation curing. The difference of curing method played more dominate role on the penetration of chloride ions. Early carbonation curing was able to significantly reduce the chloride penetration in both OPC and fly ash-OPC concretes.

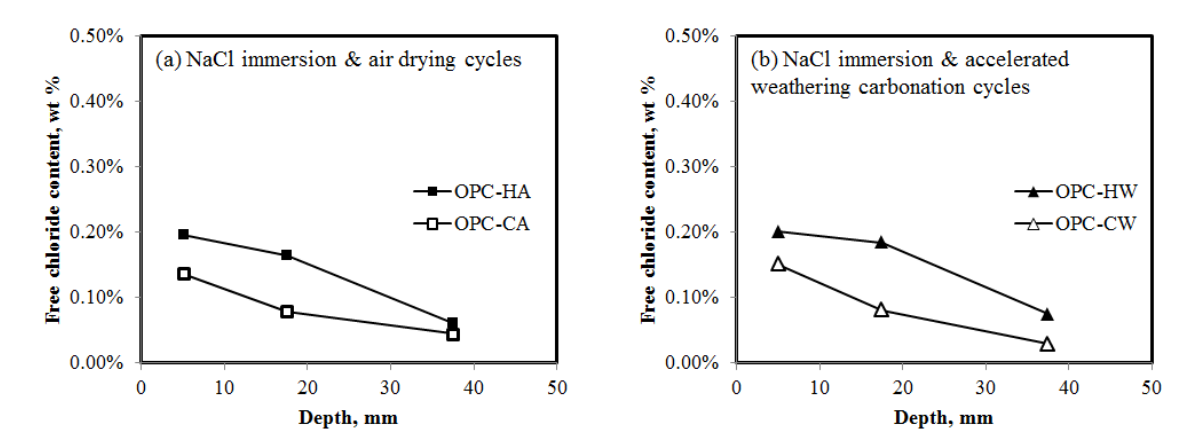


Fig. 6.14. Free chloride content in OPC concrete after 50th cycle

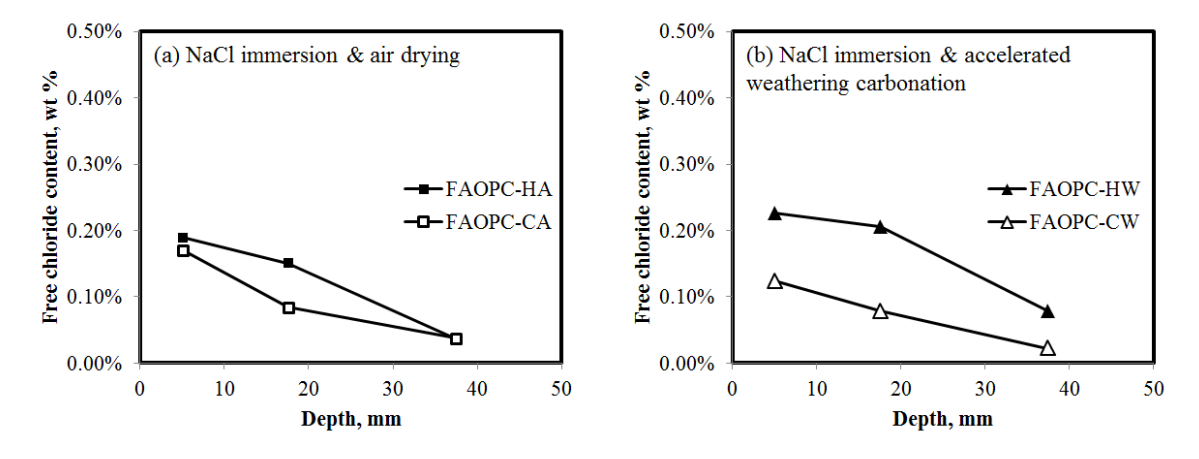


Fig. 6.15. Free chloride content in fly ash-OPC concrete after 50th cycle

# 6.3.7. Effect of early carbonation curing on free chloride profile

Chlorides in concrete was categorized into two different states: bound and free based on their solubility in pore solution (<u>Arya and Xu, 1995</u>; <u>Glass and Buenfeld, 2000</u>). The bound chloride was chemically combined by reaction product of cementitious materials or physically adsorbed by internal surface area of pore structure. The bound

chloride was not soluble in pore solution and thus showed no direct effect on steel corrosion. The free chloride, however, existed in pore solution and increased the corrosion potential. Usually free chloride content at steel rebar location was compared with threshold value to determine the state of corrosion. In laboratory experiment, chloride ions were tested as acid-soluble or water-soluble by titration test following ASTM C1152 or ASTM C1218, respectively. The acid-soluble test represented the total chloride content while the water-soluble the free chloride. Fig. 6.14 compares the free chloride profile in concrete cured by the two different methods after 50<sup>th</sup> cycle. Early carbonation cured concrete showed less free chloride content in both exposure conditions comparing to hydration reference. At layer 2 (10-25 mm) free chloride content was reduced by more than 50% in carbonation cured concrete. The same phenomenon was also observed in the scenario of fly ash-OPC concrete in Fig. 6.15. In concrete cured by early carbonation, free chloride ions seemed to be accumulated on concrete surface (layer 1). The penetration rate was significantly reduced. Since free chloride played the critical role on corrosion initiation, it was suggestive that early carbonation curing was beneficial on concrete resistance to chloride-induced corrosion as exposed to both chloride and weathering carbonation.

The ability of reaction products to bind chloride ions was quantified by binding capacity. It was reported that binding capacity was highly related to C<sub>3</sub>A content in cement composition. The chemical binding of chloride through C<sub>3</sub>A formed Friedel's salt (Taylor, 1997; Hilsdorf and Kropp, 2004) which was decomposed in exposure of weathering carbonation. Chloride was released from binding state and the binding

capacity at this area was reduced as a result. The effect of early carbonation curing on binding capacity was estimated after the 50<sup>th</sup> cycle.

Table 6.6. The bound chloride to total chloride ratio (%)

Sample	Location	HA	CA	HW	CW
OPC	Layer 1	34	33	25	25
	Layer 2	35	39	33	34
Fly ash-OPC	Layer 1	31	27	25	25
	Layer 2	33	34	32	33

Table 6.6 shows the ratio of bound chloride to total chloride at each layer after 50<sup>th</sup> exposure cycle. In layer 1 of OPC concrete, it was obvious that the accelerated weathering carbonation significantly reduced the bound chloride. The value was reduced from 34% to approximately 25%. The difference between early carbonation curing and hydration, however, was not significant. It seemed that early carbonation showed no impact on binding capacity as much as the weathering carbonation. The portion of bound chloride in layer 2 was found increased comparing to layer 1 especially in concretes exposed to accelerated weathering carbonation. This was in agreement with the measurements of weathering carbonation depth which was basically limited within layer 1. Fly ash-OPC concrete exhibited similar profile of bound chloride. It seemed that early carbonation curing made no obvious difference from normal hydration on chloride binding capacity. In contrast, weathering carbonation released chloride ions from binding state and led to higher portion of free chloride content.

#### **6.4. SUMMARY AND CONCLUSIONS**

Effect of early carbonation curing on chloride penetration and weathering carbonation in both OPC and OPC-fly ash concretes were studied. Tests of cyclic exposure to chloride solution immersion and accelerated weathering carbonation were carried out in one year period on carbonation cured and normally hydrated concretes. Total chloride and free chloride contents were measured. Conclusions were drawn as follows:

- 1. Carbonation curing reduced pH of concrete immediately after the process. However, this reduction in alkalinity was able to be compensated after 27 d subsequent hydration, at which time concrete gained pH comparable to hydration references at heavily carbonated surface area. The one year alternation test between chloride immersion and accelerated weathering carbonation suggested that carbonation curing and hydration curing made no obvious difference on concrete resistance to weathering carbonation in service life.
- 2. In alternation between chloride immersion and air drying, total chloride content was reduced in carbonation cured concrete than in hydration reference. At the location of 10-25 mm from surface, total chloride content was reduced over 50% by carbonation curing. It seemed that concretes subjected to carbonation curing were more resistant to chloride penetration in both short and long term exposure. Under the effect of both chloride and weathering carbonation, concrete cured by early carbonation was seen less chloride content comparing to hydration as well. It was indicative that carbonation curing

reduced corrosion risk or delayed corrosion initiation in concrete serving in marine environment.

- 3. Total chloride content at layer of 10-25 mm was increased as concrete exposed to both chloride and weathering carbonation comparing to chloride environment alone. In the meantime, the ratio of free chloride to bound chloride was increased with weathering carbonation involved. More chloride ions were released and steel rebar became more vulnerable to chloride corrosion deterioration.
- 4. Free chloride and binding capacity was evaluated based on one year tests. Free chloride content was considerably reduced by more than 60% in early carbonation cured concrete comparing to hydration reference. However, the ratio of bound chloride to total chloride seemed not significantly changed by different curing methods.
- 5. Carbonation curing effect on fly ash concrete was also studied. Both total and free chloride contents were largely reduced. The effect was more apparent at layer of 10-25 mm where carbonation cured concrete was shown more than 50% less chloride content than hydration reference. Accordingly, corrosion risk of reinforcing steel was highly reduced in concrete subjected to carbonation curing. Carbonation curing of fly ash concrete significantly reduced carbon emission due to the carbon uptake and the cement replacement in addition to the improved resistance to chloride penetration.
- 6. It was conclusive that carbonation curing at early age did not promote weathering carbonation in in the long term. It was able to reduce corrosion risk and delay corrosion initiation by reducing chloride penetration. Accordingly early age carbonation was applicable as curing method on reinforced concrete production.

# ACKNOWLEDGEMENT

The financial supports by Natural Sciences and Engineering Research Council (NSERC) of Canada and by Climate Change and Emissions Management Corporation (CCEMC) of Alberta are gratefully acknowledged.

### REFERENCES

- AHMAD, S. 2003. Reinforcement corrosion in concrete structures, its monitoring and service life prediction—a review. *Cement and Concrete Composites*, 25, 459-471.
- ALONSO, C., ANDRADE, C. & GONZALEZ, J. 1988. Relation between resistivity and corrosion rate of reinforcements in carbonated mortar made with several cement types. *Cement and concrete research*, 18, 687-698.
- ANN, K. Y. & SONG, H.-W. 2007. Chloride threshold level for corrosion of steel in concrete. *Corrosion Science*, 49, 4113-4133.
- ARYA, C. & XU, Y. 1995. Effect of cement type on chloride binding and corrosion of steel in concrete. *Cement and Concrete Research*, 25, 893-902.
- ATIŞ, C. D. 2003. Accelerated carbonation and testing of concrete made with fly ash. *Construction and Building Materials*, 17, 147-152.
- BASTIDAS-ARTEAGA, E., CHATEAUNEUF, A., SÁNCHEZ-SILVA, M., BRESSOLETTE, P. & SCHOEFS, F. 2010. Influence of weather and global warming in chloride ingress into concrete: A stochastic approach. *Structural Safety*, 32, 238-249.
- BERGER, R., YOUNG, J. & LEUNG, K. 1972. Acceleration of hydration of calcium silicates by carbon dioxide treatment. *Nature*, 240, 16-18.
- BERKELEY, K. & PATHMANABAN, S. 1990. Cathodic protection of reinforcement steel in concrete.
- GLASS, G. & BUENFELD, N. 1997. The presentation of the chloride threshold level for corrosion of steel in concrete. *Corrosion Science*, 39, 1001-1013.
- GLASS, G. & BUENFELD, N. 2000. The influence of chloride binding on the chloride induced corrosion risk in reinforced concrete. *Corrosion Science*, 42, 329-344.
- GLASS, G., PAGE, C. & SHORT, N. 1991. Factors affecting the corrosion rate of steel in carbonated mortars. *Corrosion Science*, 32, 1283-1294.

- HENG, M. & MURATA, K. 2004. Aging of concrete buildings and determining the pH value on the surface of concrete by using a handy semi-conductive pH meter. *Analytical sciences*, 20, 1087-1090.
- HILSDORF, H. & KROPP, J. 2004. Performance criteria for concrete durability, CRC Press.
- HONG, K. & HOOTON, R. 1999. Effects of cyclic chloride exposure on penetration of concrete cover. *Cement and Concrete Research*, 29, 1379-1386.
- HUSSAIN, S., AL-MUSALLAM, A. & AL-GAHTANI, A. 1995. Factors affecting threshold chloride for reinforcement corrosion in concrete. *Cement and Concrete Research*, 25, 1543-1555.
- LEE, M. K., JUNG, S. H. & OH, B. H. 2013. Effects of carbonation on chloride penetration in concrete. *ACI Materials Journal*, 110.
- LI, D., CHEN, Y., SHEN, J., SU, J. & WU, X. 2000. The influence of alkalinity on activation and microstructure of fly ash. *Cement and Concrete Research*, 30, 881-886.
- MCCARTER, W., STARRS, G. & CHRISP, T. 2000. Electrical conductivity, diffusion, and permeability of Portland cement-based mortars. *Cement and Concrete Research*, 30, 1395-1400.
- NEVILLE, A. 1995. Chloride attack of reinforced concrete: an overview. *Materials and Structures*, 28, 63-70.
- PAPADAKIS, V. G. 2000. Effect of supplementary cementing materials on concrete resistance against carbonation and chloride ingress. *Cement and concrete research*, 30, 291-299.
- RICHARDSON, M. G. 1988. Carbonation of reinforced concrete: its causes and management, Citis.
- ROSTAMI, V., SHAO, Y. & BOYD, A. J. 2011a. Carbonation curing versus steam curing for precast concrete production. *Journal of Materials in Civil Engineering*, 24, 1221-1229.
- ROSTAMI, V., SHAO, Y. & BOYD, A. J. 2011b. Durability of concrete pipes subjected to combined steam and carbonation curing. *Construction and Building Materials*, 25, 3345-3355.

- SHAO, Y., MIRZA, M. S. & WU, X. 2006. CO<sub>2</sub> sequestration using calcium-silicate concrete. *Canadian Journal of Civil Engineering*, 33, 776-784.
- STEWART, M. G., WANG, X. & NGUYEN, M. N. 2011. Climate change impact and risks of concrete infrastructure deterioration. *Engineering Structures*, 33, 1326-1337.
- TAYLOR, H. F. 1997. Cement chemistry, Thomas Telford.
- THOMAS, M. 1996. Chloride thresholds in marine concrete. *Cement and concrete Research*, 26, 513-519.
- YOON, I.-S., ÇOPUROĞLU, O. & PARK, K.-B. 2007. Effect of global climatic change on carbonation progress of concrete. *Atmospheric environment*, 41, 7274-7285.
- ZHANG, D. & SHAO, Y. 2016. Early age carbonation curing for precast reinforced concretes. *Construction and Building Materials*, 113, 134-143.

## CHAPTER 7

\_

# CONCLUSIONS AND FUTURE WORK

#### 7.1. CONCLUSIONS

Carbonation curing of precast concrete with high workability was studied in an attempt to extend its application to reinforced concrete. The performance of concrete subject to the innovative carbonation curing process was evaluated in both short and long period. Chemical and physical structure of carbonated concrete was investigated through various experimental approaches. Laboratory simulation on marine concrete structure was conducted to acquire realistic evaluation on potential risk of rebar corrosion. According to the experimental results and theoretical analysis, conclusions were drawn as following:

(1) Following the process of initial hydration - carbonation - subsequent hydration, carbonation curing was able to be controlled on surface of wet-mix concrete. The carbonated layer was carbonate-rich while the concrete pH maintained normal level. The technique of carbonation curing improved early performance without affecting the core area in concrete.

- (2) The improved early strength was primarily due to the accelerated reaction of Portland cement. The 1 day cement reaction degree was increased to above 60% to 80% depending on carbon dioxide uptake. The advantage in the reaction extent remained in the long term comparing to conventional hydration in moist condition.
- (3) Fly ash reaction was weakened primarily due to the reduced alkalinity as a consequence of carbonation curing. Subsequent hydration of Portland cement provided calcium hydroxide which accounted for the pozzolanic reaction. It was feasible to maintain both improved early performance and desirable pozzolanic reaction degree by well controlled carbonation uptake and suitable fly ash addition.
- (4) The physical pore structure in microscope was significantly changed by carbonation curing. Total porosity measured by mercury intrusion porosimetry was found to be reduced by 40% and 22% in plain cement and fly ash cement at the age of 360 days after 12 hours carbonation treatment. Pore size was reduced as well. The critical pore diameter reduced by approximately 50% for both plain cement and fly ash cement. The component of pore structure was substantially changed due to carbonation curing. The primary governing pore type shifted from medium capillary pores ( $10 \sim 50 \text{ nm}$ ) to small capillary and gel pores (less than 10 nm). In the meanwhile, the ink-bottle effect seemed more considerable after carbonation curing which further accounted for better resistance to permeation. As a consequence, carbonation curing served densification effect on the pore structure. The same effect was observed on concrete by water absorption. Carbonation curing reduced permeable porosity by 18% and 23% in plain OPC and fly ash-OPC concrete, respectively.

- (5) Carbonation curing showed significant effect on concrete resistance to freeze-thaw damage. Pore with diameter less than 10 nm occupied more than 50% in volume of total porosity. Water in small pores required lower temperature to exert freeze damage on the solid. The densification effect of carbonation curing on pore structure accounted for the improved freeze-thaw resistance.
- (6) The ingress of chloride in concrete was considerably prevented by carbonation curing. The penetration depth was reduced while the total chloride content in concrete became less. Free chloride was reduced as well after 50 wet/dry cycles. The binding capacity maintained high in spite of carbonation curing.
- (7) Early age carbonation followed by proper subsequent hydration was able to maintain concrete pH above 12.5. The depth of weathering carbonation in the long term was not found intensified. However, in the presence of both weathering carbonation and chloride penetration, the ingress of chloride ions was considerably reduced. The corrosion risk, as a whole, was reduced specifically regarding to chloride-induced corrosion.

Consequently, carbonation curing on wet cast concrete was capable to solve the problem of insufficient performance in the early age including strength gain and durability specifically as supplementary cementitious materials incorporated. Curing period could be reduced and thus higher producing efficiency was possibly achieved. Durability in cold weather, especially the resistance to frost damage, was significantly improved. Reinforced concrete subjected to carbonation curing gained higher resistance to rebar corrosion specifically in regard of chloride-induced corrosion.

# 7.2. SUGGESTIONS FOR FUTURE WORK

Based on the presented work, some subjects are suggested as future work:

- (1) Large scale research requires to be conducted as to spread the technique of carbonation curing on reinforced concrete. Low pressure (including vacuum) as well as flue gas cycling network are necessary for industrialization.
- (2) Corrosion test is required on steel rebar. Parameters including corrosion initializing age and corrosion rate need to be quantitatively evaluated in reinforced concrete.
- (3) Other than fly ash, more supplementary cementitious materials need to be studied the potential of carbonation in wet cast mixture. The effect of carbonation curing on long term performance should also be clarified.
- (4) More techniques are required to visualize the geometric shape of micro pores.

  The nanostructure and gel pores in C-S-H are necessary to be characterized.

#### **DUO ZHANG**

Department of Civil Engineering & Applied Mechanics
McGill University

Macdonald Engineering Building, 817 Sherbrooke Street West, Room 165
Montreal, Quebec, H3A 0C3

Email: duo.zhang3@mail.mcgill.ca

#### **EDUCATION**

# September, 2013 – present

McGill University, Montreal, Canada

Ph.D. Candidate, Civil Engineering (GPA: 4.0/4.0)

Thesis Title: Performance Evaluation of Precast Reinforced Concrete after Early-Age Carbonation Curing

# <u>September, 2011 – June, 2013</u>

Southwest Jiaotong University, Chengdu, China

Master of Engineering, Civil Engineering (GPA: 3.7/4.0)

Thesis Title: Mechanical analysis of FRP cable in 2000m-span cable-stayed bridge (Outstanding Thesis Award)

#### September, 2007 – June, 2011

Southwest Jiaotong University, Chengdu, China

Bachelor of Engineering, Civil Engineering (GPA: 92/100)

Bachelor of Business Administration, Management (GPA: 87/100)

#### SELECTED PUBLICATIONS (PEER REVIEWED)

- ➤ <u>Duo Zhang</u>, Yixin Shao. (2016), Effect of early carbonation curing on chloride penetration and weathering carbonation in concrete, *Construction and Building Materials*, in press.
- ➤ <u>Duo Zhang</u>, Xinhua Cai, Yixin Shao. (2016), Carbonation curing of precast fly ash concrete, Journal of Materials in Civil Engineering, ASCE, 04016127
- ➤ <u>Duo Zhang</u>, Yixin Shao. (2016), Early age carbonation curing for precast reinforced concrete, *Construction and Building Materials*, 113, 134-143.
- ➤ <u>Duo Zhang</u>, Xiaozhen Li. (2014). Theoretical solution of dynamic reaction of simply supported beam under vertical moving harmonic force series, *Chinese Journal of Applied Mechanics*, 31(1), 144-149.
- ➤ <u>Duo Zhang</u>, Wei He, Changjiang Jiang, & Linyu Yuan. (2012). Construction monitoring and control of cantilever casting arch of New Midi Bridge. *Bridge Construction*, 42(4), 87-92.